

INFORMATION TO USERS

This reproduction was made from a copy of a document sent to us for microfilming. While the most advanced technology has been used to photograph and reproduce this document, the quality of the reproduction is heavily dependent upon the quality of the material submitted.

The following explanation of techniques is provided to help clarify markings or notations which may appear on this reproduction.

1. The sign or "target" for pages apparently lacking from the document photographed is "Missing Page(s)". If it was possible to obtain the missing page(s) or section, they are spliced into the film along with adjacent pages. This may have necessitated cutting through an image and duplicating adjacent pages to assure complete continuity.
2. When an image on the film is obliterated with a round black mark, it is an indication of either blurred copy because of movement during exposure, duplicate copy, or copyrighted materials that should not have been filmed. For blurred pages, a good image of the page can be found in the adjacent frame. If copyrighted materials were deleted, a target note will appear listing the pages in the adjacent frame.
3. When a map, drawing or chart, etc., is part of the material being photographed, a definite method of "sectioning" the material has been followed. It is customary to begin filming at the upper left hand corner of a large sheet and to continue from left to right in equal sections with small overlaps. If necessary, sectioning is continued again—beginning below the first row and continuing on until complete.
4. For illustrations that cannot be satisfactorily reproduced by xerographic means, photographic prints can be purchased at additional cost and inserted into your xerographic copy. These prints are available upon request from the Dissertations Customer Services Department.
5. Some pages in any document may have indistinct print. In all cases the best available copy has been filmed.

**University
Microfilms
International**

300 N. Zeeb Road
Ann Arbor, MI 48106

8508719

Mohammed, Abdel-Raouf Eid

DENSITY-FUNCTIONAL THEORY STUDIES OF CORRELATION ENERGY
EFFECTS AT METALLIC SURFACES

City University of New York

PH.D. 1985

University
Microfilms
International 300 N. Zeeb Road, Ann Arbor, MI 48106

Density-Functional Theory Studies
of
Correlation Energy Effects at Metallic Surfaces

by

Abdel-Raouf Eid Mohammed

A dissertation submitted to the Graduate Faculty
in Physics in partial fulfillment of the requirements
for the degree of Doctor of Philosophy, The City
University of New York.

1985

This manuscript has been read and accepted for the Graduate Faculty in Physics in satisfaction of the dissertation requirement for the degree of Doctor of Philosophy.

Nov 16, 1984

date

Viraht Sahni

Chairman of Examining Committee

Nov. 20, 1984

date

[Signature]

Executive Officer

Viraht Sahni
Joseph B. Krieger
Lawrence B. Mendelsohn
C. R. Fischer
John P. Perdew

Supervisory Committee

The City University of New York

Abstract

Density-Functional Theory Studies of Correlation Energy Effects at Metallic Surfaces

by

Abdel-Raouf Eid Mohammed

Advisor: Professor Viraht Sahni

In this thesis we study the effects of correlation in the inhomogeneous electron gas at metallic surfaces. These studies are performed within the context of density-functional theory (DFT). Using accurate representations of the electronic density profile, we have estimated variationally the surface correlation energy of jellium metal. The accuracy of these estimates is founded in the assumption that the exchange-correlation energy functional of the density is approximated accurately by the wave-vector analysis method, and by the fact that the non-local exchange energy contributions are treated exactly. In contrast to the previously accepted conclusion that for surfaces correlation effects are as significant as exchange, our results indicate the ratio of these energies to lie between 34% - 97% over the metallic density range, the smaller ratios corresponding to the higher

density metals. In this work we have also examined the local density (LDA) and gradient expansion approximations(GEA) (to $O(\nabla^2)$) for the correlation energy. We have demonstrated for realistic metal surface densities the cancellation of the errors in the LDA for exchange and correlation, and shown that the density profiles at surfaces would have to be unphysically slowly varying for the correlation energy GEA to converge. We have also studied the effects of correlation at surfaces by screening the exchange, and observe that the surface exchange energy for screened-Coulomb interaction decreases as the screening length is reduced. Thus, the more short-ranged the interaction, the easier it is to split the crystal in two. In addition we have derived the DFT first gradient correction coefficient in the GEA for the screened-Coulomb exchange energy, and shown it to be the same as that obtained within Hartree-Fock theory (HFT) for finite screening. This coefficient reduces to the DFT bare-Coulomb interaction value in the limit of no screening in which limit the HFT coefficient is singular. The GEA for the screened-Coulomb surface exchange energy in both HFT and DFT are also examined and both expansions shown not to converge to the exact values as a function of the density profile. An explanation for these surprising results is presented and suggestions made for future work based on the wave-vector method.

Dedication

To: My Parents,
wife Shadia,
son Hosam and daughter Doaa.

Acknowledgements

I wish to express my deepest gratitude to my advisor Professor Viraht Sahni for his valuable guidance , constant encouragement and for being a constant source of inspiration throughout the course of this thesis work. I have a deep sense of admiration for his valuable advice , outstanding personality , and his keen interest in my work .

I like to acknowledge the many helpful comments of Professor John P. Perdew of Tulane University during the course of this thesis.

I wish to acknowledge with gratitude the department of Physics of Brooklyn College for providing me this opportunity, the Research foundation of CUNY for the financial support during the course of this work, and the Brooklyn College computer center for allowing me to use their facilities.

The final tribute must go to my wife , Shadia, whose continuing encouragement and understanding have been the most helpful solace at difficult times , and for her sacrifices which made these studies possible.

Contents

| | |
|--|-----|
| Abstract | iii |
| Dedication | v |
| Acknowledgements | vi |
| List of Tables | ix |
| List of Figures | xi |
| | |
| Chapter I: INTRODUCTION | 1 |
| 1.1 The Correlation Energy within Density-Functional Theory | 1 |
| 1.1.1 Quantitative Estimates | 10 |
| 1.1.1.1 Homogeneous Electron Gas | 10 |
| 1.1.1.2 Atoms | 11 |
| 1.1.1.3 Metallic Surfaces | 15 |
| 1.2 Local Density and Gradient Expansion Approximations | 18 |
| 1.2.1 Local Density Approximation for the Exchange , Correlation and Exchange-Correlation Energies. | 21 |
| 1.2.1.1 Atoms | 21 |
| 1.2.1.2 Metallic Surfaces | 22 |
| 1.2.2 The Lang-Sham Argument | 23 |
| 1.2.3 Gradient Expansion Approximation for the Exchange , Correlation and Exchange-Correlation Energies. | 26 |
| 1.2.3.1 Atoms | 26 |
| 1.2.3.2 Metallic Surfaces | 26 |
| 1.3 Thesis Outline | 27 |
| | |
| Chapter II: | 31 |
| 2.1 Definitions of Jellium Metal Surface Properties | 31 |
| 2.2 Exact Surface Exchange Energy for Screened-Coulomb Interaction | 38 |

| | |
|---|-----|
| Chapter III: | 50 |
| 3.1 Convergence Study of the Gradient Expansion Approximation for Screened-Coulomb Exchange Energy within Hartree-Fock Theory | 50 |
| 3.2 The Gradient Expansion Approximation for Screened- Coulomb Exchange Energy within Density-Functional Theory | 66 |
| Chapter IV: | 76 |
| 4.1 Estimates of the Surface Correlation Energy | 76 |
| 4.2 Convergence Study of the Gradient Expansion Approximation for the Surface Correlation Energy | 91 |
| Chapter V: | 102 |
| 5.1 Summary and Conclusions | 102 |
| 5.2 Future Work | 106 |
| Appendix A | 108 |
| Density-Functional Theory First Gradient Coefficient for the Screened-Coulomb Exchange Energy. | 108 |
| Appendix B | 134 |
| Linear-Potential Model of a Surface. | 134 |
| Appendix C | 141 |
| Polynomial Fit to First Gradient Correction Coefficient | 141 |
| Bibliography | 144 |

List of Tables

| | | |
|------|---|----|
| I. | Empirically determined conventional and density-functional theory correlation energies of atoms with atomic number $Z=2-18$ | 12 |
| II. | The exact, local density and gradient expansion approximation surface exchange, correlation and exchange-correlation energies as a function of the Wigner-Seitz radius for the infinite barrier model | 16 |
| III. | the surface exchange energy for screened-Coulomb interaction as a function of the density profile parameter and screening parameter in the step-potential model | 46 |
| IV. | The total surface energy for screened-Coulomb interaction for different bulk densities and density profiles of the step-potential model, as a function of the screening parameter | 48 |
| V. | The exact, local density and gradient expansion approximation surface exchange, correlation and exchange-correlation energies as a function of the Wigner-Seitz radius for the linear-potential model | 86 |
| VI. | Exact, local density and gradient expansion approximation surface correlation energies as a function of the density | |

profile parameter of the linear-potential model for a fixed
bulk density 95

List of Figures

| | | |
|-----|---|----|
| 1. | Variation of the exact surface exchange energy as a function of the density profile parameter and screening parameter | 47 |
| 2a. | Variation of the exact, LDA and GEA surface exchange energies for screened-Coulomb interaction as a function of the screening parameter. | |
| b. | The corresponding LDA and GEA percent error plots. | 54 |
| 3a. | Variation of the LDA coefficient A_{sx}/k_F^{-3} as function of the screening parameter for different bulk densities. | |
| b. | Variation of the GEA coefficient C_{sx} in the Hartree-Fock theory as a function of the screening parameter for different bulk densities | 56 |
| 4a. | Variation of the exact, LDA and GEA surface exchange energies for screened-Coulomb interaction as a function of the density profile parameter in the step-potential model . | |
| b. | The corresponding LDA and GEA percent error plots | 58 |
| 5. | Caption for parts (a) and (b) are the same as that of Fig. 4, except that these results are derived for a different value of the screening parameter | 60 |

| | | |
|-----|--|----|
| 6. | Variation of the "small" parameter of Eq.(62) as a function of the distance from the jellium edge | 61 |
| 7. | Variation of the "small" parameter of Eq. (63) as a function of the distance from the jellium edge | 62 |
| 8a. | Variation of the exact, LDA and GEA for surface exchange energy for bare-Coulomb interaction as a function of the density profile parameter in the step-potential model. | |
| b. | The corresponding LDA and GEA percent error plots | 64 |
| 9. | Variation of the density-functional theory local density and gradient expansion approximation coefficients as a function of the screening parameter | 69 |
| 10. | (a) ,(b) and (c). Variation of the GEA coefficient C_{sx} within Hartree-Fock and density-functional theories as a function of the screening parameter | 71 |
| 11. | The DFT LDA and GEA percent error curves for the screened-Coulomb surface exchange energy as a function of the density profile parameter for different values of the screening parameter | 73 |
| 12. | Variation of the exact and LDA surface exchange , correlation and exchange-correlation energies as a function of the Wigner-Seitz radius | 87 |

| | | |
|-----|--|-----|
| 13. | Variation of the 'exact' (wave-vector) , LDA and GEA surface correlation energies as a function of the density profile parameter in the linear-potential model | 96 |
| 14. | Percent error plots of the LDA and GEA results of Fig. 13 | 97 |
| 15. | Variation of the surface correlation energy density as a function of the distance from the jellium edge | 99 |
| 16. | Variation of the 'small parameter' of Eq.(88) as a function of the distance from the jellium edge | 101 |

Chapter I

INTRODUCTION

1.1 The Correlation Energy within Density-Functional Theory

The Coulomb repulsion between electrons correlates their motion in such a way as to reduce the probability of two electrons approaching each other closely. These Coulomb correlations are different from the type of correlations which are due to the Pauli exclusion principle. The Hartree-Fock method which accounts for correlations of the latter type, takes no account at all of the former. Consequently, the correlation energy E_c is defined¹ as the total non-relativistic energy E^{nr} , calculated with proper allowance for Coulomb correlations, minus the Hartree-Fock energy E^{HF} . This is the conventional definition of the correlation energy. What is referred to as the correlation energy in modern density-functional theory^{2,3} (DFT), on the other hand, is a mathematical artifact. In order to understand this definition we begin with a discussion of the Hohenberg-Kohn-Sham^{2,3} theory.

According to Hohenberg and Kohn², the non-relativistic ground state energy E^{nr} of a system of N interacting electrons in the presence of an external potential $V(\mathbf{r}_1, \mathbf{r}_2, \dots, \mathbf{r}_N) = \sum_i v(\mathbf{r}_i)$ may be written as

$$E^{\text{nr}}[\rho] = \int d\mathbf{r} v(\mathbf{r})\rho(\mathbf{r}) + \frac{1}{2} \iint d\mathbf{r}d\mathbf{r}' \frac{\rho(\mathbf{r})\rho(\mathbf{r}')}{|\mathbf{r}-\mathbf{r}'|} + G[\rho] \quad (1)$$

$$= E_{\text{es}}[\rho] + G[\rho] \quad (2)$$

where the first term in Eq.(1) corresponds to the interaction between the electrons and the external potential, the second term is the classical Coulomb self-energy of the electrons, and $G[\rho]$ is a universal functional of the density $\rho(\mathbf{r})$. The sum of the first two terms constitutes the known electrostatic energy functional $E_{\text{es}}[\rho]$ of the system. The functional $G[\rho]$ is not given by the theory. In the Kohn-Sham³ version of the theory, the functional $G[\rho]$ is defined by adding and subtracting from it the kinetic energy $E_{\text{k}}[\rho]$ of a system of non-interacting electrons having the same density $\rho(\mathbf{r})$. Thus

$$G[\rho] = E_{\text{k}}[\rho] + G[\rho] - E_{\text{k}}[\rho] \quad (3)$$

$$= E_{\text{k}}[\rho] + E_{\text{xc}}[\rho], \quad (4)$$

which defines the presently unknown 'exchange-correlation' energy functional $E_{\text{xc}}[\rho]$ in which all the many-body effects are incorporated. Therefore, $E_{\text{xc}}[\rho]$ is comprised of the sum of the density functional theory exchange and correlation energies to be defined below, plus the

actual kinetic energy of the interacting system, minus the kinetic energy of the non-interacting electrons with the same density. It has been shown^{2,3} that the energy functional of Eq.(1) is stationary and minimum for the true density, subject to the constraint that all the densities considered conserve the total number of electrons.

Employing a Lagrangian multiplier μ (which can be shown to correspond to the chemical potential of the system) to incorporate the constraint that the total number of particles must be conserved, the Euler equation for the true density on application of the variational principle for the energy is then

$$\frac{\delta E^{\text{nr}}[\rho]}{\delta \rho(\mathbf{r})} = \mu . \quad (5)$$

Using Eq.(1) and Eq.(4) this Euler equation for the density may be put in the form

$$\frac{\delta E_{\text{k}}[\rho]}{\delta \rho(\mathbf{r})} + V_{\text{es}}(\mathbf{r}) + \frac{\delta E_{\text{xc}}[\rho]}{\delta \rho(\mathbf{r})} = \mu , \quad (6)$$

where $V_{\text{es}}(\mathbf{r})$ is the electrostatic potential due to all the charges . Thus

$$V_{\text{es}}(\mathbf{r}) = v(\mathbf{r}) + v_{\text{H}}(\mathbf{r}) , \quad (7)$$

where $v_H(\mathbf{r})$ is the Hartree potential

$$v_H(\mathbf{r}) = \int d\mathbf{r}' \frac{\rho(\mathbf{r}')}{|\mathbf{r}-\mathbf{r}'|} . \quad (8)$$

The ground state density may then be obtained by solution of Eq.(6) in conjunction with Eq.(7).

However, since the kinetic energy $E_k[\rho]$ within this theory is treated as that for a system of non-interacting electrons, Kohn and Sham showed that solution of the Euler Equation (6) was entirely equivalent to solving a set of single-particle Schrodinger-like equations for non-interacting electrons moving in a local effective potential $V_{\text{eff}}(\mathbf{r})$. The self-consistent solution of these equations are the orbitals from which the exact ground state density and energy of the interacting system may be determined . The Kohn-Sham equations are

$$[-\frac{1}{2}\nabla^2 + V_{\text{eff}}(\mathbf{r})] \psi_i(\mathbf{r}) = \epsilon_i \psi_i(\mathbf{r}) \quad (9)$$

with the density being given by

$$\rho(\mathbf{r}) = \sum_i^N |\psi_i(\mathbf{r})|^2 . \quad (10)$$

Here the local effective potential $V_{\text{eff}}(\mathbf{r})$ is defined as

$$V_{\text{eff}}(\mathbf{r}) = V_{\text{es}}(\mathbf{r}) + v_{\text{xc}}(\mathbf{r}) , \quad (11)$$

where v_{xc} , the exchange-correlation potential, is the functional derivative, with respect to the density, of the exchange-correlation energy functional :

$$v_{xc}(\mathbf{r}) = \frac{\delta E_{xc}[\rho]}{\delta \rho(\mathbf{r})} . \quad (12)$$

The kinetic energy, which within this self-consistent scheme may be determined exactly, is then obtained by multiplying Eq.(9) by ψ_i^* , summing over all the particles, and integrating over the electronic coordinates. Thus

$$E_k[\rho] = \sum_i^N \varepsilon_i - \int V_{eff}(\mathbf{r}) \rho(\mathbf{r}) d\mathbf{r} . \quad (13)$$

With the substitution of this expression for the kinetic energy into Eqs.(1) and (4) , the ground state energy of the interacting system is then given by

$$E^{nr}[\rho] = \sum_i^N \varepsilon_i - \frac{1}{2} \iint d\mathbf{r} d\mathbf{r}' \frac{\rho(\mathbf{r})\rho(\mathbf{r}')}{|\mathbf{r}-\mathbf{r}'|} - \int d\mathbf{r} v_{xc}(\mathbf{r})\rho(\mathbf{r}) + E_{xc}[\rho] . \quad (14)$$

In their original work, Kohn and Sham³ pointed out that the eigenvalues ε_i of Eq.(9) have no direct physical significance and cannot be interpreted as electron removal energies. More recently however, it has been shown⁴ that the highest occupied orbital energy $\varepsilon_{\max}^{\text{KS}}$ is equal to the chemical potential μ .

Thus we see that the most significant attribute of the Kohn-Sham theory is that the effective potential in which the electrons move is local, and consequently solution of Eq.(9) is similar to that of the Hartree equations. The principle drawback of the formalism, on the other hand, is that the exchange-correlation energy functional is unknown and must be approximated. As a consequence, the bounds to the ground state energy are no longer rigorous.

In the Kohn-Sham density-functional theory context, the correlation energy $E_c^{\text{DFT}}[\rho]$ is defined by subtracting from $E_{\text{xc}}[\rho]$, the density-functional theory exchange energy functional $E_x^{\text{DFT}}[\rho]$ defined below.

Thus

$$E_c^{\text{DFT}}[\rho] = E_{\text{xc}}[\rho] - E_x^{\text{DFT}}[\rho], \quad (15)$$

where

$$E_x^{\text{DFT}}[\rho] = -\frac{1}{2} \sum_i^N \sum_j^N \int dr \int dr' \frac{\Psi_i^*(r) \Psi_j^*(r') \Psi_i(r') \Psi_j(r)}{|r-r'|}. \quad (16)$$

(// Spins)

The orbitals in the definition of $E_x^{\text{DFT}}[\rho]$ are solutions of Eq.(9) with $v_{xc}(\mathbf{r})$ replaced by the sum of the corresponding functional derivatives $v_x(\mathbf{r})$ and $v_c(\mathbf{r})$. These orbitals are, of course, the same as those obtained by solution of Eq.(9). As is the case with $E_{xc}[\rho]$, the functional $E_c^{\text{DFT}}[\rho]$ is also presently unknown.

However, we note that there is nothing in the Hohenberg-Kohn theorem which precludes the addition and subtraction of any auxiliary kinetic energy from the interacting-fermion energy functional. In fact, one is free to choose the statistics of the fictitious non-interacting particles, or even their masses and spins. Consequently, the corresponding 'exchange-correlation' and 'correlation' energy functionals would be different from that of the Kohn-Sham definition. It is in this context that we refer to the correlation energy in density-functional theory as a mathematical artifact. The addition and subtraction of the kinetic energy of a system of non-interacting bosons of density $\rho(\mathbf{r})$, together with application of the variational principle for the energy to Eq.(1), in fact leads⁵ to a single Euler equation for the density with a different local effective potential and whose eigenvalue is the chemical potential.

Returning to the Kohn-Sham formalism the total non-relativistic energy may then be written as

$$E^{\text{nr}}[\rho] = E_{\text{k}}[\rho] + E_{\text{es}}[\rho] + E_{\text{x}}^{\text{DFT}}[\rho] + E_{\text{c}}^{\text{DFT}}[\rho] = E^{\text{XO}}[\rho] + E_{\text{c}}^{\text{DFT}}[\rho], \quad (17)$$

where the sum of the first three terms constitutes what we refer to as 'exchange-only' (XO) part of the total energy . The exchange-only energy E^{XO} can be determined independently by solving the exchange-only Kohn-Sham equations which are

$$[-\frac{1}{2}\nabla^2 + v(\mathbf{r}) + v_{\text{H}}(\mathbf{r}) + v_{\text{x}}(\mathbf{r})]\phi_i(\mathbf{r}) = \epsilon_i \phi_i(\mathbf{r}), \quad (18)$$

with

$$\rho'(\mathbf{r}) = \sum_i^N |\phi_i(\mathbf{r})|^2 \quad (19)$$

being the corresponding exchange-only density. Note that $E^{\text{XO}}[\rho] = E^{\text{XO}}[\rho']$, but that the constituent kinetic , electrostatic and exchange energy functionals are not equivalent for the two densities ρ and ρ' . Thus , the ground-state energy for the exchange-only system is doubly degenerate in these densities . Although we provide no rigorous mathematical proof of the existence of this degeneracy, the equality of the ground-state exchange-only energy for the two densities may be understood as follows. For an assumed calculational scheme, such as that due to Kohn and Sham , the correlation energy is uniquely defined and must have a specific numerical value for the fully-interacting system under consideration. Consequently , the exchange-only

component of the total energy must have the same value irrespective of whether it is being determined by the density of the fully-correlated system or that of the exchange-only system. The results of calculations to be presented in chapter IV support this conclusion. It must also be emphasized that the $\phi_i(\mathbf{r})$ are not Hartree-Fock orbitals, and that consequently, E^{XO} is not the Hartree-Fock energy. The distinction arises because one set of orbitals are derived from a local effective potential while the other are obtained via a non-local potential. Of course, it is possible⁶ to construct a local effective potential which will give rise to the Hartree-Fock density and total energy, but this is then not the optimized local effective potential.

There are two ways by which the conventional and density-functional theory correlation energies may be estimated. The first is to resort to experiment. The non-relativistic ground state energy may be obtained by subtracting out from the experimental value theoretically determined relativistic effect contributions. Empirical values for the correlation energies may then be obtained by subtracting out the Hartree-Fock and exchange-only energies. The second approach is entirely theoretical. For the conventional correlation energy, one assumes a many-parameter correlated wave function to determine variationally a rigorous upper bound to the ground state energy, from which the Hartree-Fock value is then subtracted. For density-

functional theory values , one must approximate the exchange-correlation or correlation energy functionals as accurately as possible , solve the Kohn-Sham equations self-consistently to determine the ground state energy , and from this result subtract the exchange-only terms using the same orbitals . As indicated earlier, the exchange-only energy may also be determined by an independent Kohn-Sham procedure assuming only Pauli correlations. For system in which self-consistency is difficult to achieve, the ground state energy may be approximated by treating the densities in the energy functional variationally . The exchange-only component to be subtracted should then be determined for these same energy minimized densities. In both the self-consistent and variational procedures , the fact that the total energy functional is approximated implies , as stated earlier, that the bound obtained is no longer rigorous .

1.1.1 Quantitative Estimates

1.1.1.1 Homogeneous Electron Gas

Having described the qualitative differences between the conventional and density-functional theory definitions of the correlation energy , the obvious question which arises next is what are quantitative differences between the two ? . For the homogeneous electron gas, the two correlation energies are identical since both the

Hartree-Fock and exchange-only orbitals are plane waves . Furthermore , the average correlation energy per particle ε_c as determined by a many-parameter correlated wave function calculation⁷, is 20% - 33% of the average exchange energy⁸ $\varepsilon_x = -3\bar{k}_F/4\pi$ over the metallic range of densities $\bar{r}_s = 2-6$. Here \bar{r}_s is the Wigner-Seitz radius defined in terms of the bulk Fermi momentum \bar{k}_F as⁹ $\bar{k}_F = 1/(\alpha r_s)$, $\alpha^{-1} = (9\pi/4)^{1/3}$, and where $\bar{k}_F^3/3\pi^3 = \bar{\rho}$ is the bulk density.

1.1.1.2 Atoms

For the non-uniform electron gas in atoms , the difference between the conventional and density-functional values of the correlation energy can be determined with accuracy upto an atomic number of $Z=18$. Following Veillard and Clementi¹⁰ the non-relativistic ground state energy E^{nr} is the sum of the experimentally determined ionization potentials of an atom minus a relativistic correction . To determine E^{nr} for these atoms we use the most recently determined experimental values quoted by Moore¹¹ . The relativistic corrections we employ are those due to Desclaux¹² who obtained these contributions perturbatively using self-consistently determined Dirac-Fock wavefunctions . In addition to the E^{nr} thus determined for the atoms with $Z=2-18$, we present in Table I the Hartree-Fock¹³ (E^{HF}) and exchange-only¹⁴ (E^{XO}) energies together with the corresponding conventional (E_c) and density-functional theory (E_c^{DFT}) correlation energies . That these empirical

Table I.

Empirically determined conventional (E_c) and density-functional theory (E_c^{DFT}) correlation energies in Rydbergs of atoms with atomic number $Z=2-18$. The non-relativistic ground state energy E^{nr} determined as described in the text, as well as the Hartree-Fock E^{HF} and exchange-only E^{XO} energies are also quoted. Theoretically determined values of E^{nr} for He, Li and Be are given in parentheses.

| ATOM | Atomic Number | Total Energies (Ryd) | | | Correlation Energies (Ryd) | |
|------|---------------|-------------------------------------|---------------------|---------------------|----------------------------|---------------------------|
| | | Non-Relativistic | Hartree-Fock | Exchange-only | Conventional | Density-Functional Theory |
| | Z | $-E^{\text{nr}}$ | $-E^{\text{HF(a)}}$ | $-E^{\text{XO(b)}}$ | $-E_c$ | $-E_c^{\text{DFT}}$ |
| He | 2 | 5.8068 (5.8077) ^(c) | 5.7234 | 5.7234 | 0.0834 | 0.0834 |
| Li | 3 | 14.9554 (14.9561) ^(d) | 14.8655 | 14.8648 | 0.0899 | 0.0906 |
| Be | 4 | 29.3332 (29.3347) ^(e) | 29.1460 | 29.1448 | 0.1872 | 0.1884 |
| B | 5 | 49.3058 | 49.0581 | 49.0555 | 0.2477 | 0.2503 |
| C | 6 | 75.6864 | 75.3772 | 75.3730 | 0.3092 | 0.3134 |
| N | 7 | 109.1732 | 108.8019 | 108.7964 | 0.3712 | 0.3768 |
| O | 8 | 150.1278 | 149.6188 | 149.6149 | 0.5090 | 0.5129 |
| F | 9 | 199.4568 | 198.8187 | 198.8157 | 0.6381 | 0.6411 |

Table I. (continued)

| ATOM | Atomic Number | Total Energies (Ryd) | | | Correlation Energies (Ryd) | |
|------|------------------|----------------------|------------------|-------------------|----------------------------|-------------------------------|
| | | Non- Relativistic | Hartree- Fock | Exchange- only | Conventional | Density- Functional Theory |
| | Z | $-E^{nr}$ | $-E^{HF(a)}$ | $-E^{XO(b)}$ | $-E_c$ | $-E_c^{DFT}$ |
| Ne | 10 | 257.852 | 257.0942 | 257.0910 | 0.758 | 0.761 |
| Na | 11 | 324.478 | 323.7178 | 323.7119 | 0.760 | 0.766 |
| Mg | 12 | 400.058 | 399.2293 | 399.2223 | 0.829 | 0.836 |
| Al | 13 | 484.620 | 483.7514 | 483.7462 | 0.869 | 0.874 |
| Si | 14 | 578.616 | 577.7087 | 577.7008 | 0.907 | 0.915 |
| P | 15 | 682.370 | 681.4376 | 681.4264 | 0.932 | 0.944 |
| S | 16 | 796.044 | 795.0098 | 794.9998 | 1.034 | 1.044 |
| Cl | 17 | 920.108 | 918.9641 | 918.9569 | 1.144 | 1.151 |
| Ar | 18 | 1054.844 | 1053.635 | 1053.623 | 1.209 | 1.221 |

(a) See Ref. (13)

(b) See Ref. (14)

(c) See Ref. (15)

(d) See Ref. (16)

(e) See Ref. (17)

values for the conventional correlation energy are accurate is substantiated by the results of many-parameter correlated wavefunction calculations¹⁵⁻¹⁷ for the ground state energies of He , Li and Be . These theoretically determined numbers are quoted in parentheses below the corresponding empirically determined values in the Table, and the two sets of numbers may be observed to be essentially the same . A study of the Table indicates that the conventional correlation energy is consistently larger than the density-functional theory value, their difference being $\leq 1\%$ of the former. This is , of course, due to the fact that the exchange-only results for the energy lie only slightly above those of Hartree-Fock . The orbitals as well as the constituent exchange and kinetic energies¹⁸ also closely approximate each other . That an optimized local effective potential reproduces in essence the solutions derived from a non-local potential is quite remarkable. We are unaware of any theorem that proves this must be the case . Finally, although the correlation energy increases in magnitude with electron number , as it must , the fraction it is of the exchange energy diminishes . For He,Be,Ne and Ar , the correlation energy is 4.1% , 3.5% , 3.1% and 2.4% of the density-functional theory exchange energy .

1.1.1.3 Metallic Surfaces

The problem of the inhomogeneous electron gas at metallic surfaces has proved to be far more complex. As a consequence of the fact that at present no reliable experimental numbers exist for the surface energy of simple metals, our understanding is entirely theoretical. As in the atomic physics case, there has been both a density-functional theory as well as a quantum-mechanical correlated-wavefunction approach to the surface problem. Within the context of the former theory our ideas on the separate contributions of exchange and correlation to the surface energy of jellium metal are based on calculations performed for the infinite barrier model^{19,20} of a surface. For these orbitals the 'exact' (within the random phase approximation (RPA)) surface exchange-correlation energy^{21,22} $\sigma_{xc}[\rho]$, as well as the exact (density-functional theory) surface exchange energy^{23-25,18} $\sigma_x[\rho]$ are known. (The superscript DFT will no longer be used with symbols for the surface properties since the majority of the calculations to be discussed and presented in this thesis are performed within density-functional theory). These results are quoted in Table II for the metallic range of densities. The exact exchange energy column is given¹⁸ by $(0.576/k_F^{-3})(10^{-3} \text{ a.u.})$. In the last column of the Table we give the ratio of the correlation to exchange as a percentage, and observe that the two contributions are equivalent. This indicates that

Table II.

The surface exchange , correlation , and exchange-correlation energies in ergs/cm² as a function of Wigner-Seitz radius r_s (in a.u.) for the infinite barrier model densities . The results quoted are those in the local density (LDA) and gradient expansion (GEA) approximations . The exchange energies are the exact non-local values, whereas the 'exact' exchange-correlation (and correlation) energies are the RPA results of Wikborg and Inglesfield²¹ as modified by Langreth and Perdew²² . For the LDA correlation energy we have employed the Ceperley-Alder⁷ values of the average correlation energy per particle . The quantities in parentheses in the LDA correlation energy column are those obtained using the Wigner⁵¹ expression . The GEA exchange-correlation (and correlation) energy results are determined using the Langreth-Perdew⁴¹ coefficient for the first gradient correction.

| Wigner-Seitz Radius \bar{r}_s (a.u.) | SURFACE ENERGIES (ergs/cm ²) | | | | | | | | | $\left(\frac{\text{Correlation}}{\text{Exchange}}\right) \times$ "EXACT" (RPA) |
|---|--|------|-------|-------------|------|------------------|----------------------|------|------------------|--|
| | Exchange | | | Correlation | | | Exchange-Correlation | | | |
| | LDA | GEA | EXACT | LDA | GEA | "EXACT" (RPA) | LDA | GEA | "EXACT" (RPA) | |
| 2.07 | 1110 | -392 | 715 | 118 (65) | 3542 | 675 | 1228 | 3150 | 1390 | 94 |
| 4.0 | 154 | -54 | 99 | 26 (22) | 450 | 104 | 180 | 396 | 203 | 105 |
| 6.0 | 46 | -16 | 29 | 10 (10) | 129 | 34 | 56 | 113 | 63 | 117 |

for surfaces, correlation plays as significant a role as does exchange, a result which is entirely different from the atomic and homogeneous electron gas systems discussed above. Certainly this result is reasonable and to be expected for lower density metals, but that it is the case for the higher density metals appears intuitively to be incorrect. Of course, it must be emphasized that these values are derived for the infinite barrier model which is a rather poor representation^{26,27} of a metal surface .

No RPA calculation of $E_{xc}[\rho]$ along the lines of Wikborg and Inglesfield²² for accurate metal surface densities exists although one is presently being attempted by Qian and Kohn²⁸ . However, rigorous upper bounds to the surface energy in the exchange-only

approximation (with non-local exchange) have been determined by Sahni and Ma²⁹ for wavefunctions generated by the linear-potential model^{30,31} of a metal surface . Thus we do have an accurate estimate of the DFT exchange contribution to the surface energy of jellium metal. A quantum-mechanical correlated wavefunction calculation of the surface energy has recently been performed by Woo and collaborators³² . However, various approximations are made in their work and it is only the kinetic energy that has been treated exactly . A self-consistent Hartree-Fock solution for the surface physics problem also does not

exist, although Bardeen¹⁹ did attempt such a calculation with many simplifying approximations^{19,29}.

1.2 Local Density and Gradient Expansion Approximations .

Within density-functional theory the most commonly employed approximation for the exchange (x), correlation (c), exchange-correlation (xc) and screened-exchange (sx) energies is the so-called local density approximation (LDA) according to which the energy density is treated as a function of the local value of the density. Thus, in this approximation,

$$E_i^{\text{LDA}}[\rho] = \int A_i\{\rho(\mathbf{r})\} d\mathbf{r} \quad (20)$$

where $i=x, c, xc$ or sx respectively. The LDA coefficient³ $A_i\{\rho(\mathbf{r})\}=\rho(\mathbf{r})\varepsilon_i\{\rho(\mathbf{r})\}$ where the ε_i are the corresponding average energies per electron of a homogeneous electron gas of density $\rho(\mathbf{r})$. By exchange-correlation we mean the sum of the exchange and correlation energies, and by screened-exchange the exchange energy obtained for the screened-Coulomb interaction of the Yukawa form:

$$u(\mathbf{r}-\mathbf{r}')=e^2 \frac{e^{-k_s|\mathbf{r}-\mathbf{r}'|}}{|\mathbf{r}-\mathbf{r}'|}, \quad (21)$$

where k_s is the screening parameter . The coefficients A_x and A_{sx} are known^{2,33-35} exactly for all densities, whereas A_c is known³⁶ for high densities but must be approximated for metallic and lower densities^{33,37} . Thus the LDA is exact in the limit of very slowly varying densities and should be accurate for densities which do not change appreciably over a Fermi or screening wavelength.

For the case where the density $\rho(\mathbf{r})$ varies slowly over distances such as the Fermi wavelength or screening length, Hohenberg and Kohn² have also suggested non-local corrections to the LDA term of Eq. (20) in the form of an expansion in gradients of the density. In this gradient expansion approximation (GEA) , the correction to the LDA to $O(\nabla^2)$ is of the form

$$\Delta E_i^{\text{GEA}} = \int B_i\{\rho(\mathbf{r})\} |\nabla\rho(\mathbf{r})|^2 d\mathbf{r} = \int C_i\{\rho(\mathbf{r})\} \frac{|\nabla\rho(\mathbf{r})|^2}{\rho^{4/3}(\mathbf{r})} d\mathbf{r} . \quad (22)$$

The coefficients B_i of this expansion can be shown to be related to the q^2 coefficient in the expansion of the reciprocal of the static density response function in powers of the wave-vector q .

Until the recent work of Sahni et al¹⁸ it was assumed that a GEA for the exchange (and hence correlation) energy did not exist and that

consequently such an expansion was mathematically valid only when exchange and correlation were considered together. This assumption was based on the work of Kleinman³⁸ and Geldart et al³⁹ who showed that for Hartree-Fock theory orbitals the coefficient B_x was singular. However, the expansion of Eq. (22) is intrinsically an expansion within the rubric of density-functional theory and what Sahni et al¹⁸ showed was that such an expansion exists for the exchange energy provided one employs density-functional theory orbitals i.e. solutions of Eq.(18). The critical difference between the two sets of orbitals is that one is derived from a non-local potential whereas the other is obtained from an effective potential which is local. The density-functional theory coefficient B_x was originally derived by Sham⁴⁰ and has been rederived recently by Langreth and Perdew⁴¹ by a wave vector analysis method. As a consequence of the fact that a density-functional theory GEA exists for the exchange energy, such an expansion must also exist for the case of the screened-Coulomb exchange energy. One of the calculations performed in this thesis is the derivation of the coefficient B_{sx}^{DFT} . Within Hartree-Fock theory (HFT), a GEA for the screened-Coulomb exchange energy is also well defined, and the corresponding coefficient B_{sx}^{HFT} is known^{38,42}. There are several calculations^{41,43-45} of the coefficient B_{xc} for metallic densities, and a value for B_c has been determined⁴⁶ in the high density limit.

In the next few subsections , we survey the existing results of the LDA and GEA for the exchange , correlation and exchange-correlation energies as applied to atoms and metallic surfaces.

1.2.1 Local Density Approximation for the Exchange , Correlation and Exchange-Correlation Energies.

1.2.1.1 Atoms

For the atoms considered in Table I , the errors in the LDA exchange energies are¹⁸ -13.6% , -8.8% and -7.5% for He,Ne and Ar respectively when compared with the exact exchange-only results. On the other hand, the magnitude of the LDA correlation energies are overestimated^{47,37} by 100-200% . This considerable overestimate has been attributed⁴⁸ principally to the fact that the expression used in Eq.(20) are derived for the infinite electron gas system which has a continuous energy spectrum, whereas the spectrum of the finite atomic system is discrete . Furthermore, the electron densities vary rapidly near the nuclei of atoms . However, the LDA exchange-correlation energy errors⁴⁹ for He,Li and Be are only 8.7% , 8.8% and 9.2% respectively when compared with exact results⁴⁹ for $E_{xc}[\rho]$. These exact values are obtained by a procedure whereby the Kohn-Sham potential v_{xc} and eigenvalues ϵ_i are first determined using the correlated wavefunctions of Refs. (15) , (16) and (17) . Then with

the exact ground state energy being known (via these correlated wavefunctions) , the exchange-correlation energy is obtained by substitution into Eq.(14).

1.2.1.2 Metallic Surfaces

The LDA surface exchange and correlation energies⁵⁰ for the infinite barrier model densities are also given in Table II. We have rederived the latter using a parameterization³⁷ of the Ceperley-Alder⁷ results for ϵ_c . In comparison with the exact results , the exchange energy which in the LDA is given¹⁸ by $(0.8939)/k_F^{-3}(10^{-3} \text{ a.u.})$ is an overestimate by 55% whereas the correlation energy is underestimated by a fifth to a third of the 'true' value . However, their sum, as in the case of the light atoms, is within 10% of the the 'exact' RPA results. The cancellation of these errors in local exchange and correlation as demonstrated by this model calculation has been the principle justification for the use of this approximation in surface physics calculations. (In the LDA correlation energy column we also give the values obtained⁵⁰ by using the Wigner⁵¹ expression for the average correlation energy per particle . Note that for the higher density metals, these LDA values are considerably different).

We observe that although in both atoms and metallic surfaces the density varies rapidly over the appropriate length scales, the LDA still

leads to fairly accurate results. There have been different explanations of this fact in the literature^{50,52,53}. We present here an argument due to Lang and Sham⁵⁰ which is relevant to the present work.

1.2.2 The Lang-Sham Argument

The argument for the de facto accuracy of the LDA for the exchange-correlation energy due to Lang and Sham⁵⁰ has been made with reference to the metallic surface. It is based on the work by Kleinman³⁸ and Geldart et al³⁹ who showed that for Hartree-Fock orbitals, a series in the gradients of the density does not exist for the bare-Coulomb exchange energy due to a divergence in the first gradient correction term. Consequently, they concluded that neither does such an expansion exist for the correlation energy. However, according to them, an expansion does exist when exchange and correlation are considered together since the singularities in the expansions for the exchange and correlation cancel. Lang and Sham⁵⁰ calculated the LDA values for the surface exchange and correlation energies within the infinite barrier model (see Table II) using the Wigner⁵¹ expression for the average correlation energy per particle. As discussed in the previous section, the LDA values differ substantially from the "exact" results when considered individually but are within 10% of them when taken together. The large discrepancies in the individual LDA terms for the exchange and correlation energies were attributed to the

assumed fact that the gradient correction had to be large since the individual series diverged . But when exchange and correlation treated locally were taken together the results were accurate because the singularities in the gradient series for each of these properties cancelled. Thus the justification for the accuracy of the LDA was based on the existence of a power series expansion in the gradients of the density. Furthermore, it is implicitly assumed in this argument that the contribution of the first gradient correction terms is small.

Further support for this argument was provided by a similar calculation by Lang and Sham⁵⁰ for the surface exchange energy assuming a screened-Coulomb interaction . Now when correlation effects are included by screening the exchange, it has also been shown by Kleinman³⁸ and Geldart et al³⁹ , as stated earlier, that a GEA exists within Hartree-Fock theory (HFT). The results of the Lang and Sham⁵⁰ calculations which were again performed for the infinite barrier model densities , indicated that the LDA was good for finite and large screening but poor for weak screening for which the interaction more closely approximated the bare-Coulomb interaction . Thus again, the existence of a GEA for screened exchange was used to justify the accuracy of the LDA .

The above argument is , however, incorrect since as indicated earlier Sahni et al¹⁸ have shown that within the density-functional theory context i.e. for orbitals derived from local effective potential, a gradient expansion does exist for the bare-Coulomb exchange energy, and thus consequently also for the correlation energy. Thus the fact that the individual LDA exchange and correlation energies are poor cannot be attributed to the lack of existence of a gradient expansion for these properties.

A second drawback of the Lang and Sham⁵⁰ argument has to do with their screened-Coulomb exchange energy calculation. They showed that the LDA was good and that it converged as a function of the screening parameter k_s for the fixed infinite barrier model density profile. Thus, it was the Hamiltonian, or equivalently, the energy functional of the interacting system which was being varied in their calculations. However, in any test of the convergence of an approximation in which the density is the intrinsic variable, it is the Hamiltonian that must be kept fixed and the density profile which must be varied.

1.2.3 Gradient Expansion Approximation for the Exchange , Correlation and Exchange-Correlation Energies.

1.2.3.1 Atoms

The only GEA correlation energy results available are those of Ma and Brueckner⁴⁶ who using the high density (constant) coefficient B_c and Hartree-Fock densities have shown that for atoms (O,Ne,Na,Ar and K) the contribution of the correction term (Eq.(22)) is too large by a factor of about five. On the other hand, the GEA for exchange as applied¹⁸ to atoms is a marked improvement over the LDA , but again the errors for the atoms considered in Table I range from 5-3% .

1.2.3.2 Metallic Surfaces

For physical density profiles at metallic surfaces the GEA for the exchange energy has been shown¹⁸ to be particularly accurate. In fact , within the exchange-only approximation, this expansion reproduces⁵⁴ the results of a calculation of the surface energy in which the non-local exchange energy is treated exactly²⁹ .

As we mentioned before, there are many different calculations^{41,43-45} of the coefficient B_{xc} for metallic densities. The results of these calculations all differ and consequently so do the surface energies obtained within this approximation. Whether the

addition of the gradient correction term for the exchange-correlation energy improves the surface energy (and through it the density and other properties), cannot be answered by comparison with experiment due to the uncertainties in the experimental values. One must thus rely strictly on a theoretical basis for determining whether the GEA for exchange-correlation is appropriate or not. One such analysis has been given by Perdew, Langreth and Sahni⁵⁵ who employing the wave-vector formalism show that the GEA leads to overestimates for surface energy. More recent work by Langreth and Perdew⁴¹ supports this conclusion. The opposite conclusion that the GEA is in fact accurate for surface energy calculations was arrived at by Rasolt and co-workers^{42,56} who studied the expansion for the screened-Coulomb interaction. An improvement in the convergence of the GEA over the LDA was observed, and this fact was used to argue indirectly the merits of the GEA for exchange-correlation as applied to metallic surfaces. However, as in the work of Lang and Sham⁵⁰ discussed above, these authors also demonstrated the convergence of the GEA as a function of the screening parameter and not as a function of the density profile or its gradients.

1.3 Thesis Outline

In this thesis we are concerned principally with the study of correlation effects at metallic surfaces, the studies performed being

within the context of density-functional theory . In section II.1 we define a jellium metal surface and the various surface properties which are employed in this work . We begin our study of the correlation effects at surfaces in section II.2 by assuming for the non-uniform electron gas a screened-Coulomb interaction. We first derive in this section exact results for the screened surface exchange energy as a function of the screening length for orbitals obtained from the step-potential model^{26,27,19} of a surface. We then study the effects of screening the exchange on the total surface energy.

Employing these exact results we then re-examine the arguments of Lang-Sham⁵⁰ and Rasolt et al⁵⁶ for the accuracy of the local density and gradient expansion approximations respectively, as applied to surfaces. In section III.1 we study the convergence of both these approximations for the screened-Coulomb exchange energy as a function of the density profile within Hartree-Fock theory . In order to study the convergence properties of the corresponding GEA in density-functional theory we first derive by the method of Sham⁴⁰ (See Appendix A for details) the first gradient correction term coefficient $B_{s x}^{\text{DFT}}$. In section III.2 we compare the density-functional theory and Hartree-Fock theory coefficients $B_{s x}^{\text{DFT}}$ and $B_{s x}^{\text{HFT}}$ respectively, and then perform a convergence study of the GEA for screened-Coulomb exchange energy in density-functional theory. The results of these

convergence studies are surprising and quite contrary to intuitive expectations of a short-ranged interaction .

As discussed previously , both for atoms and metal surfaces, the LDA for exchange-correlation is in error by approximately 10% . In order to eliminate this error, there has recently been a considerable amount of work^{41,43-45,52,53,57} on the development of non-local corrections to it . For the non uniform electron gas at metallic surfaces, the most accurate of these approximate corrections, in our opinion (with a discussion of the justification to be given later), is that obtained by the wave-vector method of Langreth and Perdew^{22,58} . In section IV.1, we employ their method in conjunction with realistic jellium metal surface densities^{30,31} to accurately estimate the (density-functional theory) surface correlation energy . In our calculations we treat the non-local exchange energy contributions exactly . These are the first realistic estimates of this property, and the results are far more physically reasonable than those obtained for the infinite barrier model. We then make comparisons with the results of existing correlated wavefunction calculations . In this section we also examine the LDA for the surface exchange and correlation energies separately in order to determine whether the cancellation of errors observed for the infinite barrier model is fortuitous or whether in fact such a cancellation does occur even for the more realistic density profiles.

Since it has now been established¹⁸ that a gradient expansion exists for the exchange and correlation energies separately, it is thus possible to study the convergence properties of the GEA for the surface correlation energy. As indicated earlier, the GEA for exchange as applied to surfaces^{18,54} is particularly accurate in reproducing the results of an exact non-local exchange energy calculation²⁹. Consequently, for surfaces, and to a lesser degree for atoms, the severe convergence criteria that have been derived^{41,53} for the exchange-correlation energy GEA must be criteria that the correlation energy GEA must satisfy. Employing the same method of estimating the surface correlation energy as described in section IV.1, we study in section IV.2 the convergence properties of both the local density and gradient expansion approximations for this property. In this section we also study a modified gradient expansion approximation for the correlation energy derived recently by Langreth and Mehl⁵³.

Finally, in chapter V we summarize our conclusions, and make suggestions for future work which would help in better understanding some of the present results and the conclusions of the others.

Chapter II

2.1 Definitions of Jellium Metal Surface Properties

In this section we present the definitions of the electron density, potential, work function and surface energy as applied to the jellium model of a metal surface . In this model the positive ions are assumed to be replaced by a uniform semi-infinite charge background of density $\rho_+(x) = k_F^3 / 3\pi^2 \theta(-x+a)$ ending abruptly at the metal surface position 'a' . Because of the reduction in symmetry in this problem , the Hamiltonian of the system is different inside and outside the metal surface , and therefore the electron momentum perpendicular to the surface is no longer a good quantum number. However, since jellium metal has no structure parallel to the surface, the momentum parallel to the surface is a good quantum number. Consequently, the electronic wave function can be written as

$$\Psi_{\mathbf{k}}(\mathbf{r}) = \left[\frac{1}{A}\right]^{\frac{1}{2}} \Psi_{\mathbf{k}}(x) \exp(i\mathbf{k}_{11} \cdot \mathbf{x}_{11}) , \quad (23)$$

where \mathbf{k}_{11} and \mathbf{x}_{11} are respectively the projections of the momentum \mathbf{k} and position \mathbf{r} of the electron on the surface plane, k and x are the corresponding quantities measured along the surface normal, and A is the cross-sectional area . The translational invariance in the direction parallel to the surface thus reduces the complex three-dimensional

calculation to one which is one-dimensional. Away from the surface region deep in the bulk, the wave function has the asymptotic form

$$\Psi_k(x) \xrightarrow{x \rightarrow -\infty} \sin[kx + \delta(k)], \quad (24)$$

where $\delta(k)$, the asymptotic phase shift, is a continuous function of k .

The electron density, which spreads into the vacuum in order to lower its kinetic energy, is defined as

$$\rho(x) = (L/2\pi^2) \int_0^{\bar{k}_F} (\bar{k}_F^2 - k^2) |\Psi_k(x)|^2 dk, \quad (25)$$

where for purposes of normalization we have assumed a crystal of length L where L is large. The electron density vanishes far into the vacuum, and approaches its bulk value ρ deep in the bulk. Inside at the crystal surface, the density exhibits the requisite Friedel oscillations. The total charge density $\rho_T(x)$ which is then

$$\rho_T(x) = \rho(x) - \rho_+(x), \quad (26)$$

must satisfy the charge neutrality condition for the system which is

$$\int_{-\infty}^{\infty} \rho_T(x) dx = 0. \quad (27)$$

It has been shown⁵⁹ that this charge neutrality condition is equivalent to a phase shift sum rule due to Sugiyama⁶⁰ according to which the

weighted Fermi surface average of the asymptotic phase shift $\delta(k)$ of the electronic wave function must equal $-\pi/4$:

$$\int_0^{\bar{k}_F} k \delta(k) dk / \int_0^{\bar{k}_F} k dk = -\pi/4 . \quad (28)$$

The jellium edge position 'a' may be determined either by the charge neutrality condition or by employing the Sugiyama sum rule. Application of the latter condition leads to a simple expression for the jellium edge position in terms of the asymptotic phase shift $\delta(k)$ which is

$$a = -3\pi/8\bar{k}_F - 3/\bar{k}_F^3 \int_0^{\bar{k}_F} k \delta(k) dk . \quad (29)$$

Due to the fact that the electronic density decays into the vacuum well beyond the jellium edge, a double layer is formed in the region about the surface. An electron trying to escape from the metal will thus experience a dipole barrier of height

$$\Delta\phi = 4\pi \int_{-\infty}^{\infty} x \rho_T(x) dx = V_{es}(\infty) - V_{es}(-\infty) , \quad (30)$$

where $V_{es}(x)$ is the electrostatic potential due to the total charge distribution of the system , and is determined as the solution to Poisson's equation

$$d^2V_{es}/dx^2 = -4\pi \rho_T(x) . \quad (31)$$

With the choice of boundary conditions $V_{es}(-\infty)=V'_{es}(-\infty)=0$, together with the charge neutrality condition; this solution may be written as

$$V_{es}(x) = \Delta\phi - 4\pi \int_{-\infty}^x dx' \int_{-\infty}^{x'} dx'' \rho_T(x''). \quad (32)$$

The contributions to the effective potential $V_{eff}(x)$, other than the electrostatic potential $V_{es}(x)$, are due to exchange and correlation effects (See Eq. 11) . In the deep interior of the metal where the electron density is uniform,

$$V_{eff}(x) \longrightarrow V_{es}(-\infty) + v_{xc}(\rho) \quad (33)$$

where $v_{xc}(\rho) = d[\rho\varepsilon_{xc}(\rho)]/d\rho$ since $E_{xc}[\rho]$ is known for the homogeneous electron gas system. Very far outside the surface, exchange and correlation effects are insignificant so that

$$V_{eff}(x \rightarrow \infty) = V_{es}(\infty) . \quad (34)$$

In the intermediate region it is not possible to give an explicit expression for $V_{eff}(x)$ since the functional $E_{xc}[\rho(x)]$ is unknown. Both from electrostatics and by a study⁶¹ of the mass operator of a Fermi-level electron in a bounded electron gas we know that well outside the surface but short of where Eq. (34) is appropriate, the effective potential is of the image form . i.e.

$$V_{eff}(x) \underset{\sim}{=} V_{es}(\infty) - 1/4x \quad (35)$$

in this region. More recently Sahni and Bohnen^{62,63} have shown that the image potential at a metal surface is strictly due to correlation effects and that exchange plays a role only when the electron is at and near the surface .

The work function ϕ which is the energy required to remove a Fermi electron to infinity may then be written as

$$\phi = [V_{\text{eff}}(+\infty) - V_{\text{eff}}(-\infty)] - \frac{1}{2}k_F^{-2} \quad (36)$$

or equivalently as

$$\phi = \Delta\phi - \frac{1}{2}k_F^{-2} - v_{\text{xc}}(\rho),$$

where $\frac{1}{2}k_F^{-2}$ is Fermi energy.

The surface energy of a metal σ_s is defined²⁰ as the energy required per unit area of new surface formed, to split the crystal in two along a plane . We consider a crystal all of whose dimensions are macroscopic, and take the two fragments into which the crystal is split to be identical . Let A be the area of the newly exposed face on each fragment . Let $\rho(\mathbf{r})$ be the electron density distribution for the fragment and $\rho'(\mathbf{r})$ be that the unsplit crystal . Then, the surface kinetic , σ_k , electrostatic, σ_{es} , and exchange-correlation , σ_{xc} , energies may be written as

$$\sigma_k = (2A)^{-1} [2E_k[\rho] - E_k[\rho']] , \quad (37)$$

$$\sigma_{es} = (2A)^{-1} [2E_{es}[\rho] - E_{es}[\rho']] , \quad (38)$$

and

$$\sigma_{xc} = (2A)^{-1} [2E_{xc}[\rho] - E_{xc}[\rho']] . \quad (39)$$

The total surface energy σ_s is then the sum of these terms.

Since the electrostatic energy in the charge neutral unsplit crystal is zero, we can write an explicit expression for the electrostatic contribution to the surface energy as

$$\sigma_{es}[\rho] = \frac{1}{2} \int_{-\infty}^{\infty} \rho_T(x) V_{es}(x) dx . \quad (40)$$

On the other hand due to the fact $E_{xc}[\rho]$ is unknown, it is not possible to write exact expressions for either $\sigma_k[\rho]$ (See Eqs. (11) and (13)) or $\sigma_{xc}[\rho]$. However, it is possible to write an expression for $\sigma_k[\rho]$ in term of $V_{eff}(x)$ and the asymptotic phase shift $\delta(k)$ which is^{20,30,60}

$$\begin{aligned} \sigma_k[\rho] = & (\bar{k}_F^{-4}/160\pi) \left\{ 1 + \frac{80}{\bar{k}_F^4} \left[\frac{3}{5} \bar{k}_F^{-2} \int_0^{\bar{k}_F} k \delta(k) dk - \int_0^{\bar{k}_F} k^3 \delta(k) dk \right] \right\} \\ & - \int_{-\infty}^{\infty} \{ V_{eff}[\rho;x] - V_{eff}[\rho;-\infty] \} \rho(x) dx . \end{aligned} \quad (41)$$

As mentioned in the introduction, we believe the most accurate method for the determination of the surface exchange-correlation energy $\sigma_{xc}[\rho]$ is the wave-vector (WV) analysis method to be discussed in section IV.1 . In this formalism we write $\sigma_{xc}[\rho]$ as

$$\sigma_{xc}^{WV}[\rho] = \sigma_{xc}^{LDA} + \Delta\sigma_{xc}^{WV} \quad (42)$$

where σ_{xc}^{LDA} is the local density approximation value given by the expression

$$\sigma_{xc}^{LDA} = \int_{-\infty}^{\infty} [\varepsilon_{xc}\{\rho(x)\} - \varepsilon_{xc}(\rho)] \rho(x) dx \quad (43)$$

and $\Delta\sigma_{xc}^{WV}$ is the non-local correction to it obtained by the wave-vector method. The non-local gradient expansion approximation correction to the LDA is, of course, given by the expression of Eq.(22). In all our calculations of the LDA surface correlation energy we employ for the average correlation energy per particle ε_c the Perdew-Zunger³⁷ parameterization of the many-parameter Monte-Carlo calculations of Ceperley and Alder⁷. The expression employed is

$$\varepsilon_c^{CA} = \frac{\gamma}{1 + \beta_1 \sqrt{\bar{r}_s} + \beta_2 \bar{r}_s} \quad (44)$$

where $\gamma = -0.1423$ $\beta_1 = 1.0529$ $\beta_2 = 0.3334$

In the surface physics literature, however, the most commonly used expression for ε_c is the Wigner⁵¹ interpolation formula which is $\varepsilon_c = -0.44/(\bar{r}_s(\bar{\rho})+7.8)$. The Ceperley-Alder values are, of course, more accurate and, as indicated in the introduction, lead to substantially different results for the LDA surface correlation energy of high density metals (See Table II).

2.2 Exact Surface Exchange Energy for Screened-Coulomb Interaction⁶⁴

In this section we study⁶⁴ the effects of correlation at surfaces by considering the exchange energy for the screened-Coulomb interaction. The exchange energy functional for any arbitrary interaction is known, and consequently one can determine (at least in principle) the surface exchange energy exactly. In order to demonstrate the explicit dependence of the exchange energy on the density $\rho(\mathbf{r})$ we rewrite Eq. (16) as

$$E_x[\rho] = \frac{1}{2}e^2 \iint d\mathbf{r}d\mathbf{r}' u(\mathbf{r}-\mathbf{r}') \rho(\mathbf{r}) \rho_x(\mathbf{r}, \mathbf{r}') , \quad (45)$$

where $\rho_x(\mathbf{r}, \mathbf{r}')$ is the exchange hole density defined in terms of the electronic wavefunctions $\Psi_{\mathbf{k}}(\mathbf{r})$ of momentum \mathbf{k} as

$$\rho(\mathbf{r}) \rho_x(\mathbf{r}, \mathbf{r}') = - \sum_{\mathbf{k}} \sum_{\mathbf{k}'} \Psi_{\mathbf{k}}^*(\mathbf{r}) \Psi_{\mathbf{k}'}^*(\mathbf{r}') \Psi_{\mathbf{k}}(\mathbf{r}') \Psi_{\mathbf{k}'}(\mathbf{r}) , \quad (46)$$

and where $u(\mathbf{r}-\mathbf{r}')$ is the Yukawa interaction of Eq. (21). The orbitals $\Psi_{\mathbf{k}}(\mathbf{r})$ are the solutions of the Kohn-Sham exchange only equations Eq. (18). For the jellium metal surface problem it has not been possible to solve these equations. Consequently we resort to the use of a non-self consistently determined wavefunction in order to calculate the surface exchange energy. The wavefunctions we employ are those generated by the step-potential model^{26,27,19} of a surface. These wavefunctions

satisfy all the constraints on the density discussed in the previous section. Our choice of these wavefunctions rather than the more accurate wavefunctions generated by the linear-potential model^{30,31} was governed by the following considerations. First, since we are dealing with a short-ranged interaction, we believe the step-potential wavefunctions to be adequate to demonstrate the general trends of any effects that might arise due to the nature of this interaction. Secondly, the arguments of Rasolt et al^{42,56} for the accuracy of the GEA for exchange-correlation are based on the use of these wavefunctions. Our calculations thus enable a meaningful evaluation of their arguments and conclusions. (See chap. III).

For the step-potential model^{26,27,19} of a surface the effective potential $V_{\text{eff}}(x)$ is defined as

$$V_{\text{eff}}(x) = W \theta(x) , \quad (47)$$

where W is the barrier height, and $\theta(x)$ the step function. With the assumption of translational invariance in the plane parallel to the surface (the jellium model approximation), the electronic wavefunctions generated by solution of the Schrodinger equation are

$$\psi_{\mathbf{k}}(\mathbf{x}) = \sqrt{\frac{2}{L}} \left\{ \sin[kx + \delta(k)]\theta(-x) + \frac{k}{h} \exp[-(h^2 - k^2)^{\frac{1}{2}}] \theta(x) \right\} . \quad (48)$$

where the phase shift $\delta(k) = \sin^{-1}(k/h)$ and $h^2=2W$. The range of density variation in the step-potential model is described by the density profile parameter $\beta=\bar{k}_F/h$. The case $\beta=0$ is the infinite barrier model, whereas $\beta=1$ corresponds to the case where the Fermi level is at the barrier height.

The exchange energy of Eq. (45) is the sum of bulk $E_{x,b}$ and surface σ_x contributions

$$E_x = \Omega E_{x,b} + A\sigma_x , \quad (49)$$

where Ω is the crystal volume and A the area of a crystal face . Using the method of Ma and Sahni²⁹ , and the wavefunctions of Eq. (48), we have⁶⁴ recalculated⁵⁶ the exact non-local surface exchange energy σ_{sx} assuming a screened-Coulomb interaction between the particles. The semi-analytical expression for σ_{sx} may be written⁶⁴ as a universal function of the density profile parameter β for specific screening defined by the parameter $\gamma = k_s/\bar{k}_F$. The expression is thus also a universal function of γ for fixed β . The case²⁹ $\gamma = 0$ corresponds to the bare-Coulomb interaction. The bulk exchange energy for the screened-Coulomb interaction $E_{sx,b}$ is also a universal function³⁵ of the screening parameter γ . The surface kinetic σ_k and electrostatic σ_{es} energies in this model can also be written²⁷ in terms of universal functions of the density profile parameter β . These properties are

independent of the type of interaction and are thus independent of the parameter γ . We present below the analytical and semi-analytical expressions for the universal functions involving the total charge density $\rho_T(x)$, the electrostatic potential $V_{es}(x)$, the kinetic energy σ_k , the bulk exchange energy $E_{sx,b}$, and the surface exchange energy σ_{sx} . The expression for σ_{sx} is given in terms of the infinite barrier model expression σ_{sx}^{IBM} .

Total Charge Density²⁷

$$\frac{\rho_T(z)}{\bar{k}_F^3} = \begin{cases} (\beta^2/\pi) \int_0^1 (1-q^2)q^2 \exp[-\beta^{-1}(1-\beta^2q^2)^{\frac{1}{2}} z] dq, & \text{for } z \geq 0 \\ (1/\pi) \int_0^1 (1-q^2) \sin^2[\frac{1}{2}zq - \gamma(q)] dq - (1/3\pi^3)\theta(-z-z_a), & \text{for } z \leq 0 \end{cases} \quad (50)$$

Electrostatic Potential²⁷

$$\frac{V_{es}(z)}{\bar{k}_F} = \begin{cases} -\frac{\beta^4}{\pi} \int_0^1 \frac{(1-q^2)q^2}{1-\beta^2q^2} \exp[-\beta^{-1}(1-\beta^2q^2)^{\frac{1}{2}} z] dq + \frac{\Delta\phi}{\bar{k}_F}, & \text{for } z \geq 0 \\ \frac{\beta^2}{\pi} \int_0^1 (1-q^2) \left(\frac{1-2\beta^2q^2}{2\beta^2q^2} (1-\cos zq) - \frac{(1-\beta^2q^2)^{\frac{1}{2}}}{\beta q} \sin zq \right) dq \\ + \frac{1}{\pi} \left[-\frac{1}{6} (z+z_a)^2 \theta(z+z_a) + 1 + \frac{2}{3}\beta^2 - \frac{1}{2}\beta\pi + \frac{1}{4}z\pi \right], & \text{for } z \leq 0, \end{cases} \quad (51)$$

where $z=2\bar{k}_F x$, $z_a=2\bar{k}_F a$, and where the surface dipole barrier $\Delta\phi$ is

given²⁶ as

$$\frac{\Delta\phi}{k_F} = \frac{1}{\pi} \left(2 - \frac{2}{3} y_a^2 - \frac{1}{2}\beta\pi + \frac{\beta^2 - 1}{2\beta} \ln \frac{1+\beta}{1-\beta} \right),$$

and where y_a , the jellium edge position, is given²⁶ by

$$y_a = \bar{k}_F a = \frac{3}{2} \left[\frac{\pi}{4} - \left(1 - \frac{1}{2\beta^2} \right) \sin^{-1}\beta - \frac{1}{2\beta} (1-\beta)^{\frac{1}{2}} \right].$$

Surface Kinetic Energy²⁷

$$\sigma_k = \sigma_k^{(1)} - \sigma_k^{(2)}, \quad (52)$$

where

$$\begin{aligned} \frac{\sigma_k^{(1)}}{\bar{k}_F^4} &= \frac{1}{160\pi} \left[1 - \frac{4}{\pi} \left(1 - \frac{3}{\beta^2} + \frac{15}{8\beta^4} \right) \sin^{-1}\beta \right. \\ &\quad \left. - \frac{1}{\beta\pi} \left(7 - \frac{15}{2\beta^2} \right) (1 - \beta^2)^{\frac{1}{2}} \right], \end{aligned}$$

and

$$\begin{aligned} \frac{\sigma_k^{(2)}}{\bar{k}_F^4} &= \frac{1}{160\pi} \left[\frac{4}{\pi} \left(\frac{5}{\beta^2} - \frac{15}{4\beta^4} \right) \sin^{-1}\beta \right. \\ &\quad \left. + \frac{1}{\beta\pi} \left(-10 + \frac{15}{\beta^2} \right) (1 - \beta^2)^{\frac{1}{2}} \right]. \end{aligned}$$

Bulk Exchange Energy³⁵

$$\frac{E_{sx,b}}{\bar{k}_F^4} = \frac{1}{4\pi^3} F(\gamma), \quad (53)$$

where

$$F(\gamma) = 1 - \frac{\gamma^2}{6} + \frac{1}{2} \gamma^2 \left(1 + \frac{\gamma^2}{12} \right) \ln \left[1 + \frac{4}{\gamma^2} \right] - \frac{4}{3} \gamma \tan^{-1} \left[\frac{2}{\gamma} \right]. \quad (54)$$

Surface Exchange Energy⁶⁴

(55)

$$\begin{aligned} \frac{\sigma_{sz}}{\bar{k}_F^3} &= \frac{\sigma_{sz}^{IBM}}{\bar{k}_F^3} + \frac{3}{8\pi^3} \left[\left(1 - \frac{1}{2\beta^2} \right) \sin^{-1} \beta + \frac{\sqrt{1-\beta^2}}{2\beta} \right] F(\gamma) \\ &\quad - \frac{1}{4\pi^4} \int_0^2 dp \int_0^1 dq \int_0^1 dq' p H(p, q, q') \\ &\quad \left[\frac{1}{\gamma^2 + p^2 + q_+^2} \left(\frac{\sin 2\delta_+}{2q_+} - \frac{\sin 2\delta}{2q} - \frac{\sin 2\delta'}{2q'} \right) \right. \\ &\quad \left. + \frac{1}{\gamma^2 + p^2 + q_-^2} \left(\frac{\sin 2\delta_-}{2q_-} - \frac{\sin 2\delta}{2q} - \frac{\sin 2\delta'}{2q'} \right) \right. \\ &\quad \left. - \sqrt{\gamma^2 + p^2} \left\{ \left(\frac{\cos \delta_-}{\gamma^2 + p^2 + q_-^2} - \frac{\cos \delta_+}{\gamma^2 + p^2 + q_+^2} \right)^2 - \left(\frac{1}{\gamma^2 + p^2 - q_-^2} - \frac{1}{\gamma^2 + p^2 + q_+^2} \right) \right\} \right. \\ &\quad \left. + \frac{1}{\sqrt{\gamma^2 + p^2}} \left(\frac{q_- \sin \delta_-}{\gamma^2 + p^2 + q_-^2} - \frac{q_+ \sin \delta_+}{\gamma^2 + p^2 + q_+^2} \right) \right] \\ &\quad - \frac{1}{\pi^4} \int_0^2 dp \int_0^1 dq \int_0^1 dq' \frac{p H(p, q, q')}{\sqrt{\gamma^2 + p^2}} \frac{\sin^2 \delta \sin^2 \delta'}{(\sqrt{\gamma^2 + p^2 + \alpha + \alpha'}) (\alpha + \alpha')} \end{aligned}$$

$$\begin{aligned}
& - \frac{1}{\pi^4} \int_0^2 dp \int_0^1 dq \int_0^1 dq' \frac{pH(p,q,q')}{\sqrt{\gamma^2+p^2}} \frac{\sin\delta\sin\delta'}{(\sqrt{\gamma^2+p^2+\alpha+\alpha'})} \\
& \left[\sqrt{\gamma^2+p^2} \left(\frac{\cos\delta_-}{\gamma^2+p^2+q_-^2} - \frac{\cos\delta_+}{\gamma^2+p^2+q_+^2} \right) \right. \\
& \left. + \frac{q_- \sin\delta_-}{\gamma^2+p^2+q_-^2} - \frac{q_+ \sin\delta_+}{\gamma^2+p^2+q_+^2} \right]
\end{aligned}$$

where

$$\begin{aligned}
\frac{\sigma_{sz}^{IBM}}{k_F^3} &= - \frac{y_\alpha^{IBM}}{4\pi^3} F(\gamma) + \frac{1}{4\pi^4} \int_0^2 dp \int_0^1 dq \int_0^1 dq' p H(p,q,q') \\
& \sqrt{\gamma^2+p^2} \times \left[\frac{1}{\gamma^2+p^2+q_-^2} - \frac{1}{\gamma^2+p^2+q_+^2} \right]^2 \\
& - \frac{1}{(2\pi)^3} \int_0^2 dp \int_0^1 dq p \left[\frac{H(p,q,q)}{\gamma^2+p^2} \right. \\
& \left. - \frac{1}{\gamma^2+p^2+q^2} (H(p,q,0) + H(p,0,q)) \right], \\
y_\alpha^{IBM} &= \frac{3\pi}{8},
\end{aligned}$$

F (δ) is given by Eq. (54).

$$\sin\delta = q\beta, \quad \sin\delta' = q'\beta, \quad q_+ = q + q', \quad q_- = q - q', \quad \delta = \delta(q),$$

$$\delta' = \delta(q'), \quad \delta_+ = \delta + \delta', \quad \delta_- = \delta - \delta', \quad \alpha = \sqrt{1-q^2\beta^2}/\beta, \quad \alpha' = \frac{1}{\beta} \sqrt{1-q'^2\beta^2}$$

and where

$$H(p, q, q') = \begin{cases} \pi(q'^2 - q^2) & \text{for } \xi \geq 1 - q'^2 \text{ and } \xi > 0 \\ \pi[(1 - q'^2) + (1 - q^2)] & \text{for } \xi^2 \geq 1 - q'^2 \text{ and } \xi < 0 \\ \pi(1 - q^2) - 2[(1 - q'^2) \sin^{-1}(\xi/\sqrt{1 - q'^2}) + \xi\sqrt{1 - q'^2 - \xi^2}] & \text{for } \xi^2 < 1 - q'^2 \end{cases}$$

and

$$\xi = (p^2 + q^2 - q'^2) / 2p \quad .$$

In the Table III we present the results for the universal function σ_{sx}/k_F^{-3} for different γ as a function of the density profile parameter β . In obtaining these universal values we have performed the multi-dimensional integrations in the expression for σ_{sx}/k_F^{-3} by an iterative and adaptive Monte-Carlo scheme with a new algorithm due to Lepage⁶⁵. The universal functions are plotted in Fig. 1. We note that for a specific density profile (i.e. for fixed value β), the surface exchange energy decreases as the interaction is made more short-ranged (i.e. as γ is increased). Since neither the surface kinetic nor electrostatic energies (See Eqs. (40) , (50) and (52)) depend explicitly on the type of interaction (i.e. whether the e-e interaction is screened or is the bare-Coulomb interaction) for fixed form of the effective potential , we can then conclude that the total surface energy decreases as the screening length is decreased. This is demonstrated in Table IV where

Table III.

Values of the universal function σ_{sx}/k_F^3 for the exact surface exchange energy σ_{sx} for screened-Coulomb interaction as a function of the density profile parameter β for different screening as specified by the parameter $\gamma = k_s/k_F$. The $\gamma = 0$ column are the results for bare-Coulomb interaction .

| DENSITY PROFILE PARAMETER β | σ_{sx}/k_F^3 (10^{-3} a.u.) | | | | | | |
|--|--|----------------|----------------|----------------|----------------|----------------|----------------|
| | $\gamma = 0^*$ | $\gamma = 0.5$ | $\gamma = 1.0$ | $\gamma = 1.5$ | $\gamma = 2.0$ | $\gamma = 2.5$ | $\gamma = 3.0$ |
| 0.0 | 0.5754 | 0.5259 | 0.3443 | 0.2246 | 0.1524 | 0.1082 | 0.0799 |
| 0.1 | 0.5755 | 0.5261 | 0.3445 | 0.2247 | 0.1525 | 0.1082 | 0.0800 |
| 0.2 | 0.5791 | 0.5277 | 0.3455 | 0.2254 | 0.1529 | 0.1085 | 0.0802 |
| 0.3 | 0.5854 | 0.5325 | 0.3485 | 0.2273 | 0.1542 | 0.1094 | 0.0809 |
| 0.4 | 0.5991 | 0.5422 | 0.3545 | 0.2311 | 0.1568 | 0.1113 | 0.0822 |
| 0.5 | 0.6248 | 0.5591 | 0.3649 | 0.2377 | 0.1612 | 0.1144 | 0.0845 |
| 0.6 | 0.6638 | 0.5861 | 0.3814 | 0.2482 | 0.1682 | 0.1193 | 0.0881 |
| 0.7 | 0.7257 | 0.6274 | 0.4064 | 0.2640 | 0.1788 | 0.1268 | 0.0937 |
| 0.8 | 0.8155 | 0.6898 | 0.4441 | 0.2878 | 0.1947 | 0.1380 | 0.1019 |
| 0.9 | 0.9648 | 0.7873 | 0.5024 | 0.3244 | 0.2191 | 0.1551 | 0.1145 |
| 1.0 | 1.2706 | 0.9742 | 0.6114 | 0.3920 | 0.2639 | 0.1865 | 0.1375 |

*see Ref. (25)

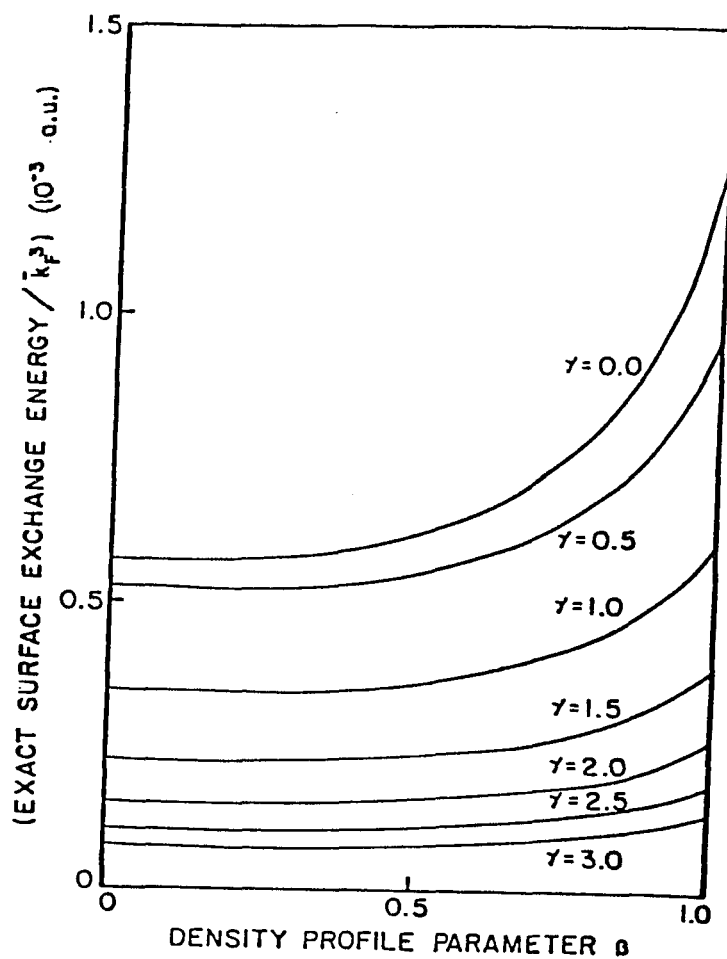


Figure 1

Variation of the universal function σ_{sx}/\bar{k}_F^3 , where σ_{sx} is the exact surface exchange energy for screened-Coulomb interaction as a function of the density profile parameter β for different screening defined by the parameter $\gamma=k_s/\bar{k}_F$. The $\gamma=0$ curve correspond to the case of bare-Coulomb interaction.

Table IV.

The total surface energy σ_s in ergs/cm² for different bulk densities ($\bar{r}_s = 2, 4$ and 6) and density profiles ($\beta=0, 0.5$ and 1.0), as a function of the screening parameter χ .

| Screening parameter χ | Total Surface Energies σ_s (erg/cm ²) | | | | | | | | |
|----------------------------------|--|---------------|---------------|-------------------|---------------|---------------|-------------------|---------------|---------------|
| | $\bar{r}_s = 2.0$ | | | $\bar{r}_s = 4.0$ | | | $\bar{r}_s = 6.0$ | | |
| | $\beta = 0.0$ | $\beta = 0.5$ | $\beta = 1.0$ | $\beta = 0.0$ | $\beta = 0.5$ | $\beta = 1.0$ | $\beta = 0.0$ | $\beta = 0.5$ | $\beta = 1.0$ |
| 0.0 | 3571 | 1329 | -1027 | 282 | 147 | 77 | 67 | 42 | 43 |
| 0.5 | 3503 | 1234 | -1435 | 274 | 135 | 26 | 65 | 38 | 28 |
| 1.0 | 3253 | 966 | -1934 | 242 | 102 | -36 | 56 | 28 | 9 |
| 1.5 | 3089 | 791 | -2236 | 222 | 80 | -74 | 50 | 22 | -2 |
| 2.0 | 2989 | 686 | -2412 | 209 | 67 | -96 | 46 | 18 | -8 |
| 2.5 | 2928 | 621 | -2519 | 202 | 59 | -110 | 44 | 16 | -12 |
| 3.0 | 2889 | 580 | -2586 | 197 | 54 | -118 | 42 | 14 | -15 |

we give the results for the total surface energy σ_s for different bulk densities ($\bar{r}_s = 2, 4$ and 6) and density profiles ($\beta = 0, 0.5$ and 1.0), as a function of the screening parameter γ . The decrease in σ_s as γ is increased is evident. Thus, the more short-ranged the interaction, the easier it is to split the crystal in two, a result expected on purely physical grounds. Yet another result that could be predicted, and is demonstrated by the Table, is that for fixed profile and fixed interaction strength, the greater the density the higher the magnitude of the surface energy. There are more electrons per unit volume interacting with each other and thus more work has to be done in order to split the crystal.

Chapter III

3.1 Convergence Study of the Gradient Expansion Approximation for Screened-Coulomb Exchange Energy within Hartree-Fock Theory

In this section, we study the convergence properties of the GEA for the surface exchange energy for screened-Coulomb interaction . The expansion examined is that which is valid within Hartree-Fock theory (HFT).

The LDA coefficient³⁵ A_{sx} for screened exchange as well as the corresponding expression^{38,42} for the first gradient correction coefficient C_{sx}^{HFT} within Hartree-Fock theory are given below. The expressions are given in terms of the screening parameter $\gamma = k_s/\bar{k}_F$. When these expressions are used in the local and gradient expansion approximations expressions expressions , Eqs. (20) and (22) , the local value $\gamma(\rho) = \gamma\bar{k}_F/k_F(\mathbf{r})$, where $k_F(\mathbf{r}) = [3\pi^2\rho(\mathbf{r})]^{1/3}$ must be employed.

Local Density Approximation Coefficient

$$A_{sx}[\rho] = a_{sx}[\rho(\mathbf{r})]^{4/3}$$

$$a_{sx} = - [3(3\pi^2)^{1/3}/4\pi] F(\gamma) \quad (56)$$

where $F(\gamma)$ is given by Eq. (54) .

Gradient Expansion Approximation Coefficient

$$B_{sx} = C_{sx} / [\rho(r)]^{4/3} \quad (57)$$

where C_{sx} within Hartree-Fock Theory is^{38,42}

$$C_{sx}^{HFT} = - [\pi / \{24(3\pi^2)^{4/3}\}] [\frac{1}{6}(5 - 2\pi k_F + G + D)] \quad (58)$$

where

$$G = (1 - 2\gamma^2) \ln(1 + 4/\gamma^2) - (64 - 4\gamma^2 - 3\gamma^4) / (4 + \gamma^2)^2$$

$$D = \frac{-2[1 + \pi k_F \gamma^2 / (4 + \gamma^2) - (\gamma^2/2) \ln(1 + 4/\gamma^2)]^2}{1 - \pi k_F^{-\frac{1}{2}} (1 + \gamma^2/2) \ln(1 + 4/\gamma^2)}$$

From the above expressions we observe that the LDA coefficient A_{sx} is a universal function of the parameter γ but that the HFT first gradient correction term is not .

We perform our calculations for the same densities as employed by others who have previously studied⁵⁶ this expansion viz., those of the step-potential model of a surface^{26,27,19} . The expression for the density is given in Eq. (50), and for purposes of studying the GEA we also need the first derivative of the density . As is the case with the

density, the first derivative can also be written as a universal function of the density profile parameter β . The expression for this universal function is

$$\frac{\rho'(y)}{\bar{\rho}} = \begin{cases} 3 \int_0^1 dq (1-q^2) q \sin[2(qy - \delta(q, \beta))] , & \text{for } y \leq 0 \\ -6\beta \int_0^1 dq (1-q^2) q^2 \sqrt{1-q^2\beta^2} \exp(-2y \sqrt{1-q^2\beta^2}/\beta) , & \text{for } y \geq 0 \end{cases} \quad (59)$$

It is evident from the above remarks on universality, that as with the exact surface exchange energy σ_{sx} , the LDA expression for the surface exchange energy σ_{sx}^{LDA} can also be written in terms of a universal function of the parameter β for fixed screening as defined by the parameter χ . The universal function involving σ_{sx}^{LDA} is

$$\frac{\sigma_{sx}^{\text{LDA}}}{\frac{-3}{k_F}} = \frac{F(\chi)}{4\pi^3} \int_{-\infty}^{\infty} dy \left[1 - \frac{F(\chi(\rho))}{F(\chi)} \left(\frac{\rho(y)}{\bar{\rho}} \right)^{1/3} \right] \frac{\rho(y)}{\bar{\rho}} . \quad (60)$$

On the other hand, since the GEA coefficient C_{sx}^{HFT} within Hartree-Fock theory is not a universal function of χ , the GEA correction term cannot be written in terms of a universal function of χ for fixed β even though the first derivative of the density is a universal function of β . Thus, one is forced into performing calculations for specific value of the bulk density as defined by the Wigner-Seitz radius \bar{r}_s .

We begin our analysis by first re-examining the test of the GEA for the surface exchange energy for screened-Coulomb interaction within HFT as performed by others⁵⁶. We replot in Fig. 2a the exact, LDA and GEA surface exchange energies as a function of the screening parameter k_s for $\bar{r}_s = 4$. These results are obtained for the fixed density profile chosen such that the Budd-Vannimenus sum rule⁶⁶ is exactly satisfied for this \bar{r}_s value. This corresponding value^{19,26} of the density profile parameter obtained is $\beta=0.733$. The Budd-Vannimenus sum rule relates the difference in the electrostatic potential between that at the surface and in the bulk, to the total energy per particle ε_T of a uniform electron gas. According to the Budd-Vannimenus theorem

$$\Delta V = V_{es}(a) - V_{es}(-\infty) = \bar{\rho} d\varepsilon_T / d\bar{\rho}. \quad (61)$$

The significance of this theorem lies in the fact that it relates a surface property to those of the more well understood bulk. In model-potential calculations, this theorem can thus be used as a constraint on the electrostatic potential. Of course, the choice of barrier height, or equivalently the density profile is arbitrary, but we believe that in any model-potential calculation it is imperative that the criterion used for the adjustment of the parameters be as physically based as possible. The use of this sum rule is possibly the best such criterion : it enables

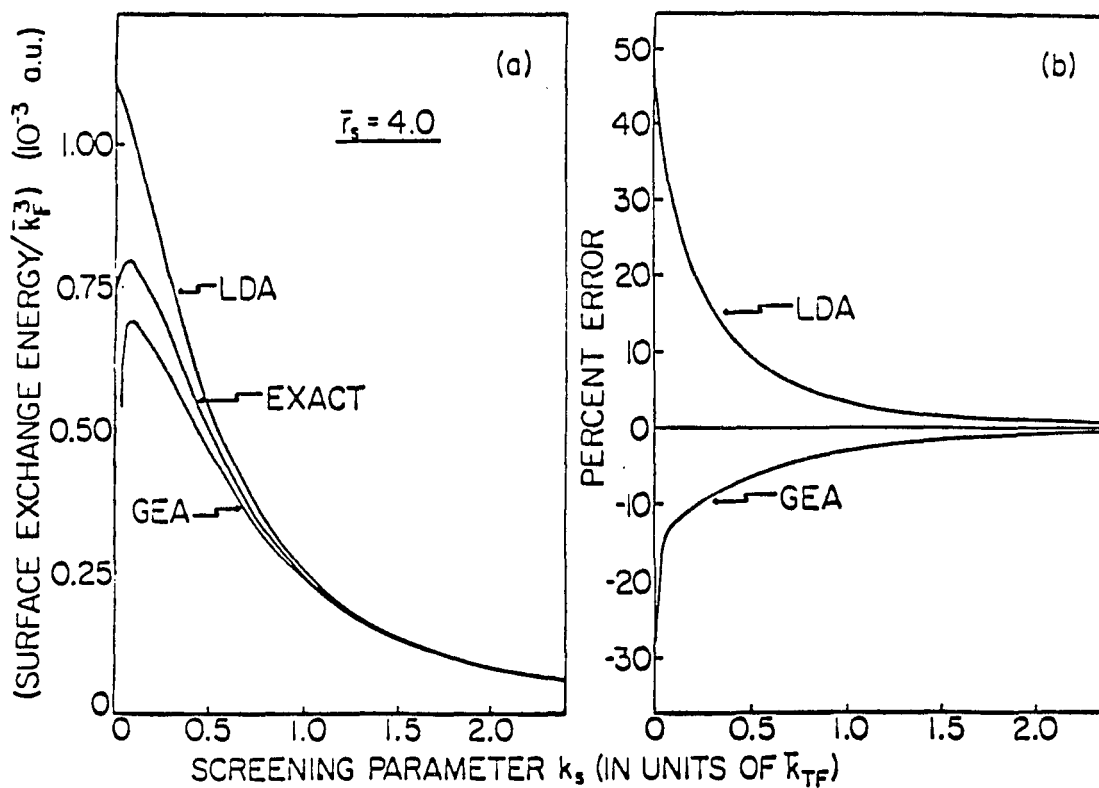


Figure 2

(a) Variation of the exact, local density (LDA) and gradient expansion (GEA) approximations for the surface exchange energy for screened-Coulomb interaction σ_{sx}/\bar{k}_F^3 as a function of the screening parameter k_s in units of Thomas-Fermi wave-vector $k_{TF} = \sqrt{4\bar{k}_F}/\pi$. The calculations are for a bulk density of $\bar{r}_s = 4$, with a density profile chosen so as to satisfy the Budd-Vannimenus theorem. The corresponding value of the density profile parameter is $\beta=0.733$.

(b) Percent error plots of the LDA and GEA results.

the contribution to the surface dipole barrier due to the charge distribution inside the metal to be determined exactly, and is in fact independent of the choice of any approximate total energy functional. In Fig. 2b we plot the percent errors of the LDA and GEA results. We observe that although there is a convergence of both the LDA and GEA with the exact values, each is essentially as much in error as the other. The convergence of these results is due to the fact that the coefficients of the LDA and first gradient correction term (see Figs. 3a and 3b) decrease rapidly with increasing value of the screening parameter. Of course, any local approximation must improve as the interaction is made more short-ranged. It is interesting to note that the addition of the first gradient correction term does not improve upon the LDA error to any degree of significance.

The above analysis of the convergence of the gradient expansion has been performed for the same fixed density profile. It is the Hamiltonian or equivalently the energy functional of the interacting system which is being varied when the screening parameter is changed. However, in any test of the convergence of an expansion in the gradients of the density for a system defined by some Hamiltonian or energy functional, it is the density and its gradients that must be varied. The authors of Ref.(56) did not study the convergence properties of the GEA as a function of the variation of the density.

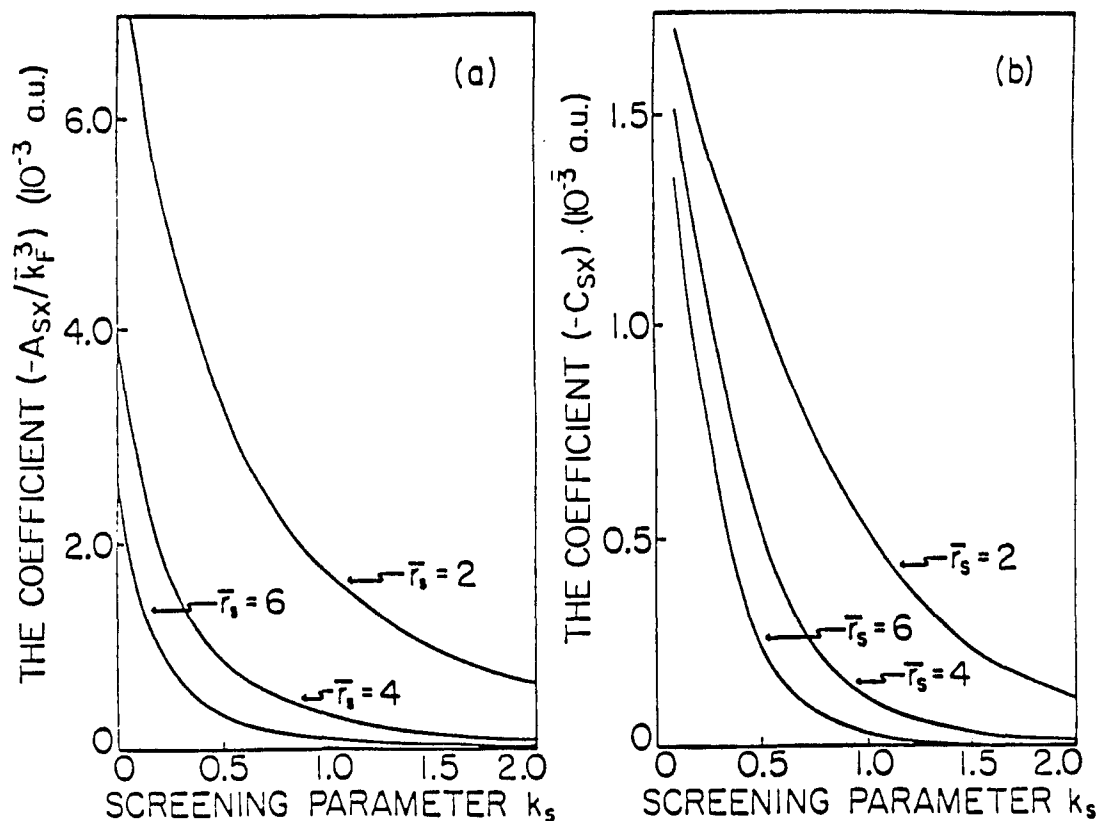


Figure 3

(a) Variation of the LDA coefficient A_{sx}/k_F^3 as function of the screening parameter k_s for $\bar{r}_s = 2, 4$ and 6.

(b) Variation of the coefficient C_{sx} (HFT) (which is related to the coefficient B_{sx} of the first gradient correction term via $B_{sx} = C_{sx}/\rho^{4/3}$) as a function of k_s for the \bar{r}_s values.

Their calculations were performed for a fixed density profile with results similar to those of Fig. 2(a). However, their density profile was chosen such that it closely resembled that derived by Lang and Kohn⁶⁷ within the LDA for the exchange-correlation energy. The corresponding value of the density profile parameter employed by these authors was $\beta=0.894$. We next perform an analysis of the GEA as a function of the variation of the density profile for the range of profiles permitted by the step-potential model ($0 \leq \beta \leq 1$). Again, due to the fact that the first gradient correction term cannot be written as a universal function of β for a specific γ , the calculations are performed for $\bar{r}_s = 4$. Furthermore, we assume the screening parameter to be of the form $k_s = \kappa k_{TF}$, where $k_{TF} = \sqrt{4k_F/\pi}$ is the Thomas-Fermi wave-vector and κ an arbitrary parameter⁶⁸. In Fig. 4a we plot the exact, LDA and GEA surface exchange energies as a function of the density profile parameter β for $k_s = 0.5k_{TF}$, and in Fig. 4b the corresponding errors in the LDA and GEA results. Observe first, that for the densities of this model the LDA is poor. Second, in the range $0 \leq \beta \leq 0.6$, even as the density is made more slowly varying, the GEA error is still greater than that due to the LDA. It is only for the most slowly varying of the densities permitted by this model that the GEA is superior to the LDA, but again not by any significant degree. These results are for a large value of the screening length. However, precisely the same trends are

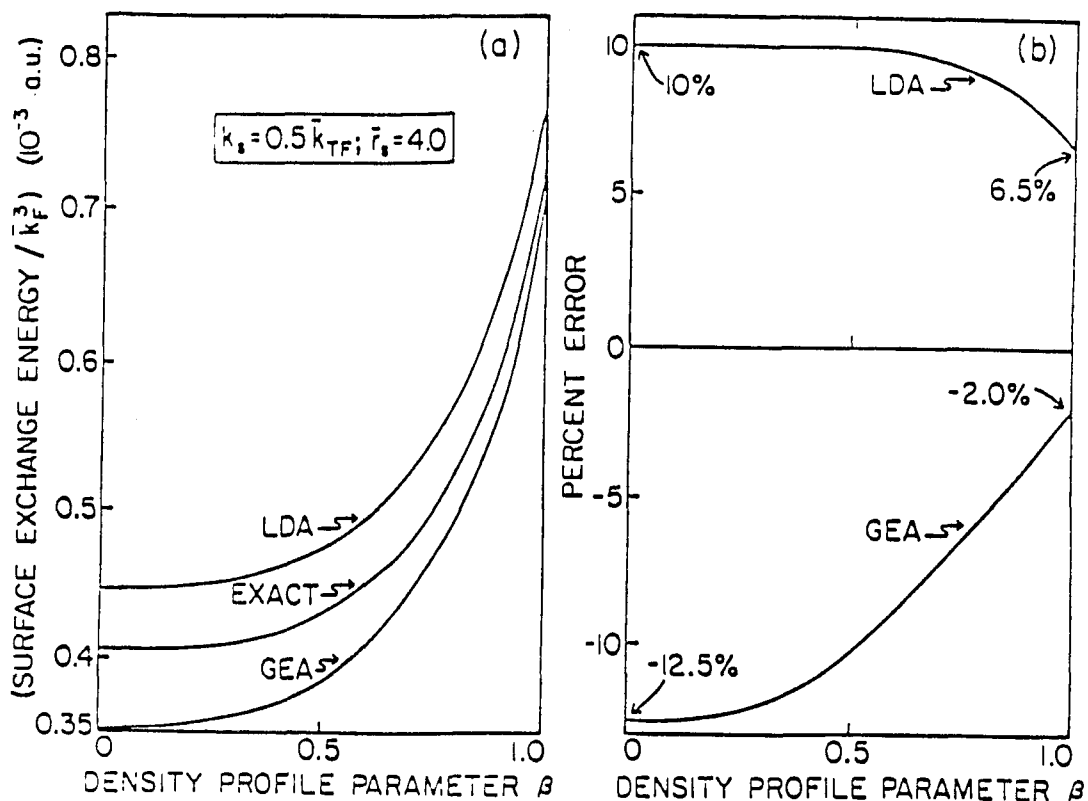


Figure 4

(a) Variation of the exact, local density (LDA) and gradient expansion (GEA) approximations for the surface exchange energy for screened-Coulomb interaction σ_{sx}/\bar{k}_F^3 as a function of the density profile parameter β . The results correspond to a bulk density of $\bar{r}_s = 4$, and for a value of the screening parameter $k_s = 0.5k_{TF}$ where k_{TF} is the Thomas-Fermi wave vector.

(b) LDA and GEA percent errors as a function of the density profile parameter β .

observed (see Figs. 5a and 5b) if the screening length is halved. The results are similar if the screening length is reduced still further. Based on these results one must conclude that both the local density and gradient expansion approximations for the surface exchange energy for screened-Coulomb interaction are poor .

These results are surprising, and the question arises as to what degree are they a consequence of the densities employed? In an attempt to answer this we have plotted in Figs. 6 and 7 respectively the "small parameters $|\nabla\rho|/2k_F\rho$ and $|\nabla\rho|/2k_S\rho$ of the convergence conditions

$$|\nabla\rho|/2k_F\rho < 1 \quad (62)$$

$$|\nabla\rho|/2k_S\rho < 1 , \quad (63)$$

as a function of the distance from the jellium edge. The satisfaction of these conditions would guarantee that the magnitude of the gradient term would be small compared to the local term. We do not consider the convergence condition $|\nabla^2\rho|/2k_F|\nabla\rho| \ll 1$, as for the step potential model densities there is a discontinuity in the second derivative at the potential barrier i.e. at $x=0$. In Fig. 6 the "small" parameter of Eq.(62) is plotted for the IBM density $\beta=0$, for $\beta=0.8$ and for the most slowly varying density permitted by this model ($\beta=1$).

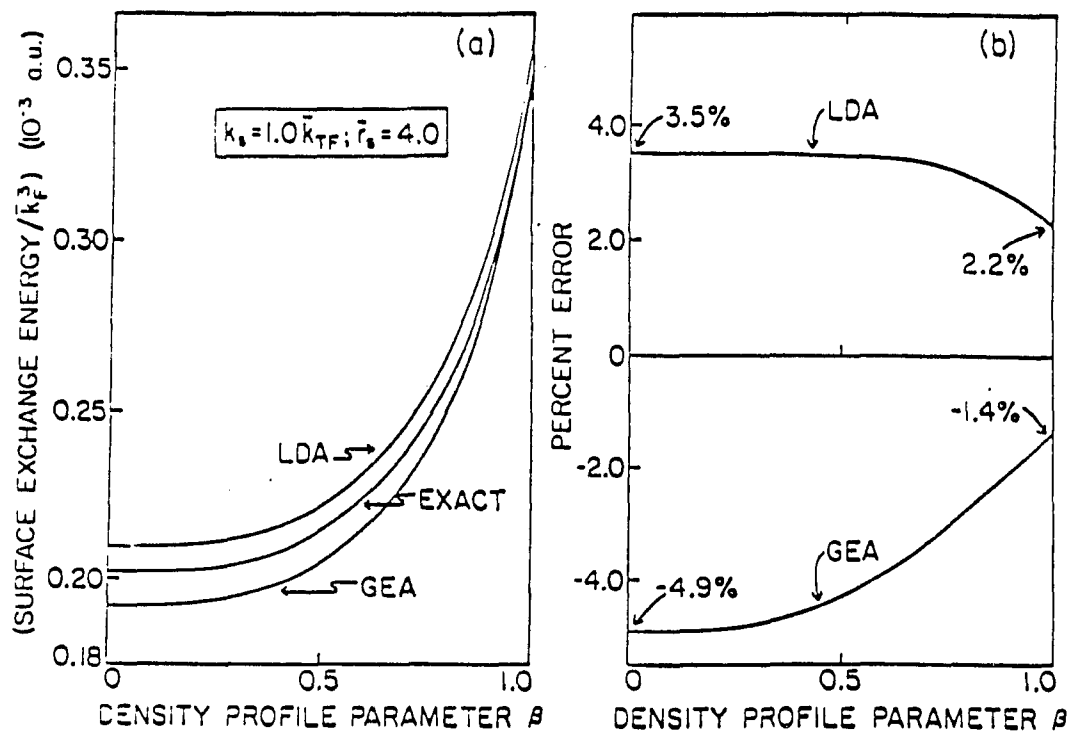


Figure 5

Caption for parts (a) and (b) is the same as that of Fig. 4, except that these results are derived for $k_s = 1.0 k_{TF}$.

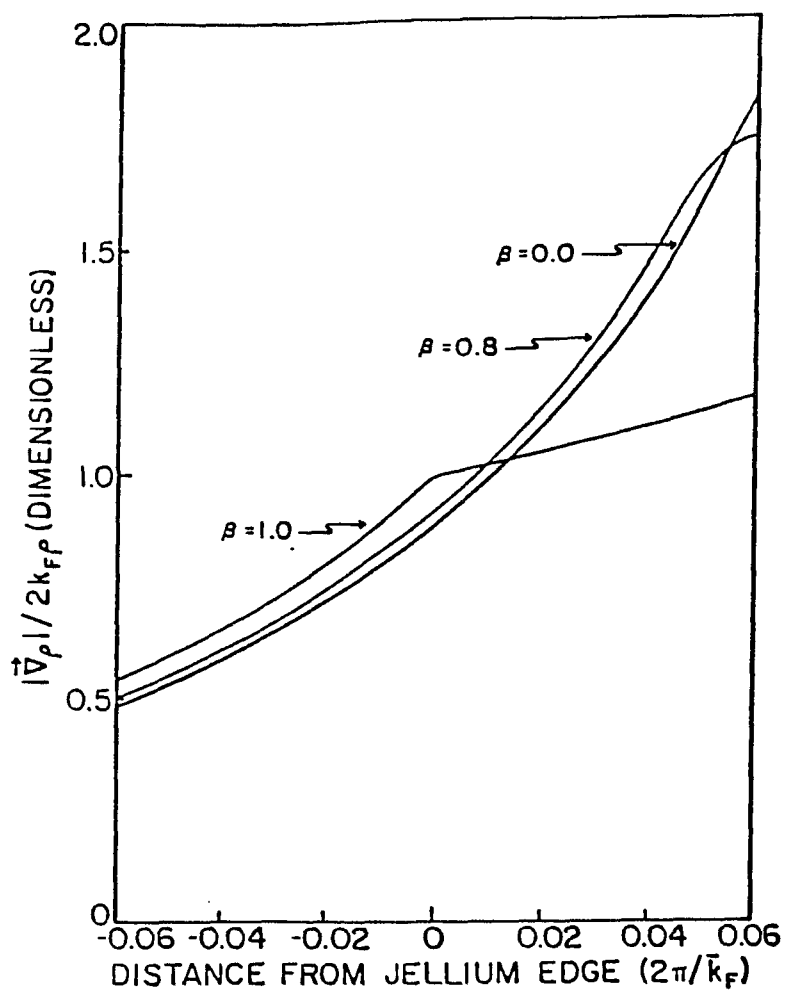


Figure 6

Variation of the "small" parameter of Eq. (62) as a function of the distance from the jellium edge for different density profiles corresponding to $\beta=0$, 0.8, and 1.0 .

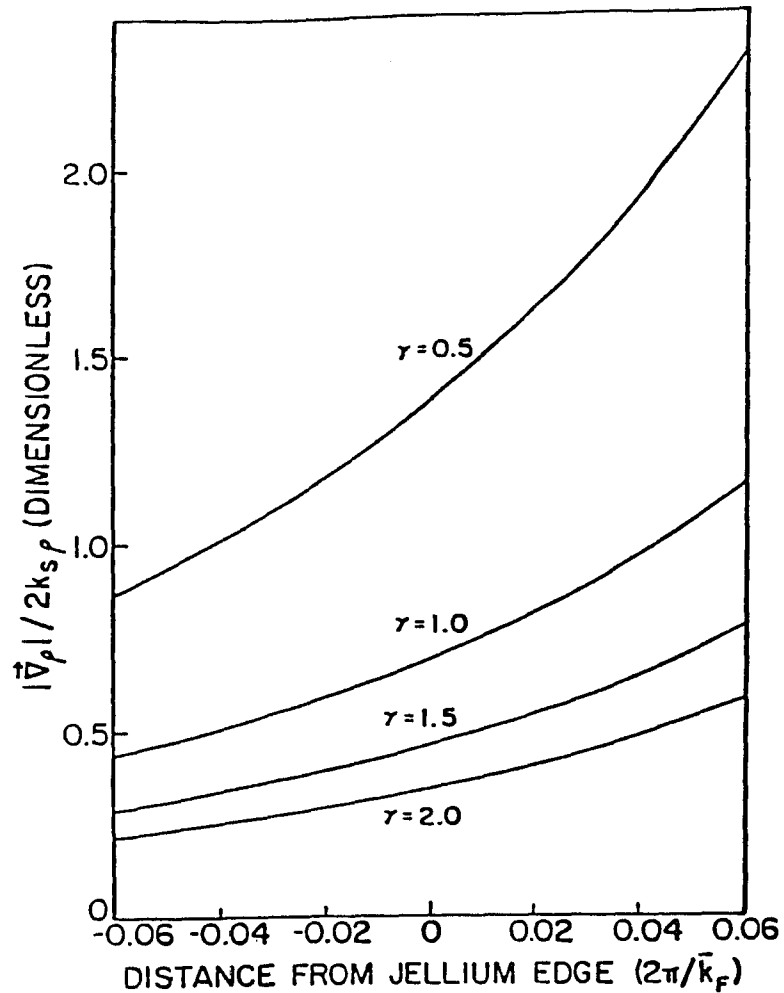


Figure 7

Variation of the "small" parameter of Eq. (63) for different values of the parameter $\gamma = k_s/\bar{k}_F$ as function of the distance from the jellium edge for fixed density profile corresponding to $\beta=0.733$. Increasing values of γ correspond to decreasing screening length.

It is evident from this graph that this convergence condition is not well satisfied, and that this is the case even for $\beta=1$ at five hundredths of a Fermi wavelength outside the surface. In Fig. 7 we plot the "small" parameter of Eq.(63) for fixed density profile ($\beta=0.733$) for different values of the parameter $\gamma = k_s / \bar{k}_F$. The diagram demonstrates that with increasing γ , i.e. decreasing screening length, the convergence condition is better satisfied. This is consistent with the idea that the LDA and GEA results should improve as the screening length is decreased. The calculations of Figs. 4 and 5 discussed previously correspond to $\gamma=0.6$ and 1.2 respectively, and as may be observed from Fig. 7 the convergence conditions for these values of γ are again not too well satisfied. Thus we conclude that one possible cause for the failure of this expansion is that the densities of this model may not be slowly varying enough.

In order to investigate this possibility further, we have also performed calculations for the case of bare-Coulomb exchange. In Fig. 8a we plot the exact, LDA and GEA surface exchange energies for the bare-Coulomb interaction, and in Fig. 8b the corresponding LDA and GEA percent errors. Note that for 70% of the densities ($0 \leq \beta \leq 0.7$) the GEA is substantially in error. For IBM densities this error is -155% and at $\beta=0.7$ it is -12%. It is only for $\beta \geq 0.8$ that the GEA is reasonably accurate. At $\beta = 0.8$ the error is -3% but at $\beta = 1$ it is 6%.

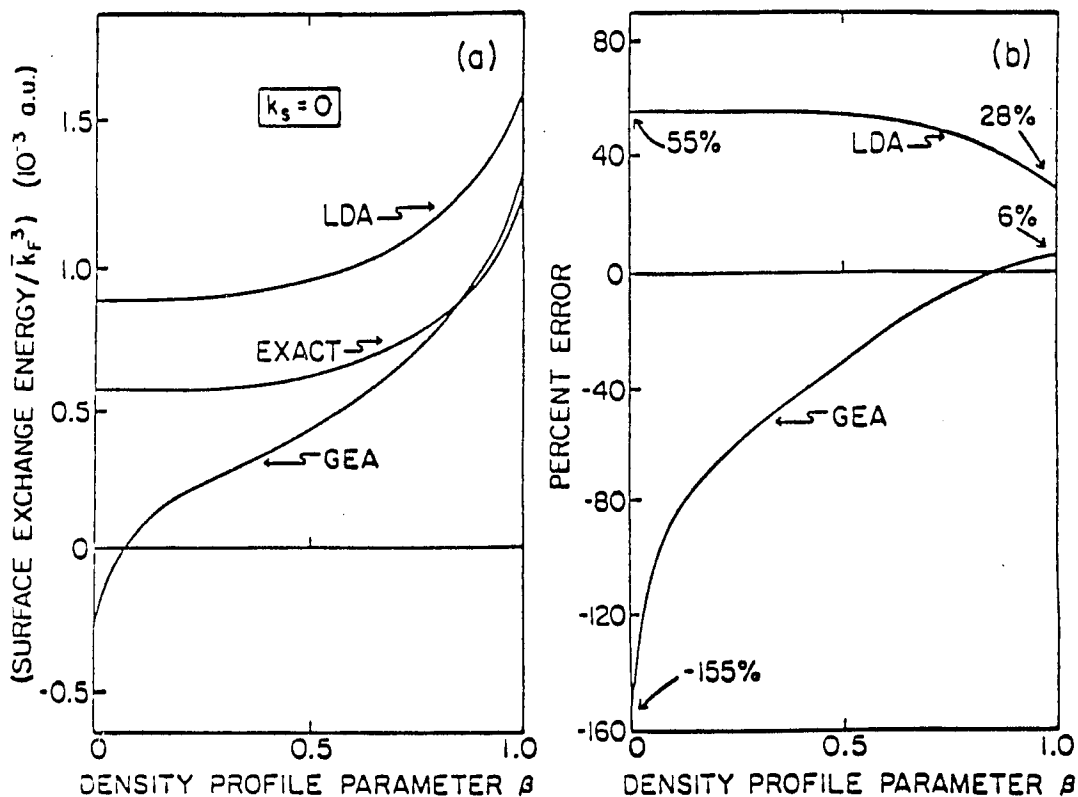


Figure 8

(a) Variation of the exact, local density (LDA) and gradient expansion (GEA) approximations for the surface exchange for bare-Coulomb interaction σ_x/\bar{k}_F^3 as a function of the density profile parameter β . These results universal curves are independent of the bulk density.

(b) LDA and GEA percent errors as a function of the density profile parameter β .

Thus, in contrast to the conclusions arrived by Sahni et al^{54,18} (see also Fig. 2 of Ref. 54), it is not possible on the basis of these results to make very strong statements with regard to the accuracy of the GEA for bare exchange as applied to surfaces. This also tends to support the conclusions of the previous paragraph . It is thus clear that the poorness of the profiles of the step-potential model play a significant role in the present conclusion that the GEA for screened exchange within Hartree-Fock theory is poor .

3.2 The Gradient Expansion Approximation for Screened-Coulomb Exchange Energy within Density-Functional Theory⁶⁹

We begin this section by a discussion of why a gradient expansion approximation for the exchange energy exists in density-functional theory but not within Hartree-Fock theory. We then derive the coefficient ($B_{s x}^{\text{DFT}}$) of the first gradient correction term for the screened-Coulomb exchange energy, the details of the derivation being relegated to Appendix A. Next we compare the coefficients $B_{s x}^{\text{HFT}}$ and $B_{s x}^{\text{DFT}}$ of Hartree-Fock and density-functional theories, and finally, using the coefficient $B_{s x}^{\text{DFT}}$ derived by us, we perform a convergence study of the corresponding gradient expansion approximation.

In DFT, the exchange energy and hence its GEA are^{18,70} purely of $O(e^2)$ where e is the electron charge. This is because the DFT orbitals are derived from a local effective potential and are functions only of the density $\rho(\mathbf{r})$. They do not in any way depend on the charge e . Thus in the calculation⁴⁰ of the DFT coefficient B_x^{DFT} , each term in the expansion of the density response function is further expanded only to terms which are first order in e^2 . Furthermore, since the first gradient correction term must⁷¹ have the dimensions of an exchange energy, this coefficient is of the form

$$B_x^{\text{DFT}}[\rho] = C_x^{\text{DFT}} / [\rho(\mathbf{r})]^{4/3} \quad (64)$$

The coefficient C_x^{DFT} was originally derived by Sham⁴⁰ and has recently been rederived via a wave-vector analysis method by Langreth and Perdew⁴¹. The correlation energy coefficient B_c^{DFT} to $O(e^2)$ valid for high densities has been derived by Ma and Brueckner⁴⁶, who also show that terms of $O(e^2 \ln e^2)$ do not exist although terms of higher order do.

On the other hand, in Hartree-Fock theory (HFT), the exchange energy contains¹⁸ terms to all orders in the electron-electron interaction, because the orbitals, (being derived from a non-local effective potential), depend explicitly on e^2 . In the evaluation of the HFT coefficient B_x^{HFT} one must thus sum to all orders in e^2 . Such a calculation has been performed by Kleinman³⁸ and Geldart et al³⁹, and the result shown to be divergent. A perturbative analysis³⁹ shows that it is terms of $O(e^4)$ and higher order that are singular. As a consequence, a gradient expansion for the exchange energy in HFT does not exist. However, a gradient series does exist within HFT provided correlation is introduced by screening the interaction via screened-Coulomb interaction of Yukawa form given in Eq.(21). In fact the authors of Refs. (38) and (39) employed this form of screened-Coulomb interaction in their calculations, and consequently arrived at their conclusions of the singular nature of B_x^{HFT} by taking the $k_s \rightarrow 0$ limit of the coefficient $B_{s x}^{\text{HFT}}$ for screened exchange .

It is evident that what remains to complete the present picture on the GEA for the exchange energy is the determination of the DFT coefficient $B_{s x}^{\text{DFT}}$ for screened-Coulomb interaction. On the basis of the discussion given above and that in Refs. (18) and (70), the GEA for the screened-Coulomb exchange energy is also purely of $O(e^2)$ and well defined. In order to derive this coefficient we have followed the method of Sham⁴⁰ described above rather than the wave-vector analysis method of Ref.(41). The details of the derivation are given in Appendix A. We quote below the final expression for the coefficient:

$$C_{s x}^{\text{DFT}} = -[\pi/\{24(3\pi^2)^{4/3}\}] [2 - (3\gamma^2/4)\ln\{1+4/\gamma^2\} - (40-6\gamma^2-3\gamma^4)/(3(4+\gamma^2)^2)] \quad (65)$$

From the above expression we observe that the DFT first gradient gradient correction coefficient $C_{s x}^{\text{DFT}}$ is a universal function of the parameter γ . Furthermore, in the limit of no screening ($\gamma \rightarrow 0$) we recover the Sham DFT result, $C_x^{\text{DFT}} = -7\pi/144(3\pi^2)^{4/3} = -0.00167$ a.u. as we must. For purposes of comparison, we plot in Fig. 9 the LDA and GEA coefficients $a_{s x}$ and $C_{s x}^{\text{DFT}}$ respectively. For all values of the screening parameter γ the two coefficients differ by two orders of magnitude. The magnitude of each coefficient also changes considerably as the screening is increased.

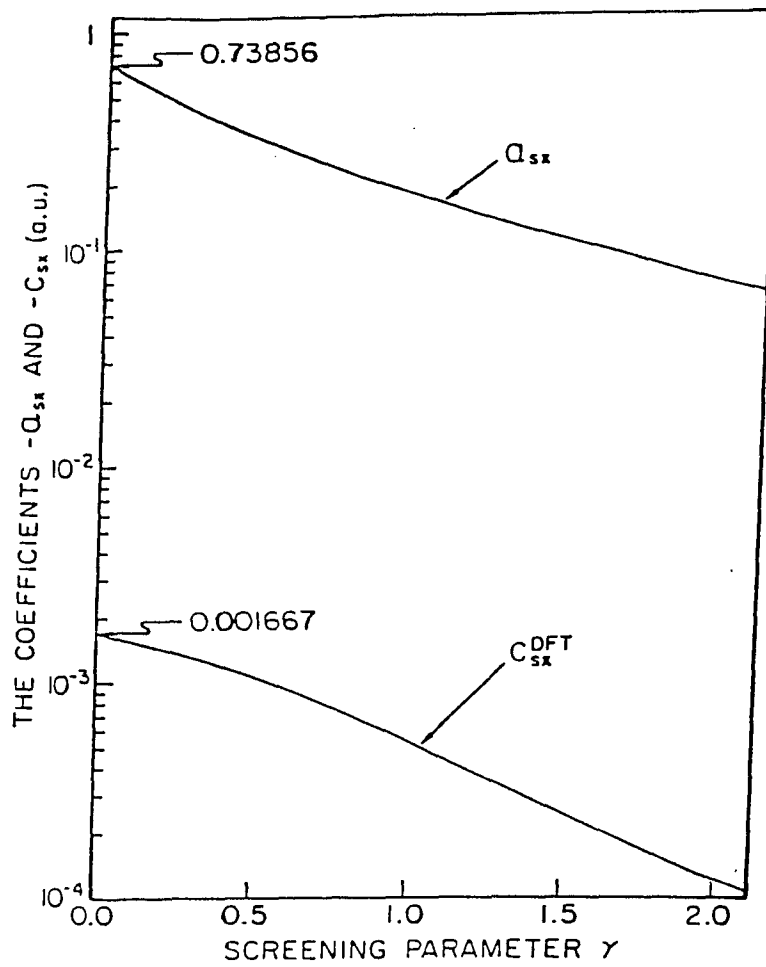


Figure 9

Variation of the Density-Functional theory (DFT) local (a_{sx}) and first gradient correction (C_{sx}^{DFT}) coefficients in the expansion for the screened-Coulomb exchange energy, as a function of the screening parameter γ . The bare-Coulomb interaction case corresponds to $\gamma = 0$.

As indicated in the previous section, the HFT first gradient correction coefficient C_{sx}^{HFT} , on the other hand, is not a universal function of the parameter γ . Consequently, comparisons with the DFT coefficient must be made for specific values of the bulk density. In Fig. 10(a), (b) and (c) we compare the DFT and HFT first gradient correction coefficients as a function of the screening parameter k_s for $\bar{r}_s = 2, 4$ and 6 . What is reassuring and readily evident from the graphs is that although the analytic expressions for the coefficients in the two theories are quite dissimilar (See Eqs. (58) and (65)), the numerical values are the same for finite screening. They become dissimilar only as one approaches the bare-Coulomb interaction case for which the HFT coefficient is singular. This, of course, implies that for finite screening in HFT the contribution of terms of order higher than e^2 are negligible. Furthermore, the higher the density, the larger is the value of the screening parameter before the two coefficients merge.

In section 3.1, we studied the convergence properties of the GEA for the screened-Coulomb exchange energy within HFT as applied to surfaces. There we showed that for the step-potential model of a surface the convergence of both the GEA and the LDA were poor and that the former did not reduce the error of the latter to any significant degree even for the most slowly varying density profile obtainable by this model. It is evident from the discussion on Fig. 10 that precisely

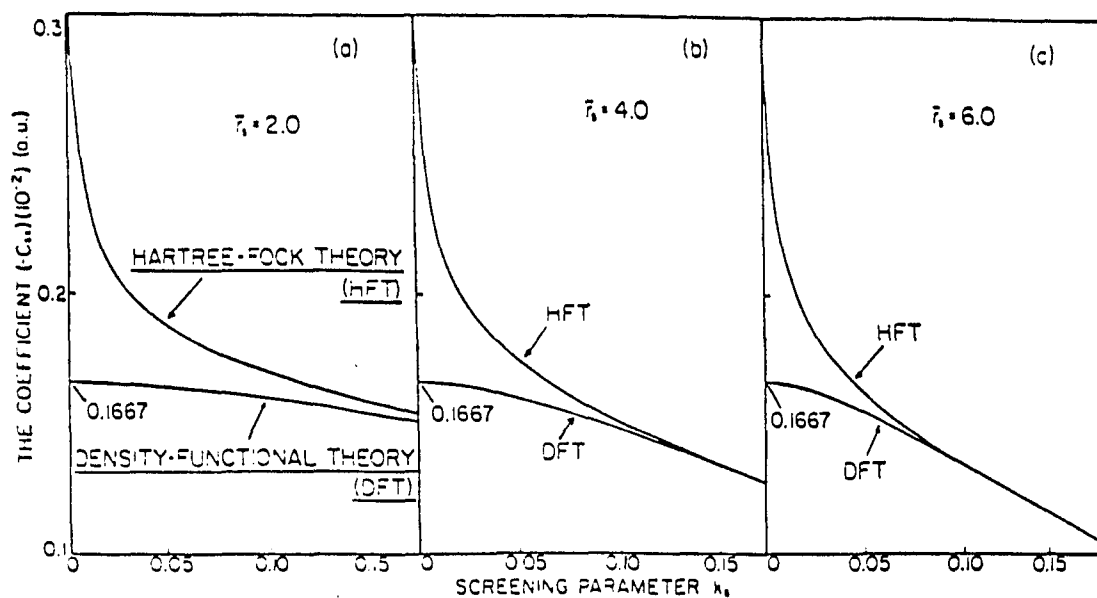


Figure 10

(a), (b) and (c). Variation of the first gradient correction coefficient C_{sx} within Density-Functional and Hartree-Fock theories, as a function of the screening parameter k_s for $\bar{r}_s = 2, 4$ and 6 .

the same conclusions must hold for the GEA within DFT for those values of the screening parameter k_s for which the coefficients in the two theories are the same. Now since in HFT the first gradient correction coefficient is not a universal function of the parameter γ , the calculations of the previous section had to be performed for a specific value of the Wigner-Seitz radius \bar{r}_s , (as had a specific value (and form) to be chosen for the screening parameter k_s). However, since in DFT the coefficient is a universal function of γ , one can study the convergence of the LDA and GEA for these step-potential model densities in a more concise and general manner, one which is entirely independent of \bar{r}_s , and thus valid for all bulk densities.

Within DFT, the exact, LDA and GEA surface exchange energies for the screened-Coulomb interaction can now all be written in terms of universal functions of the screening parameter γ for a specific density profile described by the step-model profile parameter β . Equivalently, for a specific screening γ , the exchange energies are universal functions of the density profile parameter β . In Fig. 11 we plot the universal LDA and GEA percent error curves for $\gamma = 0.5, 1.0$ and 1.5 over the entire range of densities permitted by the step-potential model. The profile becomes more slowly varying as β is increased. Note first that for each value of the screening parameter γ considered, the convergence of the LDA is poor. The GEA begins to improve upon

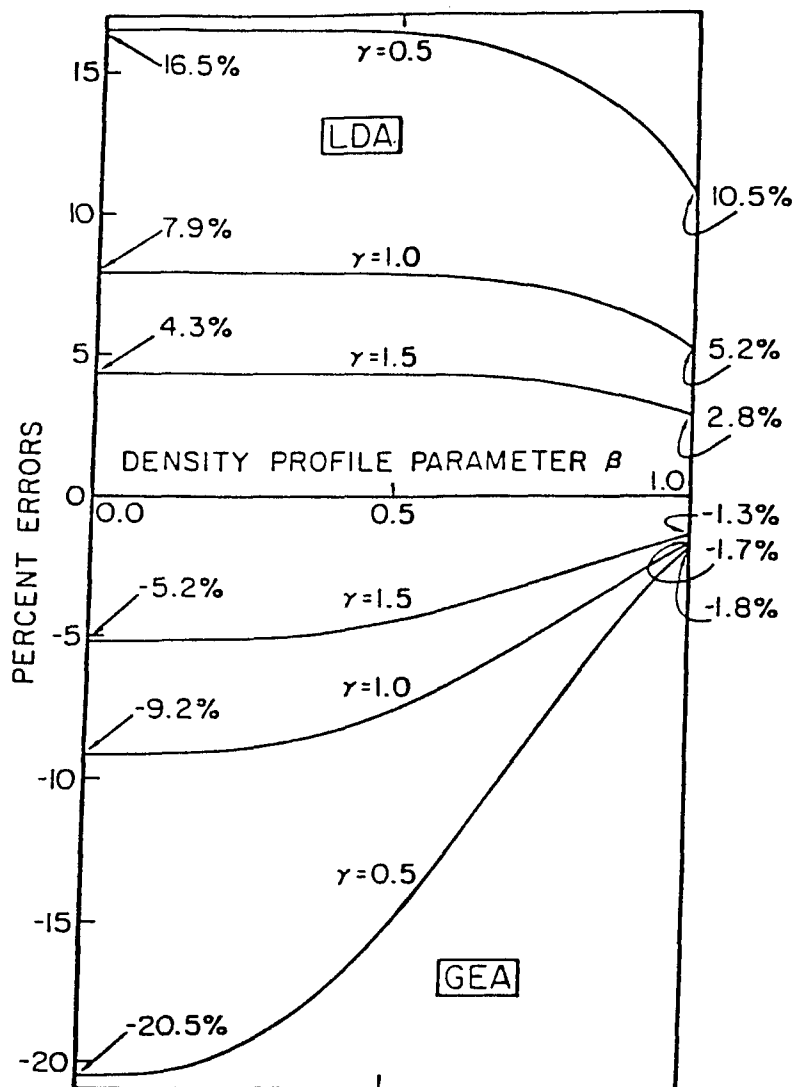


Figure 11

The universal Density-Functional theory local density (LDA) and gradient expansion (GEA) approximation percent error curves for the surface exchange energy, as a function of the density profile parameter β for different values of the screening parameter γ . Increasing values of γ imply decreasing screening lengths.

the LDA for $\beta > 0.6$, but the improvement is not significant. These were also the conclusions of the previous section . Another interesting fact is that even for the most slowly varying density ($\beta= 1$), increasing the screening improves the GEA error only slightly, going from -1.8% for $\gamma= 0.5$ to -1.3% for $\gamma= 1.5$. (See Fig. 11) .

In conclusion , we have derived the DFT coefficient of the first gradient correction term in the expansion for the screened-Coulomb exchange energy. Except for when the screening is very small, (for which this expression approaches the bare-Coulomb interaction value), the results are equivalent to those derived within HFT. However, the fact that the first gradient correction coefficient derived here has the same universal features as the LDA term is significant. After all, the GEA is intrinsically an approximation within DFT, and it is imperative that each term in the expansion exhibit the same universality as that exhibited by the exact term. This important fact consequently has enabled us to demonstrate in a far more general manner previously arrived at conclusions regarding the convergence of the expansion for screened exchange as applied to surfaces. In the previous section we had also indicated that these conclusions were surprising, and that more physically realistic densities had to be employed in any further study of the expansion. The universal characteristics of the expansion coefficients will now enable an extension, similar to that presented

here, to densities generated by other more accurate local effective potentials. The loss of this universality in HFT is, of course, strictly a consequence of attempting to replace a non-local effective potential by a local one.

Chapter IV

4.1 Estimates of the Surface Correlation Energy

In section II.2 we studied the effects of correlation at metallic surfaces by screening the exchange term. These calculations may also be interpreted in the Bohm-Pines⁷² context as being an analysis of the short-ranged part of the Coulomb interaction. In this section we accurately estimate the surface correlation energy of jellium metal via density-functional theory. In order to do this we must assume as accurate an approximation as possible for the universal exchange-correlation energy functional of the density $E_{xc}[\rho]$. For the surface physics problem specifically, we believe the most accurate of the existing formalisms to be the non-local wave-vector (WV) analysis scheme of Langreth and Perdew^{22,58}. In this theory both large as well as small wavelength fluctuations are considered in the analysis of the exchange-correlation energy functional. We begin this section by a brief description of the formalism as applied to surfaces, and then present the justification of why we think it to be the best theory for this problem. Next we describe and apply our method for the determination of the surface correlation energy, and finally, we present and discuss our results for this property.

The exchange-correlation energy E_{xc} is defined by the expression

$$E_{xc} = \int dr \rho(r) \varepsilon_{xc}(r) \quad (66)$$

where $\rho(r)$ is electron density and $\varepsilon_{xc}(r)$ the exchange-correlation energy density. In terms of the wave-vector \mathbf{k} of the fluctuations that contribute to it, the exchange-correlation energy may be written as

$$E_{xc} = \frac{1}{V} \sum_{\mathbf{k}} E_{xc}(\mathbf{k}) = \frac{1}{(2\pi)^3} \int d\mathbf{k} E_{xc}(\mathbf{k}) . \quad (67)$$

For an interelectronic interaction of the form $u(\mathbf{r}-\mathbf{r}') = \lambda e^2/|\mathbf{r}-\mathbf{r}'|$, where λ is a coupling constant, the wave-vector decomposition $E_{xc}(\mathbf{k})$ is defined as

$$E_{xc}(\mathbf{k}) = \int dr \rho(r) \frac{1}{2} \int_0^1 \frac{d\lambda}{\lambda} u(\mathbf{k}) [S_{\lambda}(\mathbf{k}, \mathbf{k}) - 1] \quad (68)$$

$$= \frac{1}{2} \int_0^1 \frac{d\lambda}{\lambda} u(\mathbf{k}) N [S_{\lambda}(\mathbf{k}, \mathbf{k}) - 1] , \quad (69)$$

where N is the electron number, $u(\mathbf{k})$ is the Fourier transform of $u(\mathbf{r})$; and

$$S_{\lambda}(\mathbf{k}, \mathbf{k}') = \int dr \int dr' e^{-i\mathbf{k} \cdot \mathbf{r}} S_{\lambda}(\mathbf{r}, \mathbf{r}') e^{i\mathbf{k}' \cdot \mathbf{r}'}, \quad (70)$$

is a double Fourier transform. The quantity $NS_{\lambda}(\mathbf{r}, \mathbf{r}') = \hat{\chi}(\mathbf{r}, \mathbf{r}')$ is the density-density correlation function, and $S_{\lambda}(\mathbf{k}, \mathbf{k}')$ is the structure factor. The function $\hat{\chi}(\mathbf{r}, \mathbf{r}')$ is related to the density and the average exchange-correlation charge density $\rho_{xc}(\mathbf{r}, \mathbf{r}')$ by the relation

$$NS_{\lambda}(\mathbf{r}, \mathbf{r}') = \hat{\chi}(\mathbf{r}, \mathbf{r}') = \rho(\mathbf{r}) [\delta(\mathbf{r}-\mathbf{r}') + \rho_{xc}(\mathbf{r}, \mathbf{r}')] . \quad (71)$$

For a large, through finite crystal, the exchange-correlation energy E_{xc} has both a bulk as well as a surface contribution. Consequently, one may write

$$S_{\lambda}(\mathbf{k}) = S_{\lambda}^B(\mathbf{k}) + S_{\lambda}^S(\mathbf{k}) , \quad (72)$$

where S_{λ}^B is the bulk contribution, and S_{λ}^S the surface correction to $S_{\lambda}(\mathbf{k})$. The quantity $NS_{\lambda}^S(\mathbf{k})$ is proportional to the area of the crystal surface. The surface exchange-correlation energy σ_{xc} may be then be written as

$$\sigma_{xc} = \frac{1}{(2\pi)^3} \int d\mathbf{k} \sigma_{xc}(\mathbf{k}) , \quad (73)$$

where $\sigma_{xc}(\mathbf{k})$, the wave-vector decomposition for the surface exchange-correlation energy, is given by

$$\sigma_{xc}(\mathbf{k}) = \frac{1}{2} \int_0^1 \frac{d\lambda}{\lambda} u(\mathbf{k}) NS_{\lambda}^S(\mathbf{k}) . \quad (74)$$

For purposes of physical interpretation and computational convenience it is preferable to work with the spherical average of $\sigma_{xc}(\mathbf{k})$ which is defined as

$$\sigma_{xc}(k) = \frac{1}{2} \int_0^{\pi} d\theta \sin\theta \sigma_{xc}(\mathbf{k}) . \quad (75)$$

In the wave-vector decomposition scheme, the local density approximation is given by an expression similar to that of Eq.(68) except that one employs the bulk structure factor $S_{\lambda}^B(\mathbf{k})$ at the local value of the density $\rho(\mathbf{r})$ rather than at the bulk value $\bar{\rho}$. Thus

$$E_{xc}^{LDA}(\mathbf{k}) = \int d\mathbf{r} \rho(\mathbf{r}) \int_0^1 \frac{d\lambda}{\lambda} u(\mathbf{k}) [S_{\lambda}^B\{\mathbf{k}; \rho(\mathbf{r})\} - 1] \quad , \quad (76)$$

and the corresponding surface energy term is

$$\sigma_{xc}^{LDA}(\mathbf{k}) = \int d\mathbf{r} \int_0^1 \frac{d\lambda}{\lambda} u(\mathbf{k}) [\rho(\mathbf{r}) S_{\lambda}^B\{\mathbf{k}; \rho(\mathbf{r})\} - \bar{\rho} S_{\lambda}^B\{\mathbf{k}; \bar{\rho}\}] \quad . \quad (77)$$

In order to describe the interpolation scheme, the surface exchange-correlation energy σ_{xc} is rewritten as

$$\sigma_{xc} = \frac{1}{(2\pi)^3} \int_0^{\infty} dk \, 4\pi k^2 \sigma_{xc}(k) = \int_0^{\infty} \frac{d\bar{k}}{2\bar{k}_F} \gamma(k) \quad , \quad (78)$$

where

$$\gamma(k) = 2\bar{k}_F [4\pi k^2 / (2\pi)^3] \sigma_{xc}(k) \quad . \quad (79)$$

Now Langreth and Perdew⁵⁸ were able to rigorously show that in the small wave-vector limit

$$\lim_{k \rightarrow 0} \gamma(k) = -\frac{\bar{k}_F k}{4\pi} (\omega_s - \frac{1}{2}\omega_p) \quad (80)$$

$k \rightarrow 0$

where $\omega_s = \omega_p / \sqrt{2}$ is the surface plasmon frequency and $\omega_p = (4\pi\rho e^2/m)^{\frac{1}{2}}$ the bulk plasmon frequency . Furthermore , they showed that in the large k limit the LDA expression Eq. (77) was exact and consequently $\gamma^{\text{LDA}}(k)$ can be obtained from it . The contribution for the intermediate wave-vectors is then obtained by interpolating in a systematic manner between the exactly known large and small wave-vector limits. The results of this interpolation scheme are accurate²² to about 1% when tested against the exactly solvable RPA results for the infinite barrier model given in Table II . The infinite barrier model represents the limit of rapid density variation. Later Perdew, Langreth and Sahni⁵⁵ also showed that this same scheme agrees with the results of the gradient expansion approximation for very slowly varying densities where the latter approximation is expected to be correct. Consequently, it was assumed that the scheme was accurate for the intermediate physical range of density profiles. In this work these authors also demonstrated that the GEA leads to overestimates of the surface energy for physical densities . In subsequent work on a wave-vector analysis of the first gradient expansion coefficient, Langreth and Perdew⁴¹ showed that this correction term made only a small contribution beyond the LDA in the intermediate wave-vector region . Furthermore, it was for small wave-vectors that the GEA compared poorly with the exact limiting behaviour . Thus the implicit assumption

of their original interpolation scheme was justified . They also showed that the densities at metallic surfaces were too rapidly varying for the GEA to give the appropriate correction to the LDA . In this work they also proposed a generalization of the gradient approximation with results which again agreed with those of the original scheme .

Arguments in support of the GEA as the most accurate representation of the exchange-correlation energy functional for surfaces are those of Rasolt and co-workers^{42,56} . As indicated in the introduction , their conclusions were arrived at indirectly by a study of the GEA for the screened-Coulomb exchange energy. To reiterate, these authors demonstrated the convergence of the GEA as a function of the screening parameter and not as a function of the density profile or its gradients. However, as we have shown in chapter II, when this expansion is tested as a function of varying density profiles, it does not converge to any appreciable degree, at least for the set of profiles employed by these authors . Other non-local representations of the exchange-correlation energy functional, such as the weighted and average density schemes^{52,57} have also proved to be inaccurate in comparison with the exact infinite barrier model results given in Table II.

Thus, from the above discussion it is evident that the most accurate method for the determination of the surface exchange-correlation energy of jellium metal is the wave-vector (WV) analysis scheme . Consequently, we write the total surface energy functional for the fully-correlated system as

$$\sigma_s[\rho] = \sigma_k + \sigma_{es} + \sigma_{xc}^{WV} \quad (81)$$

where

$$\sigma_{xc}^{WV} = \sigma_{xc}^{LDA} + \Delta\sigma_{xc}^{WV} , \quad (82)$$

where σ_k is the surface kinetic energy of a system of non-interacting electrons , σ_{es} is the electrostatic energy, σ_{xc}^{LDA} and $\Delta\sigma_{xc}^{WV}$ the LDA exchange-correlation energy and the wave-vector analysis scheme correction to it . For the LDA term we employ the same parameterization of the Monte Carlo calculation of Ceperley and Alder⁷ as used in our calculations for the infinite barrier model . In the work of Perdew, Langreth and Sahni⁵⁵ it was also shown that the non-local correction $\Delta\sigma_{xc}^{WV}$ was dependent only on the bulk value of density, and was essentially independent of the density profile at the surface . Hence we have treated this correction term as a constant ($1300/\bar{r}_s^3$ ergs/cm²) in our calculations.

We next define the surface energy for the exchange-only (XO) system as

$$\sigma_s^{XO} = \sigma_k + \sigma_{es} + \sigma_x \quad (83)$$

where σ_k and σ_{es} are as defined above and where σ_x is the exact non-local surface exchange energy, these components all being determined for the same set of orbitals used in Eq.(81) . Our estimate of the wave-vector method surface correlation energy σ_c^{WV} is then defined as the difference between the fully-correlated and exchange-only values :

$$\sigma_c^{WV} = \sigma_s[\rho] - \sigma_s^{XO} . \quad (84)$$

The Kohn-Sham equations corresponding to Eq.(81) can be solved self-consistently . However, due to the complexity of the exchange term, the task of determining the exchange-only energy with these numerically determined orbitals is prohibitive . Neither does a self-consistent optimized local-effective potential calculation of the exchange-only problem exist. Therefore, in order to determine the surface energy accurately we apply the variational principle for the energy to the functional of Eq.(81). For our variational densities we choose those generated by the linear potential model^{30,31} of a surface. Our choice is governed not only by the fact that these densities possess the requisite quantum-mechanical Friedel oscillations , but also that in a

variational procedure they reproduce³¹ the fully self-consistent LDA surface energies of Lang and Kohn⁶⁷. For this model the wavefunction of an electron, $\psi_k(x)$, is

$$\psi_k(x) = -[2/L]^{\frac{1}{2}} \{ \sin[kx+\delta(k)]\theta(-x) + \sin\delta(k)A(\xi)/Ai(-\xi_0)\theta(x) \}, \quad (85)$$

$$\delta(k) = \cot^{-1} \left[\frac{1}{\sqrt{\xi_0}} \frac{Ai'(-\xi_0)}{Ai(-\xi_0)} \right],$$

where $Ai(\xi)$ and $Ai'(\xi)$ the Airy function⁷³ and its derivative, $\xi = x(\bar{k}_F^2/x_F)^{1/3} - \xi_0$, $\xi_0 = (\bar{k}_F x_F)^{2/3} k^2/\bar{k}_F^2$. The variational or slope parameter is x_F : the case $x_F=0$ corresponds to the infinite barrier model, and as x_F is increased the density profile at the surface becomes more slowly varying. The charge neutrality is satisfied by adjusting the jellium edge position to satisfy the Sugiyama sum rule⁶⁰ of Eq.(29). With change of variables to $y = \bar{k}_F x$ ($y_F = \bar{k}_F x_F$) and $q = k/\bar{k}_F$, the density, its first derivative and other properties such as the jellium edge position $y_a = \bar{k}_F a$, the electronic surface dipole barrier ($\Delta\phi$), the electrostatic potential V_{es} , the exact non-local surface exchange σ_x , the surface kinetic σ_k , and the surface electrostatic energy σ_{es} can all be written in terms of universal functions of the slope parameter $y_F = \bar{k}_F x_F$. The semi-analytical expressions for these properties are given^{25,30,74} in Appendix B.

Our procedure for the determination of the surface correlation energy is as follows : for a specific metal defined by its bulk value of the Wigner-Seitz radius \bar{r}_s , we minimize the energy for the fully-correlated system with respect to the variational parameter y_F . Then, in the spirit of density-functional theory we determine the exchange-only energy for these same set of orbitals. From these two sets of values we obtain σ_c^{WV} via Eq.(84). (It is interesting to note that the results of the exchange-only calculations of Sahni and Ma (Ref.(29)) differ only slightly from the results of the present work for the exchange-only component of the total energy for the fully-correlated system. This supports our contention that the exchange-only energy for the fully-correlated and Pauli-correlated systems are equivalent. Had the calculations of Sahni and Ma²⁹, and those of the present work been fully-self-consistent, the exchange-only energies in each case, we believe, would have been the same.)

The results⁷⁵ for the exact non-local surface exchange energy σ_x , the 'exact' surface correlation energy σ_c^{WV} , and the percentage that the latter is of the former are given in Table V and plotted in Fig.12. We note first that the results for the magnitudes of both the exchange and correlation energies for a specific metal are considerably different from the corresponding results of the infinite barrier model (Table II). Again, in sharp contrast to the infinite barrier model results, as the

Table V.

The surface exchange, correlation, and exchange-correlation energies in ergs/cm² as a function of the Wigner-Seitz radius \bar{r}_s in (a.u.). The results quoted are those of the local density approximation (LDA), the exact non-local exchange energy, the wave-vector analysis estimates of the 'exact' exchange-correlation (and correlation) energies, and the total energy. The LDA exchange-correlation and correlation energies are determined via the Ceperley-Alder⁷ expression for the average correlation energy per particle. The energy minimized values of the variational parameter y_F are also given.

| Wigner-Seitz Radius \bar{r}_s (a.u.) | Variational Parameter y_F | SURFACE ENERGIES (ergs/cm ²) | | | | | | Total | $\left(\frac{\text{Correlation}}{\text{Exchange}} \right) \times$ "EXACT" (wave-vector) |
|---|-----------------------------------|--|-------|-------------|--------------------------|----------------------|--------------------------|-------|--|
| | | Exchange | | Correlation | | Exchange-Correlation | | | |
| | | LDA | EXACT | LDA | "EXACT" (wave-vector) | LDA | "EXACT" (wave-vector) | | |
| 2.0 | 3.3948 | 2979 | 2569 | 312 | 885 | 3291 | 3454 | -664 | 34 |
| 2.5 | 2.6677 | 1313 | 1086 | 164 | 475 | 1478 | 1561 | 187 | 44 |
| 3.0 | 2.1170 | 674 | 533 | 96 | 285 | 770 | 818 | 278 | 53 |
| 3.5 | 1.6945 | 384 | 292 | 61 | 184 | 446 | 476 | 240 | 63 |
| 4.0 | 1.3721 | 238 | 176 | 42 | 124 | 280 | 300 | 189 | 70 |
| 4.5 | 1.1257 | 157 | 112 | 30 | 88 | 186 | 200 | 146 | 79 |
| 5.0 | 0.9362 | 108 | 77 | 22 | 63 | 130 | 140 | 113 | 82 |
| 5.5 | 0.7887 | 78 | 55 | 17 | 48 | 95 | 103 | 89 | 87 |
| 6.0 | 0.6740 | 58 | 39 | 13 | 38 | 71 | 77 | 71 | 97 |

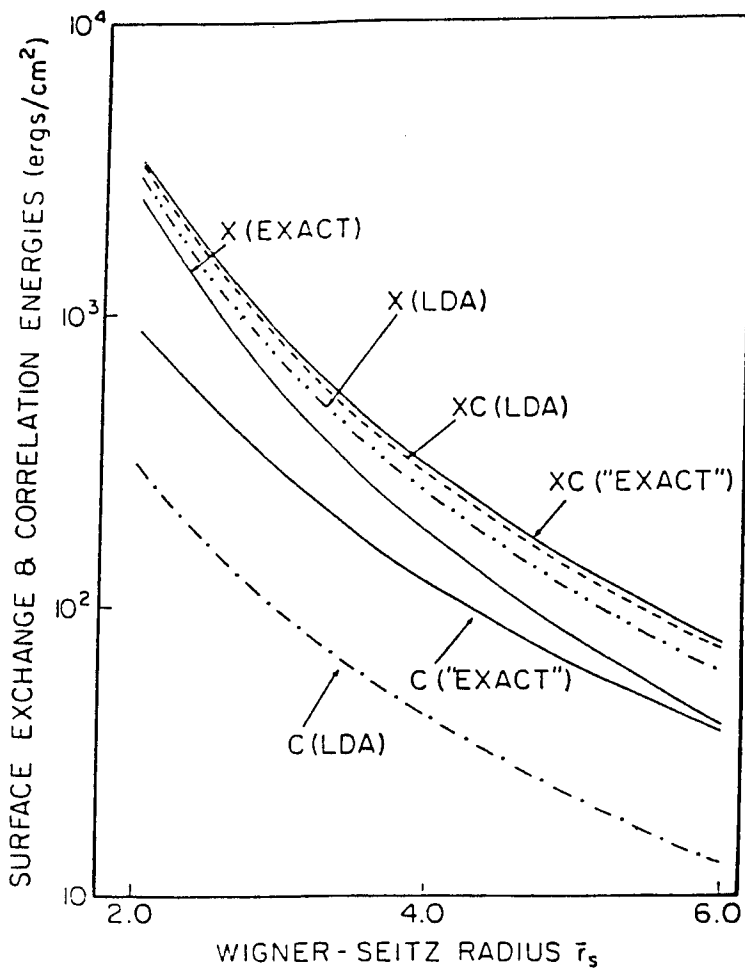


Figure 12

Variation of the exact and local density approximation (LDA) results for the surface exchange (X), correlation (C), and exchange-correlation (XC) energies as a function of the Wigner-Seitz radius \bar{r}_s . The "EXACT" C and XC results are wave-vector analysis estimates, and are considered to be exact. The non-local surface exchange X energy is determined exactly.

density is increased, the correlation energy becomes a smaller fraction of the exchange energy. (See the last column of Table V). However, for very low densities ($\bar{r}_s = 6$), the conclusion that correlation is as significant as exchange is the same. It is also interesting to observe how much more significant the effects of correlation are for the non-uniform gas at surfaces when compared to either the uniform electron gas or the non-uniform system in atoms.

In order to make comparisons between the density-functional theory and conventional definitions of the correlation energy we must assume that the present exchange-only results or those of Sahni and Ma²⁹ are equivalent to Hartree-Fock since the latter do not exist . There seems little reason to doubt this assumption in light of the closeness of the exchange-only and Hartree-Fock results in atoms . Of the many correlated wavefunction calculations of Woo and co-workers³² we use those with the lowest surface energy. Unfortunately their results do not exist for half integer values of \bar{r}_s and we have had to extrapolate to obtain these results . For $\bar{r}_s = 2.5-3.5$ their results for the correlation energy are 100-180 ergs/cm² greater than our values, whereas for $\bar{r}_s = 2$ their value is about 450 ergs/cm² greater. For $\bar{r}_s = 4.5$ the two values are the same, and for $\bar{r}_s > 4.5$ the conventional values are less than the density-functional theory values by 20-13 ergs/cm² . Thus, it is only for the high and medium density metals that the two theories give

significantly different results. Presumably, the two would more closely approximate each other if in the quantum-mechanical calculation, the expectation value of terms in the Hamiltonian other than the kinetic energy were also determined exactly. The Yamashita and Ichimaru⁷⁶ density -functional theory estimates of the surface correlation energy are about 333% greater than the present wave-vector estimates over the entire range of metallic densities . Consequently, their correlation energies are always greater than the exchange energy values.

In Table V we also quote the LDA surface exchange, correlation, and exchange-correlation energies as well as the total wave-vector exchange-correlation energies, and these results are also plotted in Fig.12 . The remarkable cancellation of the errors in the local exchange and local correlation energies is evident from the figure. Note that the energy axis in this figure is logarithmic . The local value of the correlation energy is nearly as much an underestimate of the true value as the local exchange is an overestimate. This cancellation of errors in the present work has been demonstrated for physically realistic density profiles. The fact that a similar conclusion is arrived at for the infinite barrier model densities is one of the rare instances for which this model's conclusions are in agreement with those of more realistic calculations. Finally, as in the atomic physics case , the LDA surface exchange-correlation energies obtained by the variational procedure are

within 10% of the 'exact' results . Thus , as also concluded by others^{50,58} , the LDA for exchange-correlation is a good first approximation for surface physics calculations.

4.2 Convergence Study of the Gradient Expansion Approximation for the Surface Correlation Energy .

In this section we study the GEA for the correlation energy, to $O(\nabla^2)$, as applied to jellium metal surfaces . As indicated in the introduction, the coefficient B_c of the first gradient correction term is known⁴⁶ only in the high density limit and has not been determined independently for the metallic density range . However , for these densities both the coefficients B_{xc} and B_x are known, and consequently we define the coefficient B_c as their difference . The coefficient B_{xc} was originally determined by Rasolt and Geldart⁴³ (RG) using many-body perturbation theory in a calculation along the lines of Ref.(46) that went beyond the RPA but which treated the additional terms in an approximate manner . More recently Langreth and Perdew⁴¹ (LP) have derived this coefficient within a density-functional theory version of the RPA . Although the intrinsic physics of these two calculations is the same , the coefficients differ slightly due to the approximations made in the work of RG . In our study we consider both these coefficients. (The analytic polynomial fit expression for these coefficients as well as the numerical values of the coefficients B_{xc} are given in Appendix C) . We also examine the convergence of the correlation energy modified GEA using the recently derived Langreth-Mehl⁵³ (LM) expression for the coefficient B_{xc} which is

$$B_{xc}^{LM} = a (2e^{-F} - 7/9)$$

$$F = b |\nabla\rho(\mathbf{r})| / [\rho(\mathbf{r})]^{7/6}$$

$$a = \pi / [8(3\pi^2)^{4/3}] = 4.287 \times 10^{-3} \quad (86)$$

$$b = (9\pi)^{1/6} f = 1.745 f$$

$$f = 0.15$$

where the constants a and b are given in units where the energy and length are in Rydbergs and Bohrs respectively. (In the present work we do not consider the coefficients derived by Lau and Kohn⁴⁴ nor that due to Gupta and Singwi⁴⁵. For a study of the Gupta-Singwi exchange-correlation GEA to $O(\nabla^4)$ we refer the reader to Appendix C of Ref. (74)).

Now in order to investigate the convergence of the LDA and GEA for the correlation energy we need to assume a formalism which leads to essentially exact results. As in section 4.2 we again assume that formalism to be the wave-vector analysis scheme. Thus we write the 'exact' surface correlation energy σ_c^{WV} as

$$\sigma_c^{WV} = \sigma_{xc}^{WV} - \sigma_x, \quad (87)$$

where σ_{xc}^{WV} is as defined before and σ_x is again the exact non-local surface exchange energy, both quantities being determined for the same set of orbitals. We perform our convergence studies for the orbitals of the linear-potential model which permits the density profile to change continuously from rapidly to slowly varying as the density profile parameter is increased from $y_F = 0$. (Typical real metal surface densities lie⁷⁷ in the range $1 \leq y_F \leq 4.5$. For jellium metal (see Table V) the range is $y_F = 0.6 - 3.5$).

We begin our discussion with results of the infinite barrier model ($y_F=0$) (see Table II). The GEA for the exchange energy is given¹⁸ by $(-0.3157)/k_F^3 (10^{-3} \text{ a.u.})$ and therefore underestimates the exact values by 155%, whereas the GEA for correlation is an overestimate by 430%-525%. Since the magnitude of the exchange and correlation energies are approximately the same, there is some cancellation of the errors, so that the GEA for exchange-correlation is in error by 179%-227%. It is obvious from these results that the densities are too rapidly varying for either of these expansions to be accurate. One might expect on the basis of the infinite barrier model results that the cancellation of the errors would be more effective as the density is made slowly varying. However, this is not the case since we know that the GEA for exchange converges¹⁸ rapidly to the exact results. Consequently, all the error in the GEA for exchange-correlation is due to the GEA for correlation.

In Table VI and Fig.13 we present the results for the 'exact' wave-vector surface correlation energy , as well as the LDA and various GEA values, as a function of the density profile parameter y_F for the fixed value $\bar{r}_s = 4$ which corresponds to the bulk density of Sodium . (The trends in the results, and conclusions, for both higher and lower density metals are similar and will not be presented) . As is evident from Fig.13 and the percent error plot of Fig.14 , the LDA is substantially in error over the entire range of densities considered . Even at $y_F=6$ it is in error by 32% . The GEA(LP) results (see Fig.14) are not a significant improvement over the LDA values being in error by 14% at $y_F=6$. For the physical density profile of $y_F=1.37$ (see Table V), the GEA(LP) results are as much in error as those of the LDA . Thus the density profiles have to be extremely slowly varying before the GEA for the correlation energy could be considered as being accurate . On the other hand, the GEA(LM) results are essentially exact for densities corresponding to $y_F \geq 1$ (see Fig.14). This is understandable since the GEA(LM) is based on the wave-vector method . For rapidly varying densities ($y_F < 1$) for which a key approximation made in the GEA(LM) is badly violated , the results are poor , although they are still superior to those of both the LDA and GEA(LP) (see Fig.14) .

Table VI.

Surface correlation energies in ergs/cm² as a function of the density profile parameter y_F for the fixed bulk density value of $\bar{r}_s=4$. Here the 'exact' results are those of the wave-vector scheme. The numbers in parentheses in this column correspond to the uncertainties in these values due to the uncertainties in the surface exchange energies (see Eq.(87)). The local density approximation (LDA) results are obtained via the Ceperley-Alder⁷ expression for the average correlation energy per particle. The gradient expansion approximation (GEA) values are those employing the first gradient correction coefficients of Rasolt-Geldart^{4,3} (RG), Langreth-Perdew^{4,1}(LP) and Langreth-Mehl^{5,3} (LM).

| y_F | 'EXACT' (Wave-vector) | Local-Density Approximation | Gradient Expansion Approximation | | |
|-------|--------------------------|--------------------------------|----------------------------------|-----|-----|
| | | | RG | LP | LM |
| 0.0 | 102 | 26 | 310 | 450 | 160 |
| 0.1 | 105 (1) | 28 | 198 | 274 | 147 |
| 0.2 | 106 (1) | 29 | 187 | 255 | 140 |
| 0.3 | 107 (1) | 31 | 180 | 243 | 136 |
| 0.5 | 111 (1) | 33 | 170 | 227 | 131 |
| 1.0 | 118 (2) | 38 | 157 | 204 | 127 |
| 1.5 | 121 (2) | 42 | 150 | 192 | 126 |
| 2.0 | 127 (2) | 48 | 145 | 183 | 127 |
| 2.5 | 130 (2) | 54 | 141 | 176 | 127 |
| 3.0 | 131 (3) | 59 | 139 | 170 | 128 |
| 3.5 | 134 (3) | 65 | 139 | 168 | 131 |
| 4.0 | 137 (3) | 72 | 139 | 166 | 133 |
| 4.5 | 138 (4) | 79 | 140 | 165 | 136 |
| 5.0 | 143 (5) | 87 | 143 | 166 | 141 |
| 5.5 | 148 (5) | 94 | 146 | 168 | 145 |
| 6.0 | 150 (6) | 102 | 150 | 170 | 151 |

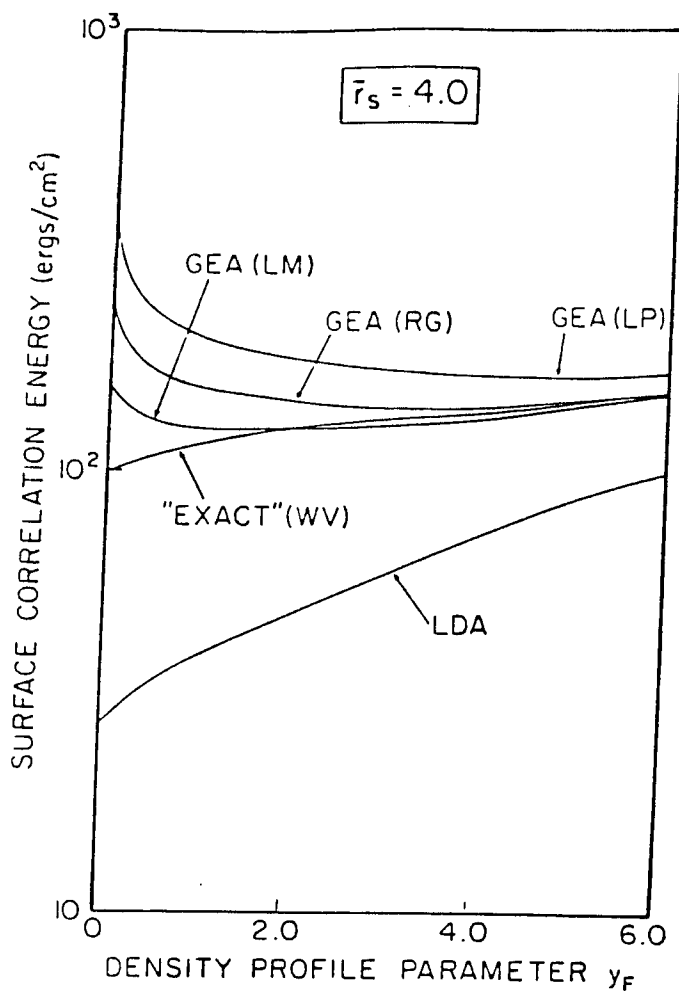


Figure 13

Variation of the 'exact' (wave-vector) (WV), local density approximation (LDA), and gradient expansion approximation (GEA) surface correlation energies, as a function of the density profile parameter γ_F for a bulk density corresponding to $\bar{r}_s = 4$. The different GEA results correspond to different coefficients of the first gradient correction term as derived by Rasolt-Geldart⁴³ (RG), Langreth-Perdew⁴¹ (LP) and Langreth-Mehl⁵³ (LM).

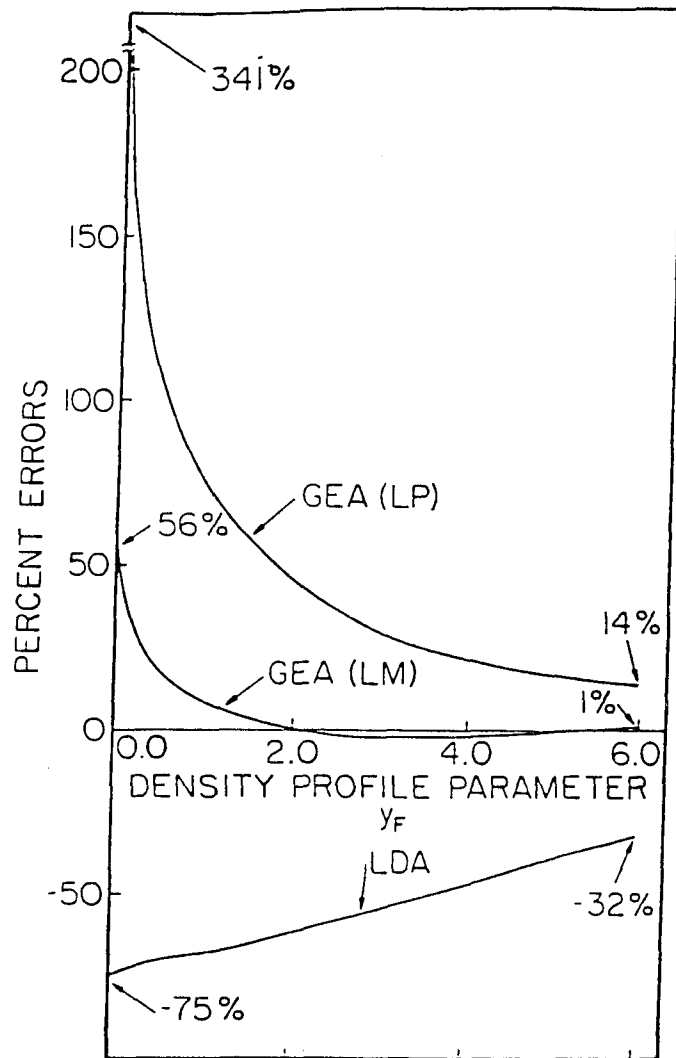


Figure 14

Percent error plots of the results of Fig. 13 corresponding to the local density approximation (LDA), and gradient expansion approximations (GEA) due to Langreth-Perdew (LP) and Langreth-Mehl (LM), as a function of the density profile parameter y_F .

Next , the fact that for the LDA and GEA functionals the corresponding energy densities are easily determined , makes it possible to plot the 'exact' correlation energy density since the GEA(LM) results are essentially exact for $y_F \geq 1$. In Fig.15 we display the LDA , GEA(LP) and the 'exact' GEA(LM) correlation energy densities for $y_F = 1 , 4$ and 6 . We observe that in general, the 'exact' energy densities lie between those of the LDA and GEA(LP) curves . This fact thus explains why it is that the LDA underestimates the exact results whereas the GEA(LP) leads to an overestimate . Furthermore , the principal contribution to the surface correlation energy comes from within half a Fermi wavelength about the jellium edge .

In their work, Langreth and Mehl⁵³ also arrived at a certain formal quantitative criterion for the validity of the GEA for the exchange-correlation energy that differs from that derived previously by Langreth and Perdew⁴¹ . This convergence condition , which is less severe by a factor of six, is

$$\frac{|\nabla\rho(\mathbf{r})|}{k_{TF}(\mathbf{r})\rho(\mathbf{r})} \ll 1 \quad (88)$$

where $k_{TF}(\mathbf{r}) = [4k_F(\mathbf{r})/\pi]^{1/2}$ is the Thomas-Fermi wave-vector . Now since Sahni et al¹⁸ have shown that the GEA for exchange converges rapidly to the exact result for the surface physics problem, this

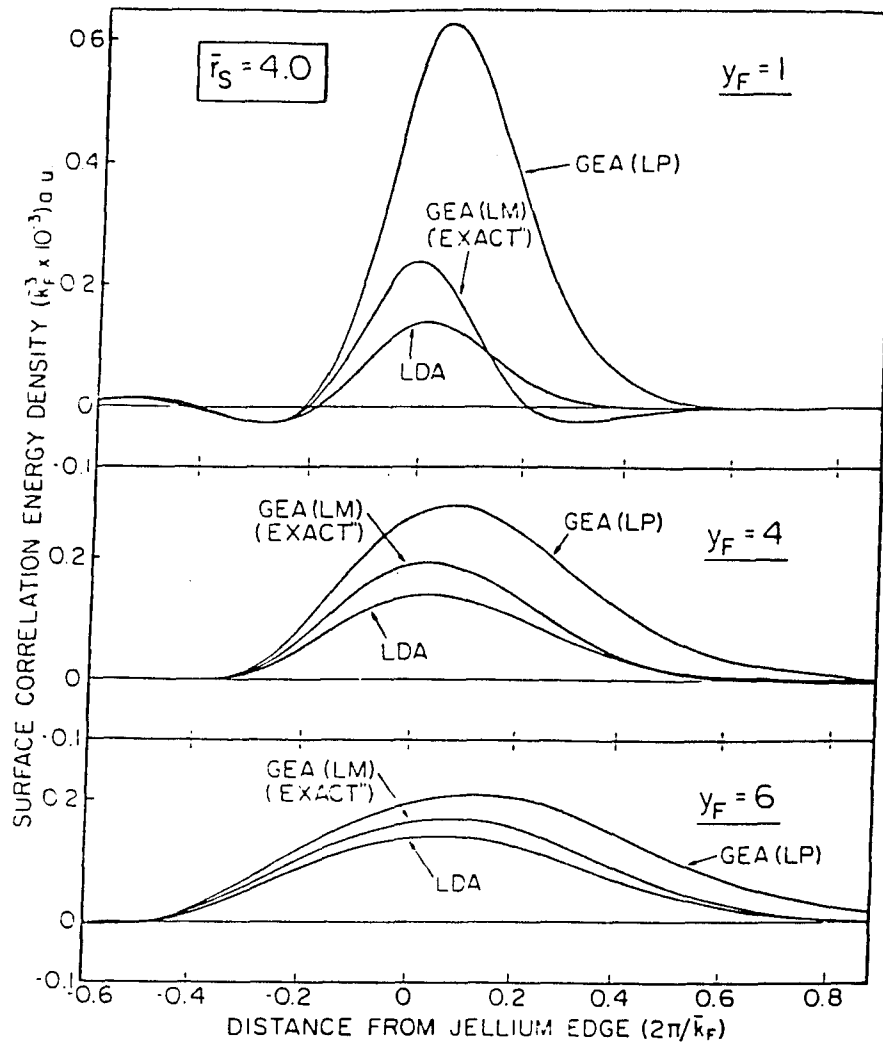


Figure 15

Variation of the surface correlation energy density as a function of the distance from the jellium edge for different values of the density profile parameter y_F for a bulk density corresponding to $\bar{r}_s = 4$. The results shown are those within the local density approximation (LDA) and the gradient expansion approximations (GEA) due to Langreth-Perdew (LP) and Langreth-Mehl (LM). The GEA (LM) results are considered essentially exact.

convergence condition may be thought of as being that for the correlation energy GEA . We display in Fig.16 the 'small parameter' of Eq. (88) corresponding to the most slowly varying profile considered in this study ($y_F = 6$) for different values of the bulk density ($\bar{r}_s = 2, 4, 6$) . Note that the convergence condition is poorly satisfied in the region about the jellium edge , a result consistent with the lack of the convergence of the GEA(LP) curve (see Fig.14) . On the other hand, the GEA(RG) results, though substantially in error at the physical energy minimized value of the density $y_F=1.37$, are inconsistent with the convergence condition results of Fig.16 . For $y_F \geq 2.5$ the GEA(RG) values are in error by less than 10% having already converged by $y_F = 4$. Thus, the differences in the LP and RG coefficients B_c of the first gradient correction term (See Appendix C) lead to significantly different conclusions with regard to the convergence of this expansion . In light of the consistency between the GEA(LP) and the convergence condition results , we conclude that the density profiles at metallic surfaces would have to be very slowly varying ($y_F > 6$) for the correlation energy GEA to be accurate .

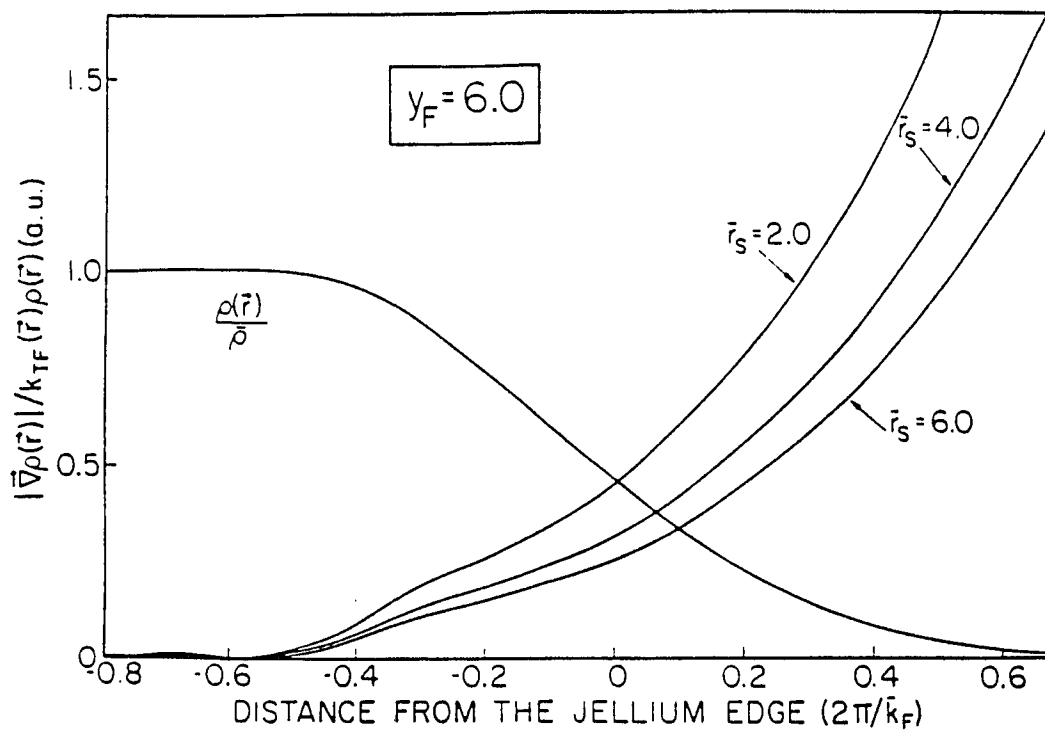


Figure 16

Variation of the 'small parameter' of Eq. (88) for different values of the bulk density ($\bar{r}_s = 2, 4, 6$), as a function of the distance from the jellium edge for the slowly varying density corresponding to $y_F = 6$. The density profile normalized to the bulk density is also plotted.

Chapter V

5.1 Summary and Conclusions

In this thesis , we have studied within density-functional theory the correlation energy at metallic surfaces. We have examined both the qualitative and quantitative differences between the conventional quantum-mechanical and Kohn-Sham density-functional theory definitions of the correlation energy of interacting non-uniform electron gas systems. Employing the most recent experimental and theoretical values existing in the literature, we observe that for atoms upto an atomic number of $Z = 18$, the two correlation energies differ by less than 1% , and that the conventional value is consistently the larger . In order to enable similar comparisons for the inhomogeneous electron gas at surfaces, we have performed variational calculations to estimate the density-functional theory surface correlation energy of jellium metal using the accurate surface density profiles generated by the linear-potential model . The accuracy of these estimates is founded in the assumption that the exchange-correlation energy functional of the density is accurately approximated by the wave-vector analysis method. These results are the first realistic estimates of this property, having been determined by treating the non-local exchange energy contributions exactly. Meaningful comparisons with correlated

wavefunction calculations cannot be made at present since these calculations do not treat the expectation value of all terms of the non-relativistic Hamiltonian exactly . However, a comparison with the existing results indicate that for high and medium density metals the conventional correlation energies are substantially larger whereas for low density metals they are slightly less than the density-functional theory values. An important result of our calculations is that in contrast to the case of atoms for which the correlation energy is less than 5% of the exchange energy, this ratio for surfaces varies from 34%-97% over the metallic density range, being the smaller percentage for the higher density metals as one might expect . This is a significant physical difference between the two non-uniform systems . In addition, these results also contrast with previous conclusions, that for surfaces correlation effects are always as significant as exchange even for medium and high density metals.

In this work we have also examined the local density approximation for the exchange-correlation and correlation energy functionals , as well as various gradient expansion approximations for the correlation energy functional, as applied to surfaces. We have first demonstrated that for realistic metal surface densities the errors in the local density approximation for exchange and correlation taken separately do in fact cancel, and that consequently the local density approximation for

exchange-correlation is a good first approximation for surface physics calculations. We have also shown, that as in case of atoms, the local density approximation for the surface correlation energy is very substantially in error , and that the density profiles would have to be unphysically slowly varying even for the correlation energy gradient expansion approximation to converge to the exact results. This latter fact is substantiated by consideration of quantitative convergence conditions for this property which are shown not to be satisfied . We have also considered a recently derived gradient expansion approximation due to Langreth and Mehl and have shown this expansion to be very accurate. As a consequence of this fact we have utilized the results of this expansion to plot and study the behaviour of the 'exact' surface correlation energy density as a function of the density profile. A comparison with the corresponding local density and gradient expansion approximation energy densities then explains why these approximations for the correlation energy fail for metal surfaces.

We have also studied the effects of correlation at surfaces by screening the exchange , or put another way, we have studied the effects of considering only the short-ranged part of the Coulomb interaction on the surface properties of jellium metal. For this interaction we have derived a semi-analytical expression for the non-local surface exchange energy for the densities of the step-potential

model. This expression is a universal function of the screening parameter. We observe that the surface exchange energy for screened-Coulomb interaction not only decreases but that it becomes more independent of the density profile as the screening length is reduced . Thus we show that the total surface energy decreases with screening length, and that consequently the more short-ranged the interaction , the easier it is to split the crystal in two. As a consequence, we can also demonstrate that for fixed density profile and interaction strength, the greater the density of the electrons, the higher the surface energy.

Next we have derived the coefficient of the first gradient correction term in the expansion for the screened-Coulomb exchange energy within the context of density-functional theory. For finite screening this coefficient is equivalent to that derived within Hartree-Fock theory. It reduces to the bare-Coulomb interaction value in the limit of no screening, in which limit, as is well known , the Hartree-Fock theory coefficient is singular. In contrast to the Hartree-Fock coefficient, the density-functional theory coefficient is a universal function of the screening parameter, as is the LDA coefficient. The fact that the gradient correction coefficient derived here has this universal feature is particularly significant since the GEA is intrinsically an approximation within density-functional theory, and it is imperative that each term in

the expansion exhibit the same universality as that exhibited by the exact term.

Finally, we have evaluated the arguments of others in support of both the LDA and GEA for the exchange-correlation energy at metallic surfaces. These arguments are based on studies assuming a screened-Coulomb interaction. By studying the local density and gradient expansion approximations for the screened-Coulomb exchange energy within both the Hartree-Fock and density-functional theories as a function of the density we have shown the arguments and conclusions of these authors to be incorrect. What we have observed is that quite contrary to intuitive expectations for a short-ranged interaction, both the GEA as well as LDA are poor. Furthermore, the former approximation does not reduce the error of the latter to any significant degree even for the most slowly varying of the densities considered. By an examination of various convergence conditions we have concluded that this lack of convergence is principally due to the limitations of the step-potential model densities employed.

5.2 Future Work

In recent work on the density-functional theory GEA for the exchange energy, Kleinman⁷⁸ has claimed that the coefficient of the

first gradient correction term is not that due to Sham⁴⁰ but rather $8/7$ ths. of Sham's value . Furthermore, his results (for this coefficient) for the screened-Coulomb case do not reduce to the bare-Coulomb value in the limit of no screening . As derived in our work , the coefficient for the screened-Coulomb case does give the Sham result in this limit . Furthermore, the coefficient that we have derived for the case of screened interaction leads to the same universal features for the GEA as those possessed by the exact and local density results for the surface exchange energy. It is evident that Kleinman's derivation and the physics involved therein must be examined.

As indicated before, our results indicating the lack of the convergence of both the LDA and GEA for screened-Coulomb interaction are surprising . Obviously the fact that the convergence conditions are not satisfied for the step-potential model densities is one explanation of this fact. Therefore, in order to arrive at more definitive conclusions with regard to the convergence of the LDA and GEA for this interaction, the analysis should be performed for the physically accurate linear-potential model densities. However, in order to better understand the results of the present work, as well as to explain the success of the GEA for bare-Coulomb surface exchange energy, a wave-vector analysis of the exact, LDA and GEA surface exchange energies for both bare- and screened-Coulomb interactions should also be performed.

Appendix A

Density-Functional Theory First Gradient Coefficient for the Screened-Coulomb Exchange Energy.

In this appendix we apply the method of Sham⁴⁰ to derive an expression for the first gradient correction coefficient in the expansion for the screened-Coulomb exchange energy within density-functional theory.

The Hartree-Fock equations for an electron of momentum k are

$$\left[-\frac{\hbar^2}{2m} \nabla^2 + v(r) + \int u(r-r') \rho(r') dr' \right] \Psi_k(r) - \int u(r-r') \rho(r, r') \Psi_k(r') dr' = \varepsilon(k) \Psi_k(r) \quad (A1)$$

where $\rho(r)$ is the density, $\rho(r, r')$ the single-particle density matrix defined as

$$\rho(r, r') = \sum_{\mathbf{k}} \Psi_{\mathbf{k}}^*(r') \Psi_{\mathbf{k}}(r) , \quad (A2)$$

$u(r)$ is an arbitrary interparticle interaction and $v(r)$ is the external potential. The eigenenergy, in an electron gas of uniform density, is

$$\varepsilon(\mathbf{k}) = \frac{\hbar^2 \mathbf{k}^2}{2m} + \varepsilon_X(\mathbf{k}) = \varepsilon_0(\mathbf{k}) + \varepsilon_X(\mathbf{k}) \quad (\text{A3})$$

where the exchange energy (for the state \mathbf{k}) is

$$\varepsilon_X(\mathbf{k}) = - \int \frac{d\mathbf{k}'}{(2\pi)^3} u(\mathbf{k} - \mathbf{k}') f[\varepsilon(\mathbf{k}')], \quad (\text{A4})$$

and where $f[\varepsilon(\mathbf{k})]$ is the Fermi function, and $u(\mathbf{k})$ the Fourier transform of $u(\mathbf{r})$.

Now it can be shown by perturbation theory and by going into momentum space (see Appendix A of the second reference of Ref.(43)) that Eq.(A3) together with the following equations (A5) - (A7)

$$\tilde{\Lambda}(\mathbf{k}+\mathbf{q}, \mathbf{k}) = 1 - \int \frac{d\mathbf{k}'}{(2\pi)^3} \Theta(\mathbf{k}'+\mathbf{q}, \mathbf{k}') u(\mathbf{k}-\mathbf{k}') \tilde{\Lambda}(\mathbf{k}'+\mathbf{q}, \mathbf{k}') \quad (\text{A5})$$

where

$$\Theta(\mathbf{k}'+\mathbf{q}, \mathbf{k}') = \frac{f_{\mathbf{k}'+\mathbf{q}} - f_{\mathbf{k}'}}{\varepsilon(\mathbf{k}'+\mathbf{q}) - \varepsilon(\mathbf{k}')}, \quad (\text{A6})$$

and

$$\chi(q) = 2 \int \frac{dk}{(2\pi)^3} \theta(k+q, k) \tilde{\lambda}(k+q, k), \quad (\text{A7})$$

constitute the self-consistent solution of the Hartree-Fock equations (A1). The function $\tilde{\lambda}(k+q, k)$ is called the irreducible vertex function and $\chi(q)$ the density response function.

From the work of Hohenberg and Kohn² we know that the coefficient B_i ($i=x, sx$) (see Eq. (22)) of the gradient expansion is the q^2 coefficient in the expansion of the function K_i which is related to the reciprocal of the density response function by

$$K_i = - \frac{1}{\chi(q)} + \frac{1}{\chi_0(q)} = K^{(0)} + q^2 K^{(2)}, \quad (\text{A3})$$

where the superscripts denote the order of q . Here $\chi_0(q)$ is the response function for the non-interacting electrons. The subscript zero denotes no interaction between the electrons i.e. $e^2=0$ where e is the electronic charge. Subscripts will denote the order of e^2 being considered. Next we expand the response function $\chi(q)$ and $\chi_0(q)$ in powers of q as

$$\chi(q) = \chi^{(0)} + q^2 \chi^{(2)} \quad (\text{A9})$$

and

$$\chi_o(q) = \chi_o^{(0)} + q^2 \chi_o^{(2)} . \quad (\text{A10})$$

From Eqs. (A8) - (A10), the coefficient B_i is then obtained as

$$B_i = K_i^{(2)} = \frac{\chi^{(2)}}{[\chi^{(0)}]^2} - \frac{\chi_o^{(2)}}{[\chi_o^{(0)}]^2} . \quad (\text{A11})$$

Now the Hartree-Fock exchange energy (see Eqs. (45) and (46) with the $\Psi_{\mathbf{k}}$ being solutions of Eq. (A1)) contains terms of $O(e^2)$, $O(e^4)$, etc. The $O(e^4)$ and higher-order terms arise from the dependence of the Hartree-Fock orbitals. Thus, in order to obtain the coefficient B_i in Hartree-Fock theory one must consider all orders of e^2 . This is what Kleinman³⁸ did. He expanded the function θ and $\tilde{\Lambda}$ to $O(q^2)$, and then showed that for the screened-Coulomb interaction, the term $\chi^{(2)}$ (and thus B_i) diverged as $\ln k_s$ as $k_s \rightarrow 0$, where k_s is the screening parameter. Geldart and Rasolt³⁹ also derived the same result, but in addition they showed that it was the e^4 contribution to $\chi^{(2)}$ that is divergent. In density-functional theory, the Kohn-Sham orbitals do not depend upon e but on the electron density. Thus, if one performed a perturbation calculation along the lines of Geldart and Rasolt, the only terms that would exist in the expansion would be of $O(e^2)$ due to the e^2 outside the exchange energy expression (see

Eq.(45)). Consequently, in density-functional theory, the gradient expansion approximation is purely of $O(e^2)$. The next significant point is that the density dependence of B_i must be $\rho^{4/3}(\mathbf{r})$ for the following reasons. First, if we scale the whole system by multiplying the linear dimension with a factor S , the total exchange energy scales by the same factor. Secondly, we know that we cannot introduce any higher order powers of e^2 because these enter as $e^2/\pi k_F$ which give rise to additional terms proportional to $\rho^{-1/3}(\mathbf{r})$. Thus, the gradient expansion approximation in density-functional theory terminates in the term of $O(\nabla^2)$ with the $\rho^{-4/3}$ dependence of B_i .

Based on the above discussion we see that in order to obtain B_i , we must expand the individual terms of $\chi(q)$ of Eq.(A9) to $O(e^2)$. Thus, we write

$$\chi^{(0)} = \chi_o^{(0)} + \chi_1^{(0)} \quad (\text{A12})$$

and

$$\chi^{(2)} = \chi_o^{(2)} + \chi_1^{(2)} \quad (\text{A13})$$

Substituting Eqs. (A10), (A12) and (A13) into (A11) we have (on retaining terms of $O(e^2)$ only) that

$$B_i = \frac{\chi_o^{(2)}}{[\chi_o^{(0)}]^2} \left[\frac{\chi_1^{(2)}}{\chi_o^{(2)}} - \frac{2\chi_1^{(0)}}{\chi_o^{(0)}} \right] \quad (\text{A14})$$

In the expression of Eq. (A3) for $\varepsilon(\mathbf{k})$, it is the $\varepsilon_x(\mathbf{k})$ term that is of $O(e^2)$ whether it be for the bare or screened-Coulomb interactions. With the expansion $\theta = \theta_o + \theta_1$ where θ_1 is the $O(e^2)$ term of θ , and where θ_o is the same as θ of Eq. (A6) with $\varepsilon(\mathbf{k})$ replaced by $\varepsilon_o(\mathbf{k})$, we have on substituting (A5) into (A7) and retaining only terms upto $O(e^2)$, that

$$\begin{aligned} \chi(\mathbf{q}) = & 2 \int \frac{d\mathbf{k}}{(2\pi)^3} \theta_o(\mathbf{k}+\mathbf{q}, \mathbf{k}) \\ & - 2 \int \frac{d\mathbf{k}}{(2\pi)^3} \theta_o(\mathbf{k}+\mathbf{q}, \mathbf{k}) \left[\int \frac{d\mathbf{k}'}{(2\pi)^3} u(\mathbf{k} - \mathbf{k}') \theta_o(\mathbf{k}'+\mathbf{q}, \mathbf{k}') \right. \\ & \left. + \frac{[\varepsilon_x(\mathbf{k}+\mathbf{q}) - \varepsilon_x(\mathbf{k})]}{[\varepsilon_o(\mathbf{k}+\mathbf{q}) - \varepsilon_o(\mathbf{k})]} \right] \end{aligned} \quad (\text{A15})$$

$$= \chi_o(\mathbf{q}) + \chi_1(\mathbf{q}), \quad (\text{A16})$$

where again in Eq.(A16) the subscripts denote the order of e^2 . For the screened Yukawa interaction

$$u(\mathbf{r}-\mathbf{r}') = e^2 \frac{e^{-k_s |\mathbf{r}-\mathbf{r}'|}}{|\mathbf{r}-\mathbf{r}'|} \quad (\text{A17})$$

whose Fourier transform is

$$u(\mathbf{k}-\mathbf{k}') = \frac{4\pi e^2}{|\mathbf{k}-\mathbf{k}'|^2 + k_s^2} \quad (\text{A18})$$

we have³⁵ from Eq. (A4) that

$$\begin{aligned} \varepsilon_{sX}(k) = & - \frac{e^2}{\pi} k_F \left[1 - \frac{k_s}{k_F} \left[\tan^{-1} \frac{k+k_F}{k_s} - \tan^{-1} \frac{k-k_F}{k_s} \right] \right. \\ & \left. + \frac{(k_F^2 + k_s^2 - k^2)}{4kk_F} \ln \left(\frac{(k+k_F)^2 + k_s^2}{(k-k_F)^2 + k_s^2} \right) \right] \quad (\text{A19}) \end{aligned}$$

(Note that in Eq. (A15) we must now use ε_{sX} rather than ε_X)

I. The Coefficient $\chi_o(q)$

From Eqs. (A15) and (A16) we have that

$$\chi_o(q) = \frac{2}{(2\pi)^3} \int dk \theta_o(k+q, k) \quad (A20)$$

$$= \frac{2}{(2\pi)^3} \int dk \frac{f(k+q) - f(k)}{\varepsilon_o(k+q) - \varepsilon_o(k)} \quad (A21)$$

Now

$$\int \frac{f(k+q) - f(k)}{\varepsilon_o(k+q) - \varepsilon_o(k)} dk = \frac{-k_F}{2\pi^2} F(q/2k_F) \quad (A22)$$

where

$$F(x) = \frac{1}{2} + \frac{1-x^2}{4x} \ln \left| \frac{1+x}{1-x} \right| \quad (A23)$$

Thus

$$\chi_o(q) = - (k_F/\pi) F(q/2k_F) \quad (A24)$$

For small x ,

$$F(x) \simeq 1 - \frac{1}{3} x^2$$

so that

$$\chi_o(q) = - \frac{k_F}{\pi^2} + q^2 \frac{1}{12\pi^2 k_F} \quad (\text{A25})$$

$$= \chi_o^{(0)} + q^2 \chi_o^{(2)} \quad (\text{A26})$$

where in Eq. (A26) , the superscripts denote the order of q^2 .

Thus

$$\chi_o^{(0)} = - \frac{k_F}{\pi^2} , \quad (\text{A27})$$

and

$$\chi_o^{(2)} = \frac{1}{12\pi^2 k_F} . \quad (\text{A28})$$

II. The Coefficient $\chi_1(q)$

From (A15) and (A16) we have that $\chi_1(q)$, the density response function to first order in e^2 , is given by

$$\chi_1(q) = -2 \int \frac{dk}{(2\pi)^3} \theta_o(k+q, k) \left[\int \frac{dk'}{(2\pi)^3} \theta_o(k'+q, k') u(k-k') + \frac{[\varepsilon_{sx}(k+q) - \varepsilon_{sx}(k)]}{[\varepsilon_o(k+q) - \varepsilon_o(k)]} \right] \quad (A29)$$

$$= \chi_1^{(0)} + \chi_1^{(2)}, \quad (A30)$$

where $\chi_1^{(0)}$ and $\chi_1^{(2)}$ are the $O(q^0)$ and $O(q^2)$ components of $\chi_1(q)$.

In order to obtain the series in q^2 from (A29) we expand the function

$\theta_o(k+q, k)$ as

$$\theta_o(k+q, k) = f'[\varepsilon_o(k)] + \frac{1}{2}[\varepsilon_o(k+q) - \varepsilon_o(k)] f''[\varepsilon_o(k)] + \dots \quad (A31)$$

where f' and f'' are the first and second derivatives of $f[\varepsilon_o(k)]$ with respect to $\varepsilon_o(k)$, and then substitute into Eq. (A29).

II.1. The q-independent term $\chi_1^{(0)}$ of $\chi_1(\mathbf{q})$

The q-independent term of Eq. (A29) is given by

$$\chi_1^{(0)} = - \frac{\varepsilon_{\text{SX}}(k_F)}{\pi^2 k_F} + I \quad (\text{A32})$$

where

$$I = 2 \frac{\partial}{\partial \varepsilon_F} \int \frac{d\mathbf{k}}{(2\pi)^3} \varepsilon_{\text{SX}}(\mathbf{k}) \frac{\partial f_{\mathbf{k}}}{\partial \varepsilon_F} \quad (\text{A33})$$

and where $\varepsilon_F = \frac{1}{2} k_F^2$. From Eq. (A19) we have

$$\varepsilon_{\text{SX}}(k_F) = - \frac{e^2}{\pi} \left[k_F - k_s \tan^{-1} \left(\frac{2k_F}{k_s} \right) + \frac{k_s^2}{4k_F} \ln \left(\frac{k_s^2 + 4k_F^2}{k_s^2} \right) \right] \quad (\text{A34})$$

so that

$$\chi_1^{(0)} = - \frac{e^2}{\pi^3} \left[1 - \frac{k_s}{k_F} \tan^{-1} \left(\frac{2k_F}{k_s} \right) + \frac{k_s^2}{4k_F^2} \ln \left(\frac{k_s^2 + 4k_F^2}{k_s^2} \right) \right] + I. \quad (\text{A35})$$

In the second term I of $\chi_1^{(0)}$ in Eq.(A32) , since $\varepsilon_{sX}(\mathbf{k})=\varepsilon_{sX}(\mathbf{k})$ i.e. it is spherically symmetric , we have

$$I = \frac{1}{\pi^2} \frac{\partial}{\partial \varepsilon_F} \int_0^{\infty} dk \, k^2 \varepsilon_{sX}(\mathbf{k}) \frac{\partial f_{\mathbf{k}}}{\partial \varepsilon_F} \quad (\text{A36})$$

Now since $f_{\mathbf{k}}=f[\varepsilon_0(\mathbf{k})]$, we have the identities

$$\frac{\partial f_{\mathbf{k}}}{\partial \varepsilon_0(\mathbf{k})} = - \delta(\varepsilon_0(\mathbf{k}) - \varepsilon_F) \quad (\text{A37})$$

and

$$\frac{\partial f_{\mathbf{k}}}{\partial \varepsilon_F} = \delta(\varepsilon_0(\mathbf{k}) - \varepsilon_F) = \delta(\frac{1}{2}k^2 - \frac{1}{2}k_F^2) . \quad (\text{A38})$$

Next using the identity

$$\delta(f(x)) = \sum_{x_i} \frac{1}{|\partial f/\partial x|_{x=x_i}} \delta(x-x_i) \quad (\text{A39})$$

where x_i are the zeros of the function $f(x)$, the first derivative of $f_{\mathbf{k}}$ with respect to ε_F in Eq.(A38) may be written as

$$\frac{\partial f_{\mathbf{k}}}{\partial \varepsilon_{\mathbf{F}}} = \frac{1}{k_{\mathbf{F}}} [\delta(k-k_{\mathbf{F}}) + \delta(k+k_{\mathbf{F}})] \quad . \quad (\text{A40})$$

Since the limit of integration over k is from 0 to ∞ in Eq.(A36), there is no contribution from the $\delta(k+k_{\mathbf{F}})$ term in Eq.(A40) . Thus we rewrite $\partial f_{\mathbf{k}}/\partial \varepsilon_{\mathbf{F}}$ in Eq.(A40) as

$$\frac{\partial f_{\mathbf{k}}}{\partial \varepsilon_{\mathbf{F}}} = \frac{1}{k_{\mathbf{F}}} \delta(k-k_{\mathbf{F}}) \quad (\text{A41})$$

By substituting for $\partial f_{\mathbf{k}}/\partial \varepsilon_{\mathbf{F}}$ given in Eq.(A41) into Eq.(A36) and using the identity

$$\int_0^{\infty} f(x) \delta(x-a) = f(a) \quad (\text{A42})$$

we obtain

$$\begin{aligned} I &= \frac{1}{\pi^2} \frac{\partial}{\partial \varepsilon_{\mathbf{F}}} \frac{k^2}{k_{\mathbf{F}}} \varepsilon_{\text{SX}}(k) \delta(k-k_{\mathbf{F}}) dk \\ &= (1/\pi^2) \frac{1}{k_{\mathbf{F}}} \frac{\partial}{\partial \varepsilon_{\mathbf{F}}} \{k_{\mathbf{F}} \varepsilon_{\text{SX}}(k_{\mathbf{F}})\} \quad , \end{aligned} \quad (\text{A43})$$

where we have used the fact that $\frac{\partial}{\partial \varepsilon_F} = \frac{1}{k_F} \frac{\partial}{\partial k_F}$. Now from (A34)

we have

$$\frac{\partial}{\partial k_F} \{k_F \varepsilon_{sx}(k_F)\} = - \frac{e^2}{\pi} [2k_F - k_s \tan^{-1} (2k_F/k_s)] . \quad (\text{A44})$$

Thus

$$I = - \frac{e^2}{\pi^3} \left[2 - \frac{k_s}{k_F} \tan^{-1} \left(\frac{2k_F}{k_s} \right) \right] , \quad (\text{A45})$$

and consequently Eq.(A32) for $\chi_1^{(0)}$ is

$$\chi_1^{(0)} = - \frac{e^2}{\pi^3} \left[1 - \frac{k_s^2}{4k_F^2} \ln \left(\frac{k_s^2 + 4k_F^2}{k_s^2} \right) \right] . \quad (\text{A46})$$

Note that in the limit as $k_s \rightarrow 0$ the above expression reduces to Sham's result

$$\chi_1^{(0)} = - \frac{e^2}{\pi^3} . \quad (\text{A47})$$

II.2. The q^2 -Coefficient $\chi_1^{(2)}$ of $\chi_1(q)$.

Finally, from Eq. (A29) and (A31), the coefficient $\chi_1^{(2)}$ is given by

$$\chi_1^{(2)} = - \frac{\varepsilon_{sx}(k_F)}{12\pi^2 k_F^3} + I_1 + I_2 + I_3 \quad (\text{A48})$$

where

$$I_1 = -\frac{1}{2} \frac{\partial}{\partial \varepsilon_F} \int \frac{dk}{(2\pi)^3} \varepsilon_{sx}(k) \frac{\partial^2 f_k}{\partial \varepsilon_F^2} \quad (\text{A49})$$

$$= - \frac{1}{4\pi^2} \int_0^\infty dk \frac{\partial f_k}{\partial \varepsilon_F} \frac{\partial P}{\partial k} \quad (\text{A50})$$

where

$$P(k) = \left[\frac{\partial}{\partial \varepsilon_F} + \frac{\partial}{\partial \varepsilon_0(k)} \right] \{k\varepsilon_{sx}(k)\}, \quad (\text{A51})$$

and

$$I_2 = \frac{1}{9} \frac{\partial}{\partial \varepsilon_F} \int \frac{d\mathbf{k}}{(2\pi)^3} \varepsilon_{s\mathbf{x}}(\mathbf{k}) \varepsilon_o(\mathbf{k}) \frac{\partial^3 f_{\mathbf{k}}}{\partial \varepsilon_F^3} \quad (\text{A52})$$

and

$$I_3 = \frac{1}{6} \int \frac{d\mathbf{k}}{(2\pi)^3} \varepsilon_{s\mathbf{x}}(\mathbf{k}) \frac{\partial^3 f_{\mathbf{k}}}{\partial \varepsilon_F^3} \quad (\text{A53})$$

We next calculate the integrals I_1 , I_2 and I_3 .

II.2.1 The Integral I_1

From Eq. (A50) , the integral I_1 is

$$I_1 = - \frac{1}{4\pi^2} \int_0^{\infty} dk \frac{\partial f_k}{\partial \varepsilon_F} \frac{\partial P}{\partial k} = - \frac{1}{4\pi^2 k_F} \frac{\partial P}{\partial k} \Big|_{k=k_F} \quad (\text{A54})$$

where we have used Eq. (A41) and where

$$P(k) = \left[\frac{\partial}{\partial \varepsilon_F} + \frac{\partial}{\partial \varepsilon_0(k)} \right] \{k\varepsilon_{SX}(k)\} . \quad (\text{A51})$$

we rewrite (A51) as

$$P(k) = \left(\frac{1}{k_F} \frac{\partial}{\partial k_F} + \frac{1}{k} \frac{\partial}{\partial k} \right) \{k\varepsilon_{SX}(k)\} \quad (\text{A55})$$

$$= P_1(k) + P_2(k) \quad (\text{A56})$$

where

$$\begin{aligned}
P_1(k) &= \frac{1}{k_F} \frac{\partial}{\partial k_F} \{k\varepsilon_{sX}(k)\} \\
&= -\frac{e^2}{\pi} \left[\frac{k}{k_F} - \frac{kk_s^2}{k_F} \left(\frac{1}{(k+k_F)^2+k_s^2} + \frac{1}{(k-k_F)^2+k_s^2} \right) \right. \\
&\quad + \frac{1}{2} \ln \frac{(k+k_F)^2+k_s^2}{(k-k_F)^2+k_s^2} \\
&\quad \left. + \frac{k_F^2+k_s^2-k^2}{2k_F} \left(\frac{k+k_F}{(k+k_F)^2+k_s^2} + \frac{k-k_F}{(k-k_F)^2+k_s^2} \right) \right] \quad (A57)
\end{aligned}$$

and

$$\begin{aligned}
P_2(k) &= \frac{1}{k} \frac{\partial}{\partial k} \{k\varepsilon_{sX}(k)\} \\
&= -\frac{e^2}{\pi} \left[\frac{k_F}{k} - \frac{k_s}{k} \left\{ \tan^{-1} \left(\frac{k+k_F}{k_s} \right) - \tan^{-1} \left(\frac{k-k_F}{k_s} \right) \right\} \right. \\
&\quad - k_s^2 \left(\frac{1}{(k+k_F)^2+k_s^2} - \frac{1}{(k-k_F)^2+k_s^2} \right) \\
&\quad - \frac{1}{2} \ln \frac{(k+k_F)^2+k_s^2}{(k-k_F)^2+k_s^2} \\
&\quad \left. + \frac{k_F^2+k_s^2-k^2}{2k} \left(\frac{k+k_F}{(k+k_F)^2+k_s^2} - \frac{k-k_F}{(k-k_F)^2+k_s^2} \right) \right] \quad (A58)
\end{aligned}$$

Thus

$$P(k) = -\frac{e^2}{\pi k} \left[2k_F - k_s \left\{ \tan^{-1} \left(\frac{k+k_F}{k_s} \right) - \tan^{-1} \left(\frac{k-k_F}{k_s} \right) \right\} \right]. \quad (\text{A59})$$

Next

$$\begin{aligned} \frac{\partial P}{\partial k} = -\frac{e^2}{\pi} \left[-\frac{2k_F}{k} + \frac{k_s}{k^2} \left[\tan^{-1} \frac{k+k_F}{k_s} - \tan^{-1} \frac{k-k_F}{k_s} \right] \right. \\ \left. - \frac{k_s^2}{k} \left(\frac{1}{(k+k_F)^2+k_s^2} - \frac{1}{(k-k_F)^2+k_s^2} \right) \right] \quad (\text{A60}) \end{aligned}$$

and

$$\left. \frac{\partial P}{\partial k} \right|_{k_F} = \frac{e^2}{\pi k_F} \left[1 + \frac{k_s^2}{4k_F^2+k_s^2} - \frac{k_s}{k_F} \tan^{-1} \frac{2k_F}{k_s} \right]. \quad (\text{A61})$$

Substituting (A61) into (A54) we have

$$I_1 = -\frac{e^2}{4\pi^3 k_F^2} \left[1 + \frac{k_s^2}{4k_F^2+k_s^2} - \frac{k_s}{k_F} \tan^{-1} \frac{2k_F}{k_s} \right]. \quad (\text{A62})$$

II.2.2 The Integral I_2

Eq. (A52) for I_2 may be written as

$$I_2 = \frac{1}{36\pi^2 k_F} \frac{\partial}{\partial k_F} \int_0^{\omega} dk k^4 \varepsilon_{sx}(k) \frac{\partial^3 f_k}{\partial \varepsilon_F^3} . \quad (\text{A63})$$

Now from Eq. (A41) we have

$$\begin{aligned} \frac{\partial^2 f_k}{\partial \varepsilon_F^2} &= \frac{1}{k_F} \frac{\partial}{\partial k_F} \left[\frac{1}{k_F} \delta(k-k_F) \right] \\ &= - \frac{\delta'(k-k_F)}{k_F^2} - \frac{\delta(k-k_F)}{k_F^3} , \end{aligned} \quad (\text{A64})$$

and consequently

$$\begin{aligned} \frac{\partial^3 f_k}{\partial \varepsilon_F^3} &= \frac{1}{k_F} \frac{\partial}{\partial k_F} \left[- \frac{\delta'(k-k_F)}{k_F^2} - \frac{\delta(k-k_F)}{k_F^3} \right] \\ &= \frac{3\delta(k-k_F)}{k_F^5} + \frac{3\delta'(k-k_F)}{k_F^4} + \frac{\delta''(k-k_F)}{k_F^3} . \end{aligned} \quad (\text{A65})$$

Substituting (A65) into (A63) we obtain

$$I_2 = \frac{1}{36\pi^2 k_F} \frac{\partial}{\partial k_F} \left[\frac{3}{k_F^5} \left(k^4 \varepsilon_{sx}(k) \right)_{k=k_F} + \frac{3}{k_F^4} \left(-\frac{\partial}{\partial k} \{k^4 \varepsilon_{sx}(k)\} \right)_{k=k_F} \right. \\ \left. + \frac{1}{k_F^3} \left(\frac{\partial^2}{\partial k^2} \{k^4 \varepsilon_{sx}(k)\} \right)_{k=k_F} \right] \quad (A66)$$

where we have used the relations

$$\int_0^{\infty} f(x) \delta'(x-a) dx = - \frac{\partial f}{\partial x} \Big|_{x=a} \quad (A67)$$

and

$$\int_0^{\infty} f(x) \delta''(x-a) dx = \frac{\partial^2 f}{\partial x^2} \Big|_{x=a} \quad (A68)$$

We rewrite I_2 as given by Eq.(A66) as

$$I_2 = \frac{1}{36\pi^2 k_F} \frac{\partial}{\partial k_F} [I_{21} + I_{22} + I_{23}]$$

where

$$I_{21} = \frac{3}{k_F^5} \{k^4 \varepsilon_{sx}(k)\}_{k=k_F} \quad (A69)$$

$$= \frac{e^2}{\pi} \left[-3 + \frac{3k_s}{k_F} \tan^{-1} \frac{2k_F}{k_s} - \frac{3k_s^2}{4k_F^2} \ln \frac{4k_F^2 + k_s^2}{k_s^2} \right] \quad (A70)$$

$$I_{22} = -\frac{3}{k_F^4} \left(\frac{\partial}{\partial k} \{k^4 \varepsilon_{sx}(k)\} \right)_{k=k_F} \quad (A71)$$

$$= -\frac{12}{k_F} \varepsilon_{sx}(k_F) - 3\varepsilon'_{sx}(k_F) . \quad (A72)$$

Now

$$\varepsilon'_{sx}(k_F) = \left. \frac{d\varepsilon_{sx}}{dk} \right|_{k=k_F} = \frac{e^2}{2\pi} \left[-2 + \frac{2k_F^2 + k_s^2}{2k_F^2} \ln \frac{4k_F^2 + k_s^2}{k_s^2} \right] \quad (A73)$$

so that

$$I_{22} = \frac{e^2}{\pi} \left[15 - 12 \frac{k_s}{k_F} \tan^{-1} \frac{2k_F}{k_s} + \frac{9k_s^2 - 6k_F^2}{4k_F^2} \ln \frac{4k_F^2 + k_s^2}{k_s^2} \right] \quad (A74)$$

Finally

$$I_{23} = \frac{1}{k_F^3} \left(\frac{\partial^2}{\partial k^2} \{k^4 \varepsilon_{sx}(k)\} \right)_{k=k_F} \quad (A75)$$

$$= \frac{12}{k_F} \varepsilon_{sx}(k_F) + 8\varepsilon'_{sx}(k_F) + k_F \varepsilon''_{sx}(k_F) . \quad (A76)$$

Using (A73) and the fact that

$$\varepsilon''(k_F) = \frac{d^2\varepsilon_{SX}}{dk^2} \Big|_{k=k_F} = \frac{e^2}{2\pi k_F} \left[2 + \frac{4k_F^2 + 2k_s^2}{4k_F^2 + k_s^2} - \frac{k_F^2 + k_s^2}{k_F^2} \ln \frac{4k_F^2 + k_s^2}{k_s^2} \right] \quad (\text{A77})$$

we have

$$I_{23} = \frac{e^2}{\pi} \left[-19 + 12 \frac{k_s}{k_F} \tan^{-1} \frac{2k_F}{k_s} + \frac{2k_F^2 + k_s^2}{4k_F^2 + k_s^2} + \frac{14k_F^2 - 6k_s^2}{4k_F^2} \ln \frac{4k_F^2 + k_s^2}{k_s^2} \right] \quad (\text{A78})$$

Thus

$$I_2 = \frac{e^2}{36\pi^3 k_F^2} \left[\frac{64k_F^4 + 3k_F^2 k_s^2 + 6k_s^4}{(k_s^2 + 4k_F^2)^2} - \frac{3k_s}{k_F} \tan^{-1} \left(\frac{2k_F}{k_s} \right) \right] \quad (\text{A79})$$

II.2.3. The Integral I_3

Eq. (A53) for I_3 may be written as

$$I_3 = \frac{1}{12\pi^2} \int_0^{\infty} dk k^2 \varepsilon_{sx}(k) \frac{\partial^3 f_k}{\partial \varepsilon_F^3} \quad (\text{A80})$$

$$= \frac{1}{12\pi^2} \left[\frac{3}{k_F^5} k_F^2 \varepsilon_{sx}(k_F) + \frac{3}{k_F^4} \left(-\frac{\partial}{\partial k} \{k^2 \varepsilon_{sx}(k)\} \right)_{k=k_F} + \frac{1}{k_F^3} \left(\frac{\partial^2}{\partial k^2} \{k^2 \varepsilon_{sx}(k)\} \right)_{k=k_F} \right] \quad (\text{A81})$$

$$= \frac{1}{12\pi^2} \left[-\frac{1}{k_F^3} \varepsilon_{sx}(k_F) + \frac{1}{k_F^2} \varepsilon'_{sx}(k_F) + \frac{1}{k_F} \varepsilon''_{sx}(k_F) \right] \quad (\text{A82})$$

where we have used Eq. (A65) to obtain (A81). Since we have already derived expressions for $\varepsilon_{sx}(k_F)$, $\varepsilon'_{sx}(k_F)$ and $\varepsilon''_{sx}(k_F)$, we have

$$I_3 = \frac{e^2}{12\pi^3 k_F^2} \left[1 + \frac{2k_F^2 + k_s^2}{4k_F^2 + k_s^2} - \frac{k_s}{k_F} \tan^{-1} \left(\frac{2k_F}{k_s} \right) \right] \quad (\text{A83})$$

Next , inserting the expressions for $\varepsilon_{sx}(k_F)$, I_1 , I_2 , and I_3 derived above into Eq. (A48), we obtain

$$\chi_1^{(2)} = \frac{e^2}{36\pi^3 k_F^2} \left[\frac{3}{4} \frac{k_s^2}{k_F^2} \ln \left(\frac{4k_F^2 + k_s^2}{k_s^2} \right) + \frac{40k_F^4 - 6k_F^2 k_s^2 - 3k_s^4}{(4k_F^2 + k_s^2)^2} \right] . \quad (\text{A84})$$

Finally on substituting the expressions for $\chi_o^{(o)}$, $\chi_o^{(2)}$, $\chi_1^{(o)}$ and $\chi_1^{(2)}$ from Eqs. (A24), (A25), (A46) and (A84) into Eq. (A14) we obtain for the coefficient B_{sx} the expression

$$B_{sx} = \frac{e^2 \pi}{24k_F^4} \left[-2 + \frac{3}{4} \frac{k_s^2}{k_F^2} \ln \left(\frac{4k_F^2 + k_s^2}{k_s^2} \right) + \frac{40k_F^4 - 6k_F^2 k_s^2 - 3k_s^4}{3(4k_F^2 + k_s^2)^2} \right] \quad (\text{A85})$$

With

$$k_F^4 = [3\pi^2 \rho(r)]^{4/3} \quad (\text{A86})$$

we can write

$$B_{sx} = C_{sx} / \rho^{4/3}(r) \quad (\text{A87})$$

where

$$C_{sx} = \frac{e^2\pi}{24(3\pi)^{4/3}} \left[-2 + \frac{3}{4} \frac{k_s^2}{k_F^2} \ln \left(\frac{4k_F^2 + k_s^2}{k_s^2} \right) + \frac{40k_F^4 - 6k_F^2 k_s^2 - 3k_s^4}{3(4k_F^2 + k_s^2)^2} \right] \quad (\text{A88})$$

As a check, we note that in the limit $k_s \rightarrow 0$

$$C_x = - \frac{7\pi}{144(3\pi^2)^{4/3}} \quad (\text{A89})$$

which is the value derived by Sham for bare-Coulomb interaction.

Appendix B

Linear-Potential Model³⁰ of a Surface.

In the linear-potential model of a metal surface, the effective potential is assumed to be

$$V_{\text{eff}}(x) = F x \theta(x) , \quad (\text{B1})$$

where F is the field strength defined in terms of the slope parameter x_F as $F = \bar{k}_F^2 / 2x_F$, $\frac{1}{2}\bar{k}_F^2$ is the Fermi energy, and $\theta(x)$ is the step function. The solution of the Schrodinger equation for this potential is given as Eq. (85) of chapter IV. In this appendix we present for this model the semi-analytical expressions^{26,30,74} for the following properties : the electronic density and its first derivative, the jellium edge position, the surface dipole barrier, the electrostatic potential, the surface kinetic, electrostatic, and the exact non-local surface exchange energies. These expressions are presented in terms of the variables $y = \bar{k}_F x$, $q = k / \bar{k}_F$ and $q' = k' / \bar{k}_F$. The slope parameter $y_F = \bar{k}_F x_F$, the jellium edge position is at $y_a = \bar{k}_F a$. The variable $\xi = y y_F^{-1/3} - \xi_0$ where $\xi_0 = q^2 y_F^{2/3}$. All the above properties can then be written in terms of universal functions of the parameter y_F and these functions are given below. With the definition

$$\kappa(q, y_F) = y_F^{1/3} \text{Ai}(-\xi_0) / \text{Ai}'(-\xi_0) \quad (\text{B2})$$

so that

$$\kappa(0) = y_F^{1/3} \text{Ai}(0) / \text{Ai}'(0) \quad (\text{B3})$$

the phase shift may be written

$$\delta(q, y_F) = \cot^{-1} [1/q\kappa(q, y_F)] \quad (\text{B4})$$

We further define

$$\Lambda(q, y_F) = \xi_0 \text{Ai}^2(-\xi_0) + \text{Ai}'^2(-\xi_0) \quad (\text{B5})$$

1. Jellium edge position

$$y_a = -3\pi/8 - 3 \int_0^l dq \, q \delta(q, y_F) \quad (\text{B6})$$

2. Electronic density and its first derivative

$$\frac{\rho(y)}{\bar{\rho}} = \begin{cases} 1 - (3/2) \int_0^l dq (1-q^2) \cos 2[qy + \delta(q, y_F)] & \text{for } y \leq 0 \\ 3y_F^{2/3} \int_0^l dq (1-q^2) q^2 \text{Ai}^2(-\xi) / \Lambda(q, y_F) & \text{for } y \geq 0 ; \end{cases} \quad (\text{B7})$$

$$\frac{1}{\bar{\rho}} \frac{d\rho(y)}{dy} = \begin{cases} 3 \int_0^l dq (1-q^2) q \sin 2[qy + \delta(q, y_F)] & \text{for } y \leq 0 \\ 6y_F^{1/3} \int_0^l dq (1-q^2) q^2 \text{Ai}(\xi) \text{Ai}'(\xi) / \Lambda(q, y_F) & \text{for } y \geq 0 . \end{cases} \quad (\text{B8})$$

3. Surface dipole barrier

$$\frac{\Delta\phi}{\bar{k}_F} = \frac{1}{\pi} \left[1 + \frac{1}{2} \pi \kappa(0) \frac{16}{105} y_F^2 - \frac{2}{3} y_a^2 \right. \\ \left. + \int_0^l dq (1-q^2) \left(\frac{\sin^2 \delta(q, y_F)}{q^2} - \frac{2}{3} y_F q \sin 2\delta(q, y_F) \right) \right] \quad (\text{B9})$$

4. Electrostatic potential

For $y \leq 0$

$$\frac{V_{es}(y)}{\bar{k}_F} = \frac{1}{\pi} \left[1 + \frac{1}{2} \pi \kappa(0) + \frac{1}{2} \pi y - \frac{2}{3} (y - y_a)^2 \theta(y - y_a) \right. \\ \left. + \int_0^1 dq \frac{(1-q^2)}{q^2} \sin^2[qy + \delta(q, y_F)] \right]. \quad (B10)$$

For $y \geq 0$

$$\frac{V_{es}(y)}{\bar{k}_F} = \frac{\Delta\phi}{\bar{k}_F} + \frac{2}{3\pi} (y - y_a)^2 \theta(y - y_a) + \frac{4 y_F^{2/3}}{3\pi} \\ \times \int_0^1 dq (1-q^2) \frac{\sin^2 \delta(q, y_F)}{\text{Ai}^2(-\xi_0)} \\ \times [2\xi\Lambda(\xi) + \text{Ai}(\xi)\text{Ai}'(\xi)] . \quad (B11)$$

5. Kinetic Energy : σ_k

$$\frac{\sigma_k}{\bar{k}_F^4} = \frac{1}{160\pi} \left[1 - \frac{64y_F}{35\pi} + \frac{4y_F^{1/3}}{3\pi} \int_0^1 dq (1-q^2)(3+5q^2) \frac{\text{Ai}(-\xi_0)\text{Ai}(-\xi'_0)}{\Lambda(-\xi_0)} \right]. \quad (\text{B12})$$

6. Electrostatic Energy : σ_{es}

$$\begin{aligned} \frac{\sigma_{es}}{\bar{k}_F^3} &= \frac{1}{4\pi^2} \left[-\frac{1}{12} + \frac{2}{3} \int_0^\infty dy \left[\frac{\rho(y)}{p} - \theta(y_a - y) \right] \frac{V_{es}(y)}{\bar{k}_F} \right. \\ &+ \frac{2}{3}y_a \left\{ (2/9\pi) y_a^2 - \frac{1}{2}y_a - \left[(1/\pi) + \frac{1}{2}\kappa(0) \right] \right\} \theta(-y_a) \\ &+ \left\{ \frac{1}{4} + \frac{2}{3}y_a/\pi \theta(-y_a) \right\} \int_0^1 dq (1-q^2) \sin^2\delta/q^2 \\ &+ \left\{ \frac{2}{3}y_a^2/\pi \theta(-y_a) - \left[(1/\pi) + \frac{1}{2}\kappa(0) \right] \right\} \int_0^1 dq (1-q^2) \sin 2\delta/2q \\ &- (2/3\pi) \int_0^1 dq (1-q^2) \frac{1}{q^2} \left\{ y_a + \frac{1}{2q} [\sin 2\delta - \sin 2(qy_a + \delta)] \right\} \theta(-y_a) \\ &+ \frac{1}{4\pi} \int_0^1 dq (1-q^2) \int_0^1 dq' (1-q'^2) \cdot \\ &\quad \left. \left[\frac{\sin 2\delta_-}{2q_-} - \frac{\sin 2\delta_+}{2q_+} - \frac{\sin 2\delta'}{2q'} \right] \right]. \quad (\text{B13}) \end{aligned}$$

7. Exact non-local Exchange Energy : σ_x

$$\begin{aligned}
\frac{\sigma_x}{\frac{-3}{k_F}} &= \frac{y_a}{4\pi^3} + \frac{1}{8\pi^3} \int_0^2 dp \int_0^1 dq p \left(\frac{H(p, 0, q) + H(p, q, 0)}{p^2 + q^2} - \frac{H(p, q, q)}{p^2} \right) \\
&\quad - \frac{1}{4\pi^4} \int_0^2 dp \int_0^1 dq \int_0^1 dq' p H(p, q, q') \\
&\quad \left[\frac{1}{p^2 + q_-^2} \left(\frac{\sin 2\delta_-}{2q_-} - \frac{\sin 2\delta}{2q} - \frac{\sin 2\delta'}{2q'} \right) \right. \\
&\quad + \frac{1}{p^2 + q_+^2} \left(\frac{\sin 2\delta_+}{2q_+} - \frac{\sin 2\delta}{2q} - \frac{\sin 2\delta'}{2q'} \right) \\
&\quad + \frac{1}{p} \left(\frac{q_- \sin \delta_-}{p^2 + q_-^2} - \frac{q_+ \sin \delta_+}{p^2 + q_+^2} \right)^2 \\
&\quad \left. - p \left(\frac{\cos \delta_-}{p^2 + q_-^2} - \frac{\cos \delta_+}{p^2 + q_+^2} \right)^2 \right]
\end{aligned}$$

$$\begin{aligned}
& - \frac{1}{\pi^4} \int_0^2 dp \int_0^1 dq \int_0^1 dq' \frac{\sin \delta \sin \delta'}{\text{Ai}(-\xi_0) \text{Ai}(-\xi'_0)} H(p, q, q') \\
& \left[p \frac{\cos \delta_-}{p^2 + q_-^2} - p \frac{\cos \delta_+}{p^2 + q_+^2} - q_- \frac{\sin \delta_-}{p^2 + q_-^2} - q_+ \frac{\sin \delta_+}{p^2 + q_+^2} \right] \\
& \times \int_0^\infty dy e^{-py} \text{Ai}(y, q) \text{Ai}(y, q') \\
& + \frac{1}{\pi^4} \int_0^2 dp \int_0^1 dq \int_0^1 dq' \frac{\sin^2 \delta \sin^2 \delta'}{\text{Ai}^2(-\xi_0) \text{Ai}^2(-\xi'_0)} H(p, q, q') \\
& \int_0^\infty dy \int_0^\infty dy' e^{-p|y-y'|} \text{Ai}(y, q) \text{Ai}(y, q') \text{Ai}(y', q) \text{Ai}(y', q') .
\end{aligned} \tag{B14}$$

where $q_+ = q + q'$, $q_- = q - q'$, $\delta' = \delta(q')$, $\delta_+ = \delta + \delta'$, $\delta_- = \delta - \delta'$ and where

$$H(p, q, q') = \begin{cases} \pi(q'^2 - q^2) & \text{for } \xi \geq 1 - q'^2 \text{ and } \xi > 0 \\ \pi[(1 - q'^2) + (1 - q^2)] & \text{for } \xi^2 \geq 1 - q'^2 \text{ and } \xi < 0 \\ \pi(1 - q^2) - 2[(1 - q'^2) \sin^{-1}(\xi/\sqrt{1 - q'^2}) + \xi\sqrt{1 - q'^2 - \xi^2}] & \text{for } \xi^2 < 1 - q'^2 \end{cases}$$

and

$$\xi = (p^2 + q^2 - q'^2) / 2p .$$

Appendix C

Polynomial Fit to First Gradient Correction Coefficient

In this appendix we give the analytic polynomial fit to the expression for the gradient correction term coefficient B_{xc} due to Rasolt and Geldart⁴³ (RG), and due to Langreth and Perdew⁴¹ (LP) .

Let $y = [\rho(r)^{4/3} B_{xc}] (10^3)$ and x be the local value of r_s

For $1 < x < 12$:

$$y = y_1 (1 - x/x_1) (1 - x/x_2) (1 - x/x_3) + y_2 . \quad (C1)$$

RG coefficient :

$$y_1 = 0.28 , y_2 = 2.42 , x_1 = -208.2 , x_2 = 1.5 , x_3 = 72.54 .$$

LP coefficient :

$$y_1 = 0.155 , y_2 = 2.5 , x_1 = -4.4 , x_2 = 8.2 , x_3 = 21.5 .$$

In our work we define the coefficient B_c of the gradient correction term for the correlation energy as

$$B_c = B_{xc} - B_x, \quad (C2)$$

where the coefficients B_{xc} due to RG and LP are given by the analytic polynomial fit expression of Eq. (C1). We write the coefficients B_{xc} and B_x in the standard form as

$$B_{xc} = C_{xc} / [\rho(r)]^{4/3}, \quad (C3)$$

and

$$B_x = C_x / [\rho(r)]^{4/3} \quad (C4)$$

where $C_x = -7\pi/144(3\pi^2)^{4/3} = -0.00167$ a.u. . Consequently, the correlation energy coefficient C_c is defined as

$$C_c = C_{xc} - C_x. \quad (C5)$$

We present below the values for the coefficients C_c due to LP and RG as a function of r_s for $1 \leq r_s \leq 12$.

| r_s | $C_c (10^{-3})$ (a.u.) | |
|-------|------------------------|--------|
| | LP | RG |
| 1.00 | 4.3265 | 4.1845 |
| 2.00 | 4.3218 | 4.0051 |
| 3.00 | 4.3095 | 3.8291 |
| 4.00 | 4.2906 | 3.6565 |
| 5.00 | 4.2664 | 3.4874 |
| 6.00 | 4.2381 | 3.3219 |
| 7.00 | 4.2068 | 3.1601 |
| 8.00 | 4.1739 | 3.0020 |
| 9.00 | 4.1404 | 2.8478 |
| 10.00 | 4.1077 | 2.6974 |
| 11.00 | 4.0767 | 2.5509 |
| 12.00 | 4.0489 | 2.4085 |

Bibliography

1. O.Sinanoglu and K.E. Brueckner, "Three Approaches to Electron Electron Correlation in Atoms" (Yale University Press, 1970).
2. P. Hohenberg and W. Kohn, Phys. Rev. 136, B864 (1964).
3. W. Kohn and L.J. Sham, Phys. Rev. 140, A1133 (1965).
4. J.P. Perdew, R.G. Parr, M. Levy and J. Balduz, Phys. Rev. Lett. 49, 1691 (1982).
5. M. Levy, J.P. Perdew and V. Sahni, Phys. Rev. A30, 2745 (1984) .
6. D.C. Langreth has informed us of recent work by U. von Barth along these lines.
7. D.M. Ceperley, Phys. Rev. B18, 3126 (1978); D.M. Ceperley and B.J. Alder, Phys. Rev. Lett. 45, 566 (1980) .
8. S. Raimes, Wave Mechanics of Electrons in Metals, (North-Holland, Amsterdam, 1961) P. 177 .
9. We employ atomic units for which $|e| = \hbar = m = 1$.
10. A. Veillard and E. Clementi, J. Chem. Phys. 49, 2415 (1968).
11. C. Moore, Ionization Potential and Ionization Limits from the Analysis of Optical Spectra, U.S. Natl. Bur. Stand., National Reference Data Series No. 34 (U.S.GPO., Washington, D.C., 1970) .

12. J.P. Desclaux, At. Data Nucl. Data Tables 12, 311 (1973) .
13. C.F. Fischer, The Hartree-Fock Method for Atoms, (John Wiley & Sons, New York 1977) .
14. K. Aashamar, T.M. Luke, and J.D. Talman, Phys. Rev. A19, 6 (1979) .
15. C.L. Pekeris, Phys. Rev. 115, 1216(1959); 126, 1470 (1962).
16. S. Larsson, Phys. Rev. 169, 49 (1968) .
17. C.F. Bunge, Phys. Rev. A14, 1965 (1976) .
18. V. Sahni, J. Gruenebaum, and J.P. Perdew , Phys. Rev. B26, 4371 (1982) .
19. J. Bardeen, Phys. Rev. 49, 653 (1936) .
20. N.D. Lang, in Solid State Physics, Advances in Research and Applications, edited by H. Ehrenreich, F. Seitz, and D. Turnbull, (Academic, New York, 1973) p. 225 .
21. E. Wikborg and J.E. Inglesfield, Solid State Commun. 16, 335 (1975).
22. D.C. Langreth and J.P. Perdew, Solid State Commun. 17, 1425 (1975).
23. H.J. Juretschke, Phys. Rev. 92, 1140 (1953) .
24. J. Harris and R.O. Jones, J. Phys. F4, 1170 (1974) .
25. C.Q. Ma and V. Sahni, Phys. Rev. B20, 2291 (1979) .

26. V. Sahni, J.B. Krieger, and J. Gruenebaum, Phys. Rev. B12, 3503 (1975) .
27. V. Sahni and J. Gruenebaum, Phys. Rev. B15, 1929 (1977).
28. G.-X. Qian and W. Kohn (private communication) .
29. V. Sahni and C.Q. Ma, Phys. Rev. B 22, 5987 (1980).
30. V. Sahni, J.B. Krieger, and J. Gruenebaum, Phys. Rev. B15, 1941 (1977) .
31. V. Sahni and J. Gruenebaum, Solid State Commun. 21, 463 (1977) .
32. X. Sun, M. Farjam, and C.-W. Woo, Phys. Rev. B27, 3913 (1983); X. Sun, M. Farjam and C.-W. Woo , Phys. Rev. B28, 5599 (1983); X. Sun, T. Li, and C.-W. Woo, in Recent Progress in Many-Body Theories, (Springer, New York, 1981), p.87 ; X. Sun, T. Li and C.-W. Woo, Acta Phys. Sin. Abstr. 31, 1466, 1474 (1982) .
33. S. Raimes, Many-Electron Theory, (North-Holland/American Elsevier, New York, 1972) PP. 64,90.
34. R. Gaspar, Acta Phys. Acad. Sci. Hung. 3,263(1954).
35. J.E.Robinson, F. Bassani, R.S. Knox, and J.R. Schrieffer, Phys. Rev. Lett. 9, 215 (1962).
36. M. Gell-Mann and K. Brueckner, Phys. Rev. 106, 364 (1957).
37. J.P. Perdew and A. Zunger, Phys. Rev. B23, 5048 (1981) .
38. L. Kleinman, Phys. Rev. B10, 2221 (1974).

39. D.J.W. Geldart, M. Rasolt and C.-O. Almbladh, *Solid State Commun.* 16, 243(1975).
40. L.J. Sham, in Computational Methods in Band Theory, edited by P.O. Marcus, J.F. Janak and A.R. Williams (Plenum, New York, 1971) P. 458.
41. D.C. Langreth and J.P. Perdew, *Solid State Commun.* 31, 567(1979); *Phys. Rev.* B21, 5469(1980).
42. J.S.-Y. Wang and M. Rasolt, *Phys. Rev.* B13, 5330 (1976).
43. M. Rasolt and D.J.W. Geldart, *Solid State Commun.* 18, 549(1976); D.J.W. Geldart and M. Rasolt, *Phys. Rev. B* 13, 1477 (1976).
44. K.H. Lau and W. Kohn, *J. Phys. Chem. Solids* 37, 99 (1976).
45. A.K. Gupta and K.S. Singwi, *Phys. Rev.* B15, 1801 (1977).
46. S.K. Ma and K.A. Brueckner, *Phys. Rev.* 165, 18(1968).
47. B.Y. Tong and L.J. Sham, *Phys. Rev.* 144, 1 (1966) .
48. B.Y. Tong, *Phys. Rev.* A4, 1375 (1971) .
49. C.-O. Almbladh and A.C. Pedroza, *Phys. Rev.* A29, 2322 (1984); C.-O. Almbladh , U. Ekenberg, A.C. Pedroza, *Physica scripta.* 28, 389 (1983) ; See also S. Jagannathan, Ph.D. Thesis, University of Georgia, Athen, Georgia (1979) (unpublished); D.W. Smith, S. Jagannathan and G.S. Handler, *Int. J. Quant. Chem.* S13, 103 (1979).

50. N.D. Lang and L.J. Sham, Solid State Commun. 17, 581 (1975)
51. D. Pines, Elementary Excitations in Solids (Benjamin, New York, 1963) , P. 94 .
52. O. Gunnarsson, M. Jonson and B.I. Lundqvist, Solid State Commun. 24, 765 (1977) ; Phys. Rev. B20, 3136 (1979) .
53. D.C. Langreth and M.J. Mehl, Phys. Rev. Lett. 47, 446 (1981); Phys. Rev. B 28, 1809 (1983).
54. V. Sahni and J. Gruenebaum, Phys. Rev. B25, 6275 (1982).
55. J.P. Perdew , D.C. Langreth and V. Sahni, Phys. Rev. Lett. 38, 1030 (1977).
56. M. Rasolt , J.S.-Y Wang and L.M. Kahn, Phys. Rev. B 15, 580 (1977).
57. J.A. Alonso and L.A. Girifalco, Solid State Commun. 24, 135 (1977) ; Phys. Rev. B17, 3735 (1978).
58. D.C. Langreth and J.P. Perdew, Phys. Rev. B15, 2884 (1977).
59. A. Sugiyama, J. Phys. Soc. Jpn. 16, 1327 (1961).
60. A. Sugiyama, J. Phys. Soc. Jpn. 15, 965 (1960) ; D.C. Langreth, Phys. Rev. B5, 2842 (1972) .
61. J. Rudnick , Ph.D. thesis, University of California, San Diego, (1970) (unpublished).
62. V. Sahni and K.-P. Bohnen, Phys. Rev. B29 , 1045 (1984).

63. V. Sahni and K.-P. Bohnen, "The Image Charge at a Metal Surface", Phys. Rev. B (submitted for publication).
64. A.-R. E. Mohammed and V. Sahni, Phys. Rev. B28, 3014 (1983).
65. G.P. Lepage, J. Comput. Phys. 27, 192 (1978).
66. H.F. Budd and J. Vannimenus, Phys. Rev. Lett. 31, 1218 (1973); 31, 1430(E) (1973).
67. N.D. Lang and W. Kohn, Phys. Rev. B1, 4555(1970).
68. This parameter, for example, could be determined by the energy minimization condition in a formalism such as that due to D. Bohm and D. Pines, Phys. Rev. 92, 609 (1953).
69. A.-R. E. Mohammed and V. Sahni, Phys. Rev. B29, 3687 (1984).
70. For a further exposition of this point see section IV(A) of D.C. Langreth and M.J. Mehl, Phys. Rev. B28, 1809 (1983).
71. F. Herman, J.P. Van Dyke, and J.B. Ortenburger, Phys. Rev. Lett. 22, 807 (1969).
72. D. Bohm and D. Pines, Phys. Rev. 92, 609 (1953).
73. M. Abramowitz and I.A. Stegun, Handbook of Mathematical Functions (Dover, New York, 1965), P. 446.
74. V. Sahni and J. Gruenebaum, Phys. Rev. B19, 1840 (1979).

75. In obtaining the numerical values of the exact non-local surface exchange energy σ_x , we have employed the iterative and adaptive Monte Carlo scheme given in Ref. (65) .
76. I. Yamashita and S. Ichimaru, Phys. Rev. B29, 673 (1984) .
77. V. Sahni, J.P. Perdew and J. Gruenebaum, Phys. Rev. B23, 6512 (1981) .
78. L. Kleinman, Phys. Rev. B30, 2223 (1984).